CHEMICAL PROBLEMS OF THE DEVELOPMENT OF NEW MATERIALS AND TECHNOLOGIES
Minsk 2003

E. N. Naumovich, A. Yaremchenko*, A. Viskup, V. V. Kharton

PEROVSKITE-RELATED OXIDE MATERIALS FOR OXYGEN-PERMEABLE ELECTROCHEMICAL MEMBRANES

INTRODUCTION

Oxide phases with cubic perovskite structure historically are first materials having the electrochemical oxygen permeability values high enough to be considered for oxygen separation membranes [1]. Electrochemical oxygen permeation was observed for fluorite-like solid electrolytes (zirkonia, toria, *etc.*) since 1960s, but typically these phenomena were treated as a parasitic consequence of minor electronic conductivity [2, 3]; negligible values of such fluxes make their use rather unlikely. The Co- and Fe-containing perovskites showed, however, oxygen permeability values 10^5-10^7 times higher than polymer-based membranes and oxygen selectivity about 100 %, on the contrary to 90-95 % selectivity for polymers and zeolites. Thus dense ceramic membranes with mixed ionic-electronic conductivity are of great interest for high-purity oxygen separation. Another application field for such membranes is the partial oxidation of light hydrocarbons. Presently, none of known mixed conductors satisfies to all criteria necessary for the electrochemical membrane reactors. Typical materials having high oxygen permeability exhibit also a very high thermal expansion [4], making them unstable on thermocycling and under temperature gradients. A deeper insight in this problem leads to chemical-induced expansion phenomena- a critical factor of the mechanical stability of the oxide ceramics under high oxygen chemical potential gradient [5, 6].

The given paper is a brief overview of the collaborative studies, mainly published in [7–15], and focused on the analysis of oxygen transport and physicochemical properties of one new group of mixed conductors based on lanthanum gallate with perovskite-type structure. Presented results were greatly contributed by F. M. B. Marques, J. R. Frade, F. M. Figueiredo, A. L. Shaula and their collaborators, from Department of Ceramic and Glass Engineering, (University of Aveiro, Portugal) and M. V. Patrakeev, E. B. Mitberg, A. A. Lakhtin, I. A. Leonidov, V. L. Kozhevnikov and their co-workers from Institute of Solid State Chemistry (Ural Division of RAS, Ekaterinburg, Russia).

* Current position-researcher in University of Aveiro, Portugal.

THERMODYNAMIC AND STRUCTURAL BACKGROUND OF OXYGEN PERMEABILITY

When a dense ceramic sample having mixed oxygen ionic and electronic conductivity is placed under an oxygen chemical potential difference, the interrelated fluxes of oxygen ions and electron charge carriers (electrons and/or holes) in the ceramics bulk will be induced. In a steady state, the sum of such fluxes represents the oxygen permeation flux through the membrane [16–19]:

$$j = \frac{1}{(4F)^2 d} \int_{\mu(O_2)_1}^{\mu(O_2)_2} \frac{\sigma_o \sigma_e}{\sigma_o + \sigma_e} d\,\mu(O_2) \qquad (1)$$

where j is the permeation flux density of molecular oxygen, d is the membrane thickness, and are the partial ionic and electronic conductivities, (O_2) is the oxygen chemical potential; $(O_2)_{1s}$ and $(O_2)_{2s}$ are the values of (O_2) in the ceramic surface layers at the membrane permeate side and feed side, respectively ($(O_2)_{2s} > (O_2)_{1s}$). Electronic conductivity of perovskite-type oxides exhibiting the highest permeation fluxes is typically predominant compared to ionic conductivity, while oxygen ionic conduction in the perovskites occurs via a vacancy mechanism [16–23]. Therefore, the permeation flux density through membrane bulk can be expressed as [16–19]:

$$j = \frac{1}{16F^2 d} \int_{\mu(O_2)_{1s}}^{\mu(O_2)_{2s}} \sigma_o d\,\mu(O_2) \qquad (2)$$

Taking in account that, in framework of Krцger-Vink formalism, oxygen vacancies should be treated as ion charge carriers

$$\sigma_O = u_O^{\cdot} [V_O^{\bullet\bullet}][O_O^x] = u_O^{\cdot} [V_O^{\bullet\bullet}]([O_\Sigma] - [V_O^{\bullet\bullet}]) \qquad (4)$$

where $u_o^{\cdot}$ is the mobility coefficient for oxygen ions, $[V_O^{\bullet\bullet}]$ and $[O_O^x]$ are the fractions of vacancies and ions in the oxygen sublattice, correspondingly, $[O_\Sigma]$ is the concentration of oxygen sites related to the A-site concentration (3 for perovskites):

$$j = \frac{u_o^{\cdot}}{16F^2 d} \int_{[V_O^{\bullet\bullet}]_{1s}}^{[V_O^{\bullet\bullet}]_{2s}} \left([V_O^{\bullet\bullet}]([O_\Sigma] - [V_O^{\bullet\bullet}]) \frac{\partial \mu(O_2)}{\partial [V_O^{\bullet\bullet}]} \right) d[V_O^{\bullet\bullet}] \qquad (5)$$

Here, the quantity $\frac{\partial \mu(O_2)}{\partial [V_o^{\bullet\bullet}]}$ may be derived from equilibrium between oxygen in the gas phase and point defects in the oxide. If assuming that the oxide phase is p-type conductor, which is typical for highly-conductive perovskites under oxidizing conditions, the equilibrium can be written as:

$$\mu(O_2) + 2\mu([V_O^{\bullet\bullet}]) = 4\mu(p) \qquad (6)$$

where $\mu(O_2)$ is the chemical potential of holes. Eq. 6 corresponds to the point defect equilibrium:

$$O_2 + 2V_O^{\bullet\bullet} \qquad 4p + 2O_O^x \tag{7}$$

As a rule, electronic transport in perovskites, where the B sublattice is dominantly occupied with Cr, Mn, Fe or Co, occurs via a polaron mechanism; in these cases p should be related to the **B**-site cations having 4+ oxidation state (*i.e.* $[B_B^{\bullet}]$), leading to the hole chemical potential

$$\mu(p) = \mu^o(p) + RT\ln\frac{[B_B^{\bullet}]}{[B_B^x]} \tag{8}$$

The oxygen-vacancy chemical potential is

$$\mu(V_o^{\bullet\bullet}) = \mu^o(V_o^{\bullet\bullet}) + RT\ln\frac{[V_o^{\bullet\bullet}]}{[O_o^x]} \tag{9}$$

Eq. 9 may be transformed to

$$RT\ln\rho(O_2) = \mu_\Sigma^0 - 2RT\ln\frac{[V_o^{\bullet\bullet}]}{[O_o^x]} + 4RT\ln\frac{[B_B^{\bullet}]}{[B_B^x]} \tag{10}$$

where μ_Σ^0 is the sum of basic chemical potentials related to the "oxide-gas" equilibrium constant:

$$K_{eq} = \exp\left(-\frac{\mu_\Sigma^0}{RT}\right) = \exp\left(-\frac{\Delta G_{eg}}{RT}\right) = \exp\left(-\frac{\Delta H_{eq} - T\Delta S_{eq}}{RT}\right) \tag{11}$$

In a simplest case, when no self-ionization in the **B**-sublattice is observed, $[B_B^{\bullet}]$ value may be derived from the electroneutrality condition:

$$2[V_o^{\bullet\bullet}] + [B_B^{\bullet}] = K_{ch} \tag{12}$$

where K_{ch} is the charge sum of all particles, not involved in the redox interactions. One should note that self-ionization may be ignored only in selected cases, including ferrites-gallates [24] or nickelates as Ni may exist only in 2+ and 3+ oxidation states. For cobaltites this phenomenon definitely can not be ignored [7,25].

$LaGaO_3$ has neither structure-predefined oxygen vacancies nor variable-valence cations, which could contribute to the electron charge carrier generation. Typically perovskite phases with low or zero oxygen-vacancy concentration possess very low ionic conductivity (Eq.4), even if the structure should support oxygen mobility. This may be illustrated by the examples of $LaCoO_3$ and $LaCo(M)O_3$ (M = Fe,Cr) solid solutions, where the ionic conductivity at relatively high $p(O_2)$ is

low (Fig 1, [7]) and the achievement of steady-state oxygen fluxes under an oxygen chemical potential gradient is associated with extremely slow transient processes (Fig. 2). The equilibration rate is essentially independent of $p(O_2)$ difference, suggesting that overall oxygen transport is limited by the ionic conductivity at the membrane feed side where the oxygen nonstoichiometry is negligible.

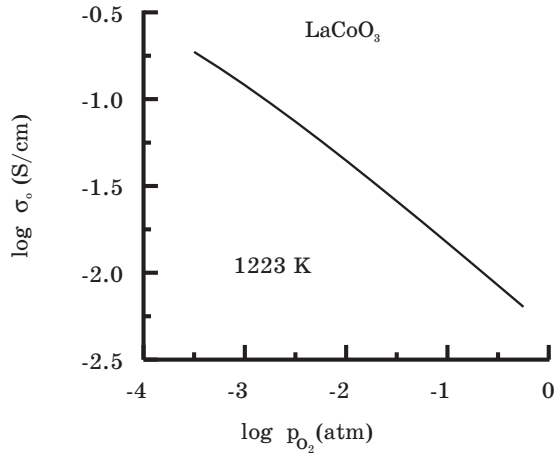

Fig. 1. Calculated oxygen ionic conductivity of $LaCoO_{3-\delta}$ vs. oxygen partial pressure [7]

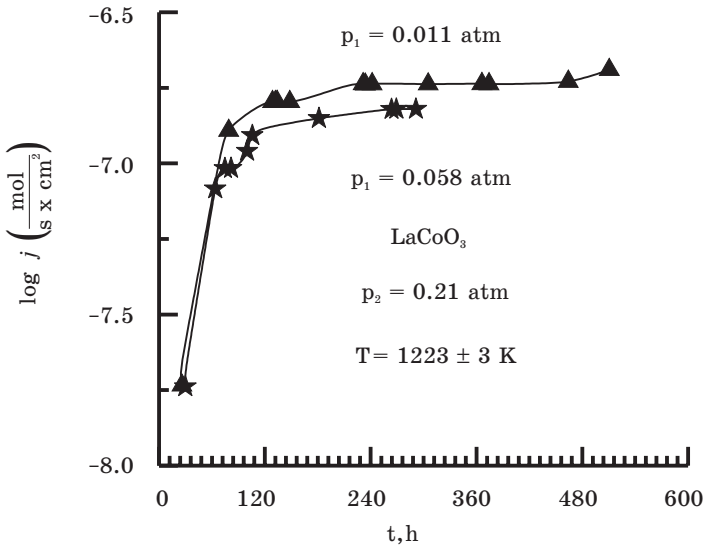

Fig. 2. Oxygen flux equilibration in $LaCoO_{3-\delta}$

Therefore, metal cations with oxidation state lower than 3+ should be introduced into **A** or **B** sublattice in order to increase K_{ch} value (Eq. 12). These cations should have an appropriate ionic radii to expand or, at least, to preserve size of the ion migration channels. Typical dopants include strontium as and magnesium as $Mg_B^{\cdot}$ [26]. To enhance electron conductivity, transition metals (e.g. Fe, Co or Ni) may be used. However, in oxidizing conditions these cations typically exist as M^{3+} or M^{4+} and cannot contribute to additional $V_o^{\bullet\bullet}$ formation. A compromise between stability, oxygen and electron conductivities should hence be achieved at moderate amounts of the transition metal dopants in the **B** sublattice; the concentrations of magnesium and strontium should be close to the corresponding solubility limits.

Experimental

The phases with perovskite structure, selected results on which are considered below, were prepared by a standard ceramic synthesis route using high-purity oxides, carbonates and nitrates of the corresponding metals as starting materials. Before weighing, lanthanum and gallium oxides were annealed at 1270–1300 K for 2 hours. The stoichiometric amounts of the precursors were dissolved in diluted nitric acid, dried and then thermally decomposed. The solid-state reaction was conducted in air at temperatures of 1370–1420 K for 10–15 hours with several intermediate grinding steps. X-ray diffraction (XRD) analysis of the prepared powder showed formation of single perovskite-type phases. After the synthesis, the powders were ball-milled. Gas-tight ceramic samples were pressed (300–400 MPa) in the shape of disks of various thickness (diameter 12 or 15 mm) and bars ($4 \times 4 \times 30$ mm^3), and then sintered in air at 1523–1700 K for 2–8 hours. The density of ceramics was higher than 90% of their theoretical density calculated from XRD data. This procedure was used for the preparation of most ceramic membranes studied in the present work.

Formation of single perovskite phases, their cation composition, and homogeneous cation distribution in the prepared materials were confirmed by XRD, emission spectroscopic analysis, and energy dispersive spectroscopy (EDS). Scanning electron microscopy (SEM) and dilatometry in controlled atmosphere were used to study ceramic microstructures and thermal expansion.

The measurements of steady-state oxygen permeation fluxes were based on the use of a stabilized zirconia solid-electrolyte cell comprising an oxygen pump and a sensor. Under steady-state conditions, the oxygen flux through the ceramics, hermetically sealed onto the measuring cell, should be equal to the flux through the electrochemical oxygen pump, while the oxygen chemical potential drop across the sample can be determined from the emf of the sensor. The reproducibility error of the permeation fluxes through different membrane samples at temperatures above 1000 K was less than 10%. At lower temperatures the reproducibility of oxygen fluxes becomes worse due to the disorder-order transitions in some phases and also owing to measurement problems associated with increasing electrode polarization in the cell. Similar cells with additional electrodes applied onto the sample surface were used to determine oxygen ionic conductivity by the faradaic efficiency technique. Unless otherwise specified, all data on oxygen permeability pre-

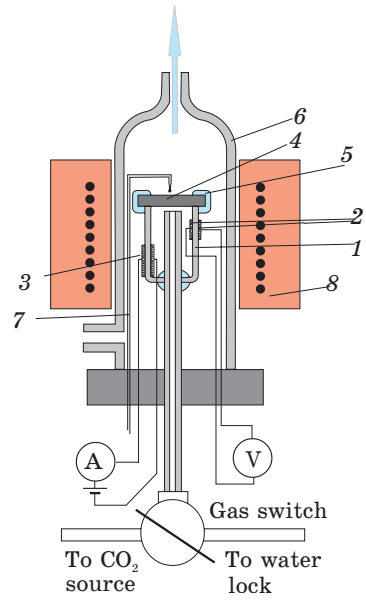

Fig. 3. Experimental cell design for the permeation measurements under high $p(O_2)$ gradients:
1 – yttria-stabilized zirconia solid electrolyte,
2 – oxygen sensor, *3* – oxygen pump, *4* – sample,
5 – sealing glass, *6* – quartz chamber,
7 – thermocouple, *8* – furnace

sented in this paper corresponds to the membrane feed-side oxygen partial pressure equal to 21 kPa (atmospheric air). The thickness of the ceramic membranes varied from 0.6 to 1.8 mm. Details on experimental procedures and equipment can be found in [7, 8, 27–31].

One special cell was designed to study oxygen fluxes through a membrane, permeating into a CO/CO_2 mixture (Fig. 3). These experiments included 3 steps. On the first step, the gas switch connects internal cell space to the water lock; the electrochemical pump is used to fill the cell with pure O_2 and to force out N_2. After achieving sensor emf values corresponding to pure oxygen inside the cell, the gas switch connects internal cell space with a CO_2 source; the pump current is reversed and carbon dioxide fills the cell. Then the switch locks internal space; the oxygen permeability measurements may be started. The values of Δ (O_2) can be calculated from the sensor emf using the only equilibrium $2CO + O_2 \rightleftarrows 2CO_2$.

RESULTS AND DISCUSSION

Doped lanthanum gallate is known as one of most conductive solid oxide electrolytes [26]. On the contrary to fluorite-type electrolytes, the substitution of gallium with transition metal cations leads to increasing electron conductivity without serious deteriorating effects for ionic transport. On the other hand, galla-

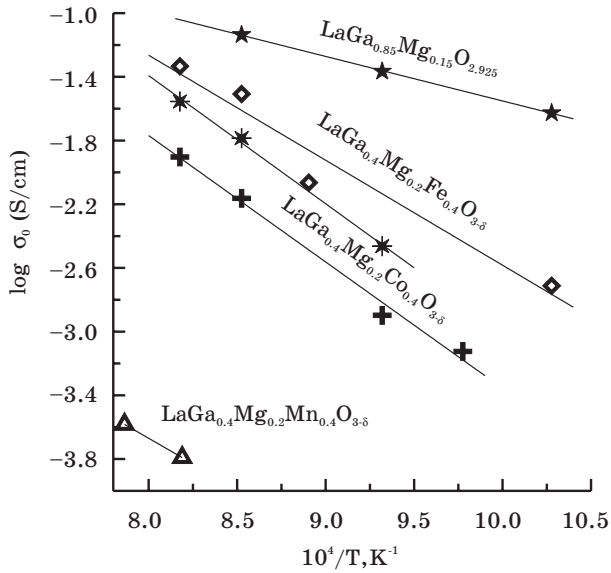

Fig. 4. Oxygen ionic conductivity of lanthanum gallate substituted with transition metal cations and magnesium in the **B**-subblatice. Detailed data presented in [12].

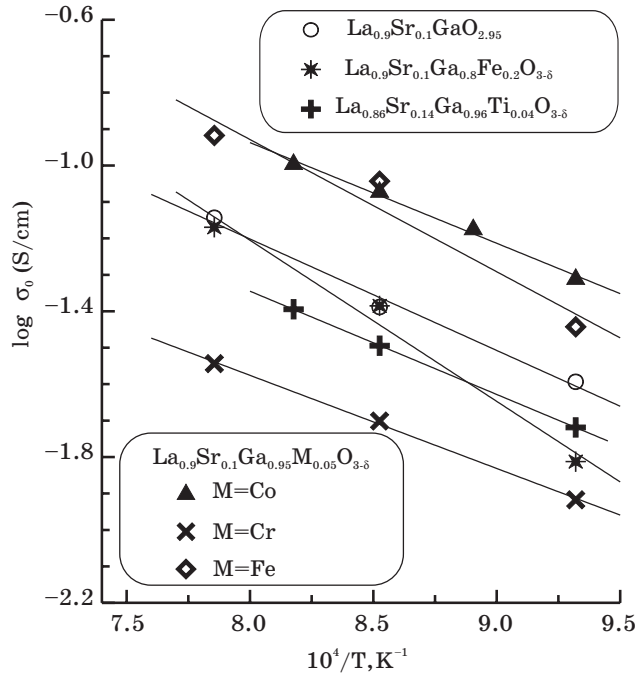

Fig. 5. Oxygen ionic conductivity of lanthanum-strontium gallate substituted with transition metal cations in the **B**-subblatice. Detailed data presented in [10]

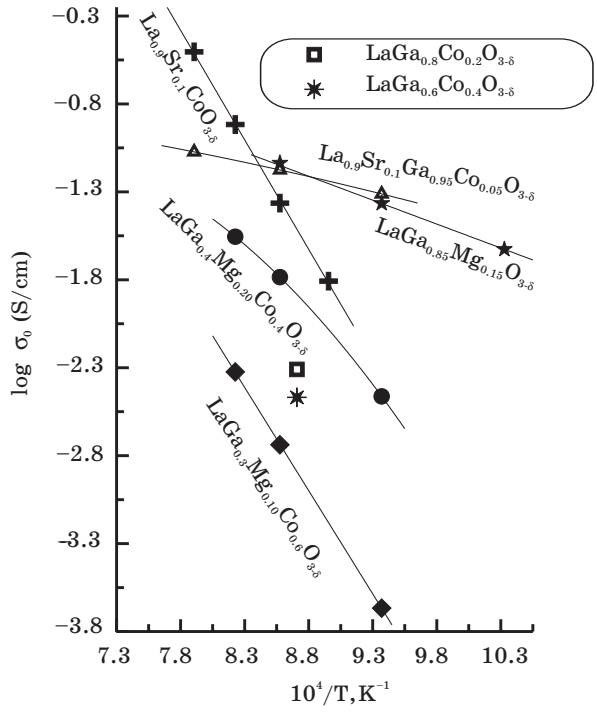

Fig. 6. Oxygen ionic conductivity of cobalt-substituted lanthanum gallates. The ionic conductivity of $La_{0.9}Sr_{0.1}CoO_{3-\delta}$ was calculated from literature data. Details presented in [10]

te-based phases are more stable with respect to reduction as compared to ferrites or cobaltites. Such features lead to a strong motivation to evaluate Ga-containing perovskites for the development of new oxygen-permeable materials operable under high oxygen chemical potential drops, like electrocatalytical methane reformers. Without considering structural stability of these perovskites, it is necessary to admit that only selected metal cations used as a basis in the **B** sublattice enable to achieve a high mobility of oxygen ions. This series includes Co, Fe, Ni and Ga. Titanium, incorporation of which may be useful in some cases [32], seems inappropriate for gallates due to dominant 4+ oxidation state, leading to reduction of the ionic conductivity. Similar situation is observed with niobium [8]. Another necessary comment is that these cations also do not provide sufficient concentration of electronic charge carriers to make the ceramics oxygen-permeable. Oxygen ionic conductivity of manganites and chromites is low [16,33], possibly due to limited oxygen-vacancy concentration and a tendency to increase covalence of the transition metal-oxygen bonds. These trends remain for the substituted lanthanum gallates (Figs. 4, 5 and 6).

Nickel-containing solid solutions are formed in a different concentration range, caused by Ni^{2+} formation. However, relatively high oxygen mobility may also be achieved (Fig. 7).

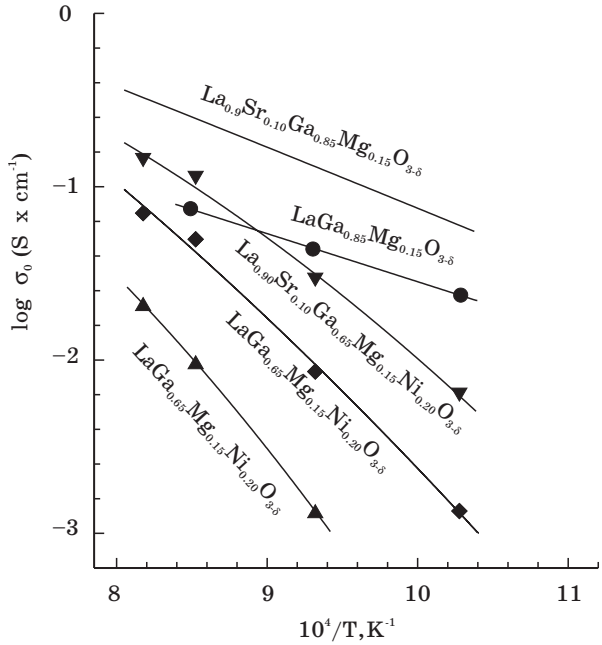

Fig. 7. Oxygen conductivity of the nickel-substituted lanthanum gallates. Detailed data presented in [13]

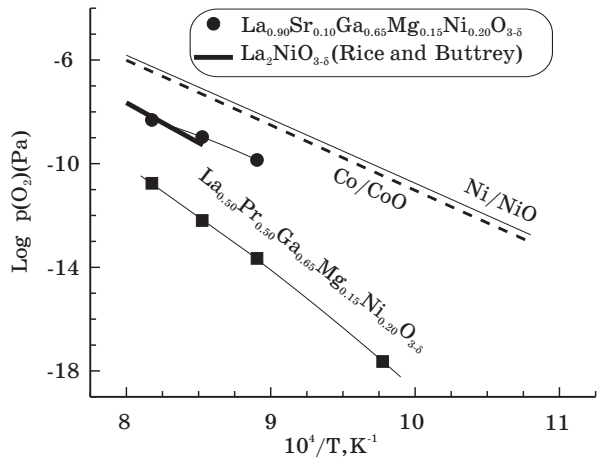

Fig. 8. Phase stability limits of Ni-containing ceramics, determined from the data on total conductivity and Seebeck coefficient. Literature data on binary metal oxides [36] and $La_2NiO_{4+\delta}$ [37] are shown for comparison. Detailed data presented in [11]

High ionic conductivity may be reached in Ni-substituted gallates by further doping with Sr in **A**- and Mg in the **B**-sublattices. Phase stability of $LaNiO_{3-\delta}$ to reducing may play a critical role [34]; special tests for nickel-containing gallates were thus carried out (Fig. 8, [35]).

The stability of $LaGa(Ni)O_3$ – based perovskites was found close to La_2NiO_4 and higher than pure NiO. Note that $La_{0.5}Pr_{0.5}Ga_{0.65}Mg_{0.15}Ni_{0.2}O_{3-\delta}$ is noticeably more stable in reducing atmospheres. Such an enhancement may be attributed to increasing oxygen content due to incorporation of praseodymium cations, keeping the oxidation state higher than 3+ and thus stabilizing the lattice. In the case of $La_{0.90}Sr_{0.10}Ga_{0.65}Mg_{0.15}Ni_{0.20}O_{3-\delta}$, critical to reduction nickel cations are expected to be mostly in 2+ state, forming oxygen-deficient Ni-O octahedra in the lattice; this state is similar to La_2NiO_4-based solid solutions, leading to similar phase existence domains.

The cobalt-substituted gallates have a lower oxygen mobility than nickel- and iron- containing phases. If comparing Co- and Ni- containing solid solutions, lower ionic conductivity of the Co-doped perovskites seems a result of stronger Co – O bonds with respect to Ni – O. Such a hypothesis might be verified if oxygen mobility data for $LaNiO_{3-\delta}$ would be accessible to compare with LaCoO3-d. However, the oxygen permeation fluxes for $LaCoO_{3-\delta}$ [38] are comparable with those of $La_2NiO_{4-\delta}$ [39]. Furthermore, the oxygen-vacancy diffusion coefficients in the perovskite-type compounds increase in the sequence Cr < Fe < Co [40, 41] which may imply that the next member of the series, Ni, has a higher diffusion coefficient. For gallates- cobaltites, the use of magnesium doping is not so fruitful as for gallates-nikelates. The positive oxygen vacancies, , are more likely tends to associate with cations with relatively lower oxidation level. Cobalt ions in perovskite lattices in air exists in three oxidation states (2+, 3+ and 4+); the 2+ and 4+ states can form either by disproportionation of Co^{3+} or charge compensation as a result of aliovalent substitution [41–43]. The **B**-subblatice in Co-substituted gallates is more oxidized in comparison with nickel-containing phases due to a limited amo-

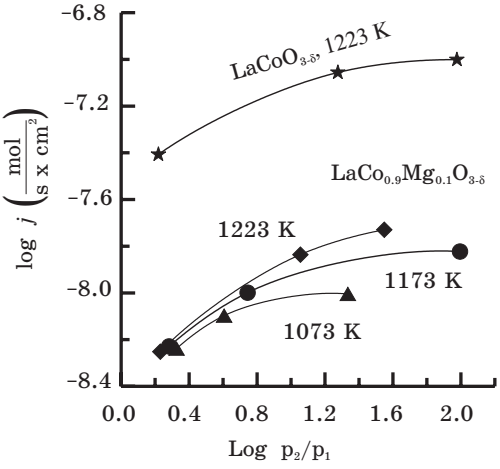

Fig. 9. Effect of magnesium doping on the oxygen permeation flux through cobaltite membranes

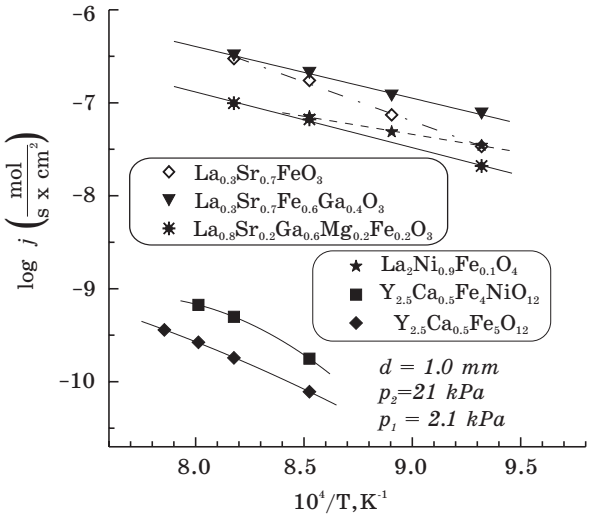

Fig. 10. Comparison of the oxygen permeation fluxes through perovskite and perovskite-related membranes

unt of Ni^{3+} existing in the latter group, compared to Co^{4+} for the former. Thus, increasing by magnesium doping may not lead to increasing mobile vacancy concentration. Such a situation is observed for $LaCo_{0.9}Mg_{0.1}O_{3-\delta}$ solid solution (Fig. 9, [44]) and may be extrapolated to other cobalt-containing perovskites.

On the other hand, bivalent Mg has a stable oxidation state; stabilization of Co^{4+}- O – Mg^{2+} clusters becomes preferable and the oxygen anions neighboring of the Co^{4+} is then less mobile. Moreover, Co^{2+} ions occupying a B-site may act as centers for oxygen-vacancy clustering which, in high enough concentration, may take the form of ordered microdomains. Evidence for this comes from $p(O_2)$-T-δ diagrams of $(La,Sr)CoO_{3-\delta}$, in which certain features are attributable to partial ordering of oxygen vacancies in microdomains at large values of δ and up to temperatures as high as 1170 K [44].

The substituted gallates containing moderate amounts of dopant cations in the B sites hence seem to be most promising materials for the membranes due to their high permeability (Fig. 10) and chemical expansion values (Fig 11).

The latter trend means that the stresses induced in gallate-based membranes under operation conditions should be much lower compared to ferrites-based materials.

The properties of gallium-containing perovskites, suitable with respect to other permeable phases, may be explained as resulting from three main factors:

1. Gallium in perovskite lattice supports a high oxygen mobility

2. Gallium do not change its oxidation state. This means that a significant part of **B**-site cations do not changes their ionic radii if the oxygen chemical potential changes; gallium incorporation in the B sites therefore suppresses chemical-induced expansion (Figs. 12, 13).

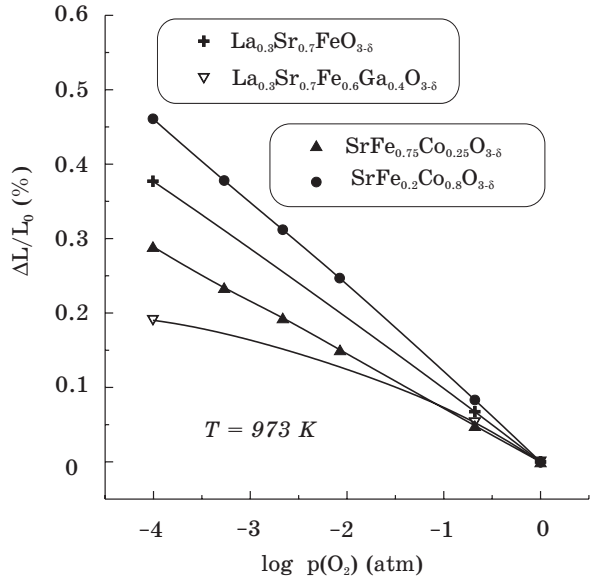

Fig. 11. Chemically-induced expansion of some highly-permeable perovskites. Data for $Sr(Fe,Co)O_{3-\delta}$ solid solution from [6]. Detailed data presented in [15].

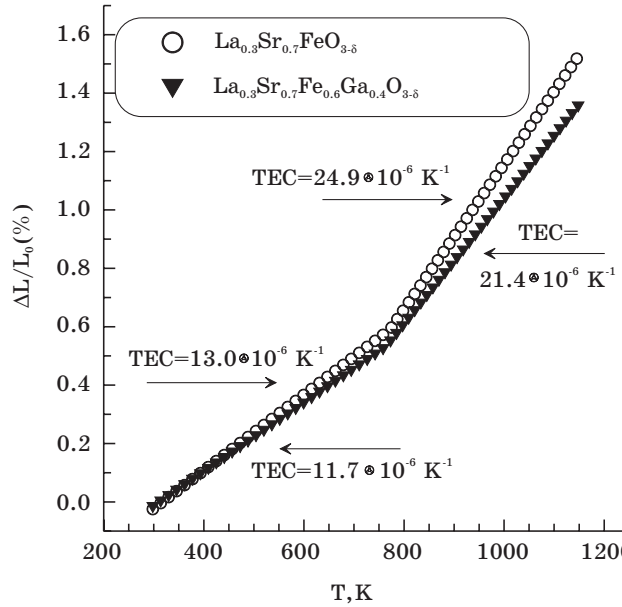

Fig. 12. The effect of Ga doping on thermal expansion [15]

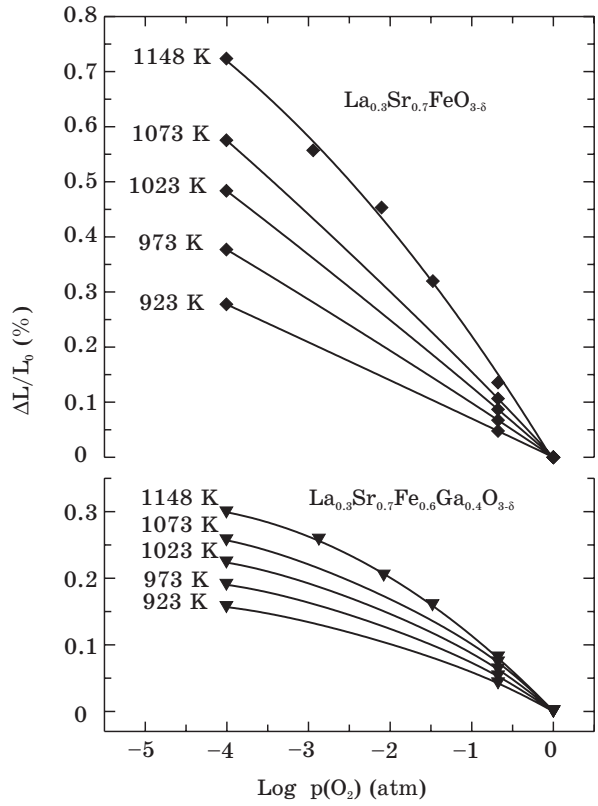

Fig. 13. The effect of Ga doping on thermal and chemically-induced expansion [15]

3. Having an average oxidation state, Ga_B^x provides rather minor contribution to the point defect association and ordering. As a rule, the ordering and defect association processes lead to suppression of the oxygen ion mobility, in particular on the permeate side of membranes [5]. Perovskites with iron in the **B**-sublattice and alkaline-earth metal cations in the **A**-sublattice show a significant tendency to ordering of various types. The substitution of iron by gallium may prevent such association, thus leading to increasing oxygen mobility (Fig. 14). As expected, this doping becomes more effective at lower temperatures.

Additional support for these conclusions was obtained when measuring oxygen permeation fluxes through $LaGa_{0.65}Mg_{0.15}Ni_{0.2}O_{3-\delta}$ membrane, one side of which was exposed to CO/CO_2 mixture (Fig. 15).

Neither chemical reduction of the permeate surface nor failure of the ceramic membranes were observed during 100–150 h under various conditions, including cycling of (O_2) and temperature. Notice than under air/CO-CO_2 gradient the permeation processes are limited by the carbon monoxide oxidation on the membrane permeate side, which tends to become a limiting stage of the overall oxygen transport. This surface should be activated with Pt layer; otherwise no steady-state

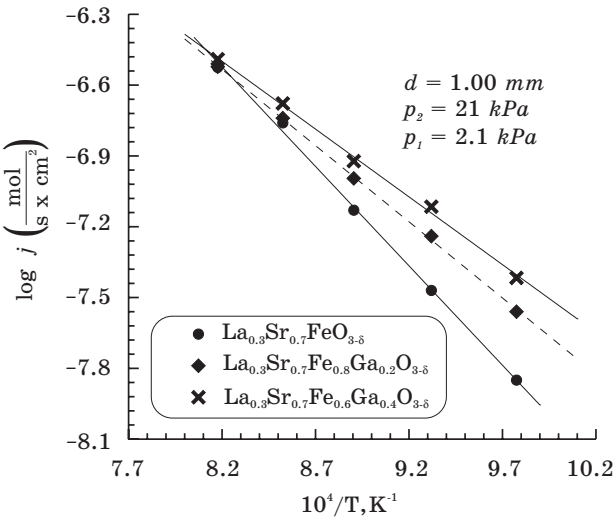

Fig. 14. The effect of Ga doping on the oxygen permeability of $Sr(La)FeO_{3-\delta}$ perovskites. Detailed data presented in [14]

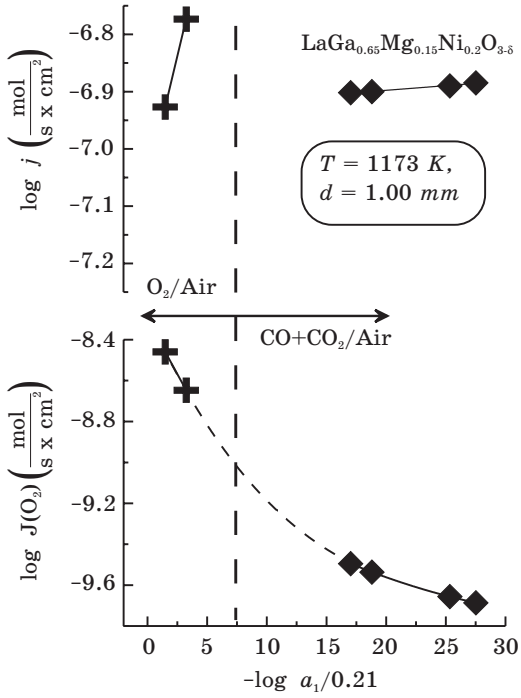

Fig. 15. Oxygen permeability under high oxygen chemical potential drop

flux can be reached. Even for the surface-activated membranes, the fluxes are comparable to those obtained in oxidizing conditions.

In summary, mixed conductors based on $LaGaO_3$ are promising materials for the electrochemical membranes. The combination of appropriate transport and mechanical properties, and a sufficiently high thermodynamic stability enables to expect that these phases may be used for the partial oxidation of light hydrocarbons.

ACKNOWLEDGEMENTS

Experimental data presented in this brief review were obtained, to a great extent, in framework of international collaboration between the Research Institute For Physical Chemical Problems (BSU, Minsk, Belarus), the Department of Ceramics and Glass Engineering (University of Aveiro, Aveiro, Portugal), and the Institute of Solid State Chemistry (Ural Division of RAS, Ekaterinburg, Russia). In Belarus this work was partially supported by the Belarus Foundation for Basic Research, the Belarussian State University, the INTAS (grant 2000-0276), and the NATO Science for Peace program (project 978002).

REFERENCES

1. *Teraoka Y., Zang H. M., Furukawa S., Yamazoe N.* Chem. Lett, Vol. 11 (1985), P. 1743.
2. *Bray D. T., Merten U.* J.Electrochem. Soc. Vol. 111 (1964), 447.
3. *Burke L. D., Rickert H., Steiner R. Z.* Phys. Chem. N. F. 1971. Vol. 74, P. 146.
4. *Kharton V. V., Tikhonovich V. N., Li Shuangbao, Naumovich E. N., Kovalevsky A. V., Viskup A. P., Bashmakov I. A.* and *Yaremchenko A. A.* J.Electrochem. Soc., 1998, Vol. 145, P. 1363.
5. *Balachandran U., Dusec J. T., Sweeney S. M., Poeppel R. B., Mieville R. L., Maiya P. S., Kleefisch M. S., Pei Sh., Kobylinski Th. P., Udovich C. A. and Bose A. C.* American Ceramic Society Bulletin, 1995. Vol. 24-1. P. 71.
6. Vashook V. V. Dr.Sci thesis, Minsk, 2000, 310 p.
7. *Kharton V. V., Naumovich E. N., Kovalevsky A. V., Viskup A. P., Figueiredo F. M., Bashmakov I. A. and Marques F. M. B.* Solid State Ionics, 2000, Vol. 138, P. 135.
8. *Kharton V. V., Viskup A.P., Naumovich E. N. and Marques F. M. B.* J. Mater. Chem., 1999, Vol. 9, P. 2623.
9. *KhartonV.V., Viskup A. P., Mather G. C., Yaremchenko A. A., Naumovich E. N. and Marques F. M. B.* Boletin de la Sociedad Espanola de Ceramica y Vidrio, 1999, Vol. 38, P. 647.
10. *Kharton V. V., Viskup A. P., Yaremchenko A. A., Baker R. T., Gharbage B., Mather G. C., Figueiredo F. M., Naumovich E. N. and Marques F. M. B.* Solid State Ionics 2000, Vol. 132, P. 119.
11. *Kharton V. V., Yaremchenko A. A., Shaula A. L., Patrakeev M. V., Naumovich E. N., Logvinovich D. I., Frade J. R. and Marques F. M. B.* Transport properties and stability of ni-containing mixed conductors with perovskite- and K_2NiF_4-type structure, J.Solid State Chem., *in press.*
12. *Kharton V. V., Yaremchenko A. A., Viskup A. P., Mather G. C., Naumovich E. N. and Marques F. M. B.* Journal of Electroceramics 2001, Vol. 7, P. 57.
13. *Yaremchenko A. A., Shaula A. L., Logvinovich D. I., Kharton V. V., Kovalevsky A. V., Naumovich E. N., Frade J. R. and Marques F. M. B.* oxygen ionic conductivity of perovskite-type $La_{1-x}Sr_xGa_{1-y}Mg_yM_{0.20}O_{3-\delta}$ (M = Fe, Co, Ni), Materials Chemistry and Physics, *in press.*

14. *Kharton V. V., Shaulo A. L., Viskup A. P., Avdeev M. Yu., Yaremchenko A. A., Patrakeev M. V., Kurbakov A. I., Casanova J. R., Naumovich E. N. and Marques F.M.B.* Solid State Ionics, 2002, Vol. 150, P. 229.
15. *Kharton V. V., Yaremchenko A. A., Patrakeev M. V., Naumovich E. N., Marques F. M. B.* Journal of the European Ceramic Society, 2003, Vol. 23, P. 1417.
16. *Bouwmeester H. J. M. and Burgraaf A. J.* Dense ceramic membranes for oxygen separation, in A.J.Burgraaf and L.Cot (Eds.), Fundamentals of Inorganic Membrane Science and Technology, Elsevier, Amsterdam-Lausanne-New York-Oxford-Shannon-Tokyo, 1996, P. 435–528.
17. *Kharton V. V., Naumovich E. N. and Nikolaev A. V.* J.Membrane Sci., 1996, Vol. 111, P. 149.
18. *Mazanec T.J., Cable T. L., Frye J. G. and Kliewer W. R.* U.S.Patent 5, 591, 315, 1997.
19. *Steele B. C. H.* Mat.Sci.Eng.B, 1992, Vol. 13, P. 79.
20. *Mazanec T. J.* Prospects for ceramic chemical reactors in industry, Solid State Ionics, 1994, Vol. 70/71, P. 11.
21. *Carter S., Selcuk A., Chater R. J., Kajda J., Kilner J. A. and Steele B. C. H.* Solid State Ionics, 1992, Vol. 53–56, P. 597.
22. *Thorogood R. M., Srinivasan R., Yu T. F. and Drake M. P.* Composite mixed conductor membranes for producing oxygen, U.S.Patent 5,240,480, 1993.
23. *Kharton V. V., Zhuk P. P., Demin A. K., Nikolaev A. V., Tonoyan A. A. and Vecher A. A.* Inorganic Materials, 1992, Vol. 28, P. 1406.
24. *Patrakeev M. V., Mitberg E. B., Lakhtin A. A., Leonidov I. A., Kozhevnikov V. L., Kharton V. V., Avdeev M., Marques F. M. B.* Journal of Materials Chemistry, 2001, Vol. 11, P. 1202.
25. *Lankhorst M. H. R., Bouwmeester H. J. M.* J.Electrochem. Soc., 1997, Vol. 144-4, P. 1268.
26. *Huang K., Tichy R. S. and Goodenough J. B.* J.Am.Ceram. Soc., 1998, 81-10, Vol. 1998, P. 2565.
27. *Kharton V. V., Naumovich E. N. and Nikolaev A. V.* J. Membrane Sci., 1996, Vol. 111, P. 149.
28. *Kharton V. V., Yaremchenko A. A., Kovalevsky A. V., Viskup A. P., Naumovich E. N. and Kerko P. F.* J. Membrane Sci., 1999, Vol. 163, P. 307.
29. *Kharton V. V., Naumovich E. N., Vecher A. A. and Nikolaev A. V.* J.Solid State Chem., 1995, Vol. 120, P. 128.
30. *Kharton V. V., Naumovich E. N., Nikolaev A. V., Astashko V. V. and Vecher A. A.* Russ. J. Electrochem., 29 (1993), 1039.
31. *Kharton V. V., Viskup A. P., Yaremchenko A. A., Kerko P. F., Naumovich E. N. and Kovalevsky A. V.* Materials Research Bulletin, 1999, Vol. 34, P. 1921.
32. V.V.Kharton, Li Shuangbao, A.V.Kovalevsky, A.P.Viskup, E.N.Naumovich and A.A.Tonoyan, Materials Chemistry and Physics, 1998, Vol. 53, P. 6.
33. *Naumovich E. N., Kharton V. V., Vecher A. A., Nikolaev A. V. and Abugoffa A. A.* Proc. Int. Symp. SOFC- IV Ed. M.Dokiya, H.Tagawa, O.Yamamoto and S.C.Singhal Yokohama, Japan, June 18-23, 1995, P. 520–527.
34. *Palguev S. F., Gilderman V. K., Zemtsov V. I.* High temperature oxide electronic conductors for the electrochemical devices, Moscow: Nauka, 1990, 197 p.
35. *Chebotin V. N. and Perfilyev M. F.* Electrochemistry of Solid Electrolytes, Khimiya, Moscow, 1978.
36. *Rice D. E., and Buttrey D. J. J.* Solid State Chem. 105 (1993), 197.
37. *Rickert H.* Electrochemistry of Solids, Springer-Verlag, Berlin-Heidelberg- N.Y., 1982.
38. *Thorogood R. M., Srinivasan R., Yu T. F. and Drake M. P.* U.S.Patent 5,240,480 (1993).
39. *Kovalevsky A. V., Kharton V. V. and Naumovich E. N.* Inorganic Materials, 32 (1996) 1230.
40. *Steele B. C. H.* Solid State Ionics, 1995, Vol. 75, P. 157.
41. *Van Hassel B. A., Kawada T., Sakai N., Yokokawa H., Dokiya M. and Bouwmeester H. J. M.* Solid State Ionics, 1993, Vol. 66, P. 295.
42. *Trofimenko N. and Ullmann H.* Solid State Ionics, 1999, Vol. 124, P. 263.
43. *Yaremchenko A. A., Kharton V. V., Viskup A. P., Kovalevsky A. V., Naumovich E. N. and Vecher A. A.* Vestnik BGU (Letters of Belarus State University), seriya 2001, Vol. 21, P. 20.
44. *Lankhorst M. H. R.* PhD Thesis, University of Twente, Enschede, The Netherlands (1997).

CHEMICAL PROBLEMS OF THE DEVELOPMENT OF NEW MATERIALS AND TECHNOLOGIES
Minsk 2003

**F. N. Kaputskii, E. V. Gert, V. I. Torgashov,
M. V. Shishonok, O. V. Zubets**

MULTIFUNCTIONALITY OF NITROGEN OXIDE COMPOUNDS AS A BASIS FOR PREPARATION OF PRACTICALLY IMPORTANT CELLULOSE MATERIALS

In the Laboratory of Physical Chemistry and Modification of Cellulose, over many years, a multitude of physical and chemical transformations of cellulose (Cel) under the action of nitrogen oxide compounds (N_2O_4, NO_2, N_2O_3, HNO_3) was studied, including determination of conditions for stimulating each type of reaction; namely, oxidation, nitrosation, nitration, hydrolytic cleavage or adduct formation. About 100 of our publications are summarized in a review [1] covering mainly fundamental aspects of this area. The amount of information accumulated thus far allowed rational approaches to be outlined concerning preparation of a number of practically important materials using nitrogen oxide compounds. Owing to multifunctionality of the latter with respect to Cel, it is often possible to do with a single reagent for a simultaneous or sequential performing several operations of chemical or structural modification of Cel. In preparation of carboxylated microcrystalline Cel, for example, using gaseous nitrogen oxide(IV) enables oxidation and hydrolytic dispersion of Cel to be performed, as well as enhancement of stability and whiteness of the final product.

Not only chemical and structural modification of Cel with nitrogen oxide compounds is of practical significance, but also participation of the latter in the process of preparation of Cel itself. High solubility of nitrates, which are mineral components of vegetal tissues, along with high reactivity of HNO_3 with respect to lignin, provides the opportunity of selective extraction of radionuclides in the course of nitric acid delignification of contaminated straw of annual plants and preparation of radionuclide-free Cel and nitrolignin. These results contribute to the development of a prospective technology for rehabilitation and deactivation of radionuclide-polluted territories. The proposed version of utilization of radionuclide-contaminated straw of technical agrocultures has won support from international scientific community.

In this review, examples are discussed of efficient use of nitrogen oxide compounds for the preparation of such practically important materials as completely or partially substituted Cel acetates soluble in organic solvents, water-soluble polysaccharide sulphates of low degree of substitution, powder forms of Cel hydrate and carboxylated Cel in structurally disordered or microcrystalline form, as well as for isolation of radiation-free Cel and nitrolignin from radionuclide-contaminated agricultural residues.

1. NITROSATION OF CELLULOSE AND OTHER POLYSACCHARIDES AS A METHOD OF «CHEMICAL ACTIVATION» FOR PREPARATION OF ACETO- AND SULPHOESTERS

Partial nitrosation of Cel in acetic acid (AA) may be of practical interest as an effective preactivation method in the preparation of cellulose acetates [2, 3]. The high reactivity of cellulose nitrite in the homogeneous transesterification reactions with acetylating agents is known [4]. This property of Cel nitrite is clearly manifested under usual acetylation conditions as well, when the reaction starts under heterogeneous conditions and ends up by a complete dissolution of the final product in the acetylating mixture (reaction up to a «clear field»).

The proposed activation procedure reduces to brief treatment of Cel with a solution of N_2O_4 in glacial AA and subsequent displacement of the free nitrogen oxides from the fibre by the same acid. The traditional industrial schemes for the activation of Cel are also based on the treatment of the fibre with AA. In Table 1, comparative data are given on Cel acetylation after activation using the conventional and the proposed methods. The activating mixture AA–N_2O_4 of composition 80:20 provides an extremely rapid conversion of Cel into the corresponding acetate with a virtually complete degree of substitution (DS). In this mixture, formation of an adduct of Cel trinitrite with AA takes place [1] and, as a result of this, very extensive swelling of the fibre occurs that complicates removal of free nitrogen oxides from it in the final stage of activation.

Table 1

Results of acetylation by the methylene chloride method of cotton Cel activated at 20 °C with AA or the N_2O_4–AA mixture

Activation conditions	Reaction time until attainment of a «clear field»/min	DS of Cel acetate	DP of Cel acetate
Initial Cel – native			
1 h, 80 % AA	180	2.85	740
20 min, N_2O_4–AA mixture (20:80)	7	2.86	400
5 min, N_2O_4–AA mixture (5:95)	30	2.92	650
Initial Cel – mercerized			
1 h, 80 % AA	180 (no homogenization)	1.62	
5 min, N_2O_4–AA mixture (5:95)	50	2.90	

Note: Acetylating mixture: acetic anhydride-acetic acid-methylene chloride (30:10:60 vol. %), catalyst – perchloric acid (~1 % of mass of C), liquor ratio 10 ml g^{-1}, temperature 26 °C.

The addition of small amounts of N_2O_4 (5 vol. %) does not induce excessive swelling of the fibre, so that the activation process occurs simply and rapidly, enabling nevertheless an appreciable increase in reactivity and higher DP of the final product to be achieved. After such activation, even mercerized cellulose that is well-known by its low reactivity in acetylation, is acetylated almost completely.

The proposed method of Cel activation provides a smooth and uniform reaction process, owing to which carrying out the reaction in acetone up to the «clear field» point makes it possible to obtain partially substituted Cel acetates (DS = 2,12 – 2,26; DP = 420–590), soluble in acetone, dioxane, DMF, AA and other solvents [3]. The properties of these products are similar to those of the secondary Cel acetates obtained via a two-stage scheme: complete acetylation of Cel – partial homogeneous hydrolysis. The known methods for the direct synthesis of such materials [5] are based on the acetylation of Cel in the presence of large amounts of H_2SO_4 (15 % – 25 % of the mass of Cel) and on the reaction being carried out in dioxane. While being more complex, these methods are based on the same principle of 'chemical activation'– by sulphate formation in this case. The mixed esterification of Cel leads to homogenization of the reaction mixture in early stages of the reaction and to uniformity of the substitution by acetyl groups that provides solubility in organic solvents of partially substituted Cel acetate. In order to isolate C acetate in a pure form and impart thermal stability to it, a special operation involving the saponification of the sulphate ester groups is carried out [5]. Preparation of similar materials based on partially nitrosated Cel is performed using the conventional acetylating mixture and does not require any additional stabilization procedures.

Biological activity is the property of not only expensive and difficult-to-isolate polysaccharide derivatives (heparin, chondroitin sulphate, etc.), but also of the sulphates of readily available polysaccharides (Cel, dextran, mannan, chitosan) [6]. An efficient procedure for a uniform conversion of polysaccharides into sulphates is the homogeneous transesterification of the respective nitrites using SO_3 in the DMF-N_2O_4 system [4]. As an alternative to the highly toxic and corrosive SO_3 in preparing sulphate esters, we have proposed [7–9] using its «stored» forms – salts of acids $H_2S_nO_{2n+1}$ (n = 1, 2) or $H_2S_nO_{3n+1}$ (n = 1–3) that generate SO_3 when acted upon by the reaction medium. Along with the system homogenization due to formation of the nitrosoester, the presence of N_2O_4 ensures sulpating activity of the potential SO_3 source.

Reactants stimulating sulphate formation can act as oxidants, or can participate in exchange processes, or can combine the oxidizing and exchange functions, depending on the type of sulphur-containing compound employed. The first role is assumed when SO_2 is converted into the sulphating complex of SO_3 with the solvent [10]. The role of N_2O_4 is not confined to only nitrosation of the polysaccharide and generation of SO_3. The equilibrium DS with respect to sulpho-groups depends on the N_2O_4/SO_3 ratio, decreasing as the latter grows.

Thus, apart from the known instability of the sulphate esters in acid media, account must be taken also of the desulphating activity of N_2O_4, i.e. the existence in the reaction systems of equilibrium between the sulphate and nitrite ester substituents in the polysaccharide:

$$R\text{–}OH + N_2O_4 \rightleftharpoons R\text{–}ONO + HNO_3$$

$$R\text{–}ONO + HNO_3 + SO_3 \longrightarrow R\text{–}OSO_3H + N_2O_4 \qquad (1)$$

When salts of $H_2S_nO_{3n+1}$ are used as a source of sulphur, the reactive sulphating agent is generated *in situ* as a result of exchange reactions involving HNO_3 and N_2O_4.

$$Na_2SO_4 + 2HNO_3 \underset{}{\overset{}{\rightleftharpoons}} H_2SO_4 + 2NaNO_3 \xrightarrow{N_2O_4} SO_3 + HNO_2 + HNO_3\ (NOSO_3OH + HNO_3) - 2HNO_3$$

$$2NOSO_3OH \xrightarrow{DMF} N_2O_3 + H_2S_2O_7 \bullet DMF; \qquad (2)$$

$$H_2S_2O_7 \rightleftharpoons H_2SO_4 + SO_3$$

The SO_3 evolved from the salts shifts the equilibrium (1) towards the formation of sulphate ester. Owing to homogeneity and equilibrated nature of the process, the displacement of nitrite by sulphate ester groups takes place uniformly. The Cel sulphates being obtained are completely soluble in water even at DS 0.2, which cannot be realized with any other known sulphate formation process.

A mixed type of activating influence of N_2O_4 and HNO_3 is manifested with respect to salts of acids $H_2S_nO_{2n+1}$:

$$Na_2SO_3 + 2HNO_3 \rightleftharpoons 2NaNO_3 + H_2SO_3 \xrightarrow{HNO_3\ (N_2O_4)} H_2SO_4 + HNO_2\ (N_2O_3) \qquad (3)$$

It follows from equations (2) and (3) that in the case of using salts with tetravalent sulphur both exchange and oxidation reactions take place. The latter lead to heating of the system and to acceleration of the reaction. Salts with hexavalent sulphur are preferable because the equilibrium is established slowly and without heating in this case, thus creating mild conditions for the synthesis, which prevent degradative transformations of macromolecules. The overall synthesis time is reduced as a result of combination of stages involving dissolution of the starting material and its conversion into sulphate on simultaneous introduction of the polymer and the salt into the DMF-N_2O_4 mixture. At the appropriate DS, the mannan and dextran sulphates synthesized in this way exhibit a distinct anticoagulant activity while being non-toxic even when applied in large doses (2–5 g kg^{-1}) [11].

The studies outlined above resulted in the development of an anti-aterosclerotic drug on the basis of mannan sulphate, which is now marketed under the name «Ronasan».

2. THE KNECHT COMPOUND AS AN ALTERNATIVE TO ALKALINE CELLULOSE FOR PREPARATION OF STRUCTURALLY AND CHEMICALLY MODIFIED POWDER FORMS OF CELLULOSE

Practical importance of Cel mercerization phenomenon based on intracrystallite swelling in alkali hydroxide solutions is well-known. The intracrystallite swelling of native Cel can also be caused by HNO_3 at concentrations close to 68.4 %, the value corresponding to azeotrope composition [12]. As a result of the swelling, crystalline phase of an additive compound, the Knecht compound (KC), is formed. Although this compound has been known for a long time [13, 14], its features remain yet obscure under many aspects [1].

On the basis of the X-ray diffraction data obtained by Andress [14], in combination with the current concepts concerning formation of Cel adducts [15], the crystalline phase of KC can be regarded as a result of insertion and stoichiometric 'fixation' of HNO_3 between the least interlinked (101) planes of the three-dimensional lattice of Cel (Fig. 1). The movement of these planes apart from one another along the large ac diagonal on the cell projection is accompanied by a decrease in the angle β, without affecting significantly the $(10\bar{1})$ and (002) planes. The (101) reflection on the X-ray diffraction pattern of the new phase is displaced towards smaller diffraction angles. According to Gess [16], KC is an oxonium-like compound by its nature, being a product of addition of HNO_3 to the oxygen of the glucoside group of Cel. Under the action of water, the polymorph Cel II is regenerated from KC, and this fact, being similar to behaviour of the alkaline Cel, allows the whole procedure to be considered as an acid version of 'mercerization' [17, 18].

The HNO_3 ability to form the Knecht additive compound with C becomes clearly apparent at the concentration of 68 % [19]. This tendency increases with increasing concentration of HNO_3. At the same time, an active accumulation of the HNO_3 pseudo form ($HO–NO_2$), which provokes nitration of Cel [20], starts from the concentration of ~ 69 % on. Hence, the stimulation of phase transformation by increasing the HNO_3 solution concentration is complicated by nitrating ability of the acid at concentrations above 69 %.

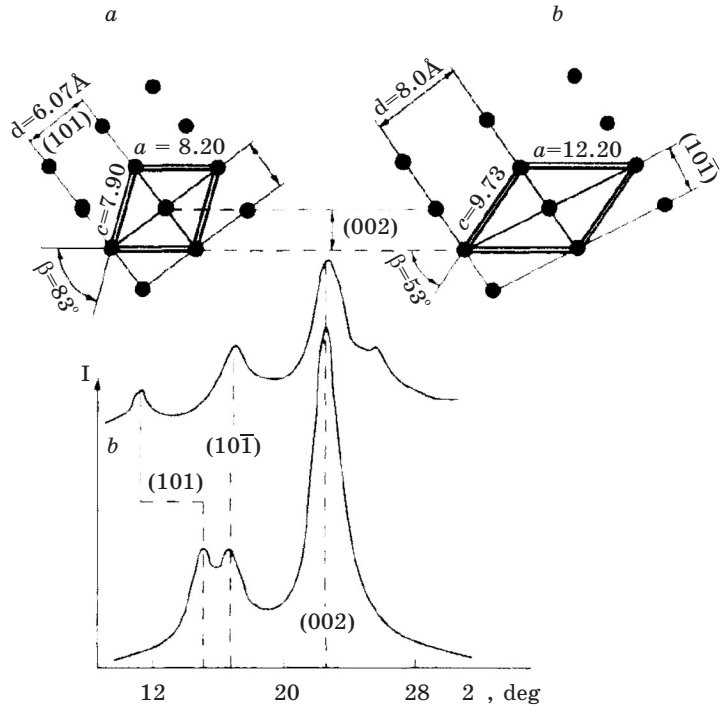

Fig. 1. Schematic illustration of the transformation of Cel-I unit cell (*a*) into KC unit cell (*b*) and the corresponding changes in the diffractogram

Lower temperatures are known to favour the process of traditional mercerization of Cel. This is usually explained by differences in temperature coefficients for the formation reaction rate and hydrolysis rate of alkaline Cel (the latter value is greater) [20]. The experimental results obtained in our studies give evidence of a peculiar effect of temperature on nitric acid «mercerization» process occuring in Cel of different origin and morphology [17, 18]. When cotton Cel (cotton Cel) is taken as starting material, the temperature dependence is similar to that observed for traditional mercerization, i.e. temperature decrease from 20 °C to 0 °C stimulates the polymorphic transformation (Fig. 2). However, a complete transformation of the starting material into the polymorph-II is not reached under these conditions. As compared to the initial cotton Cel, phase transformations are substantially slower in cotton microcrystalline Cel (cotton MCCel).

The above conditions of interaction with HNO_3 being applied to wood sulphite Cel (WCel) cause its complete and relatively rapid transformation into the polymorph-II. Unlike cotton Cel, this process occurs more rapidly at 20 °C, not at 0 °C. The anomalous character of temperature dependence is more pronounced in samples with a conventional (amorpho-crystalline) morphology (Fig. 2*a*). Wood microcrystalline Cel (WMCCel), unlike cotton MCCel, is «mercerized» at an unexpectedly high and almost temperature-independent rate, up to a conversion degree of ~ 60 %. (Fig. 2*b*). It is at the final stage only that a somewhat slower polymorphic transformation is observed at 0 °C as compared with that at 20 °C. The highest activity of sulphite WCel was noted in the traditional mercerization with NaOH solutions too, while cotton Cel and Ramie Cel were categorized among the least active [21].

It is obvious that the true dependence of the permutoid (according to Mark) reaction rate on temperature is reflected in experiments with cotton Cel, whose degree of chemical purity is superior to that of technical grade WCCel of any production methodology. The following Cel contents are found in its raw materials: up to 98 % in cotton seed fluff, and no more than 55 % in wood tissue. The destructive

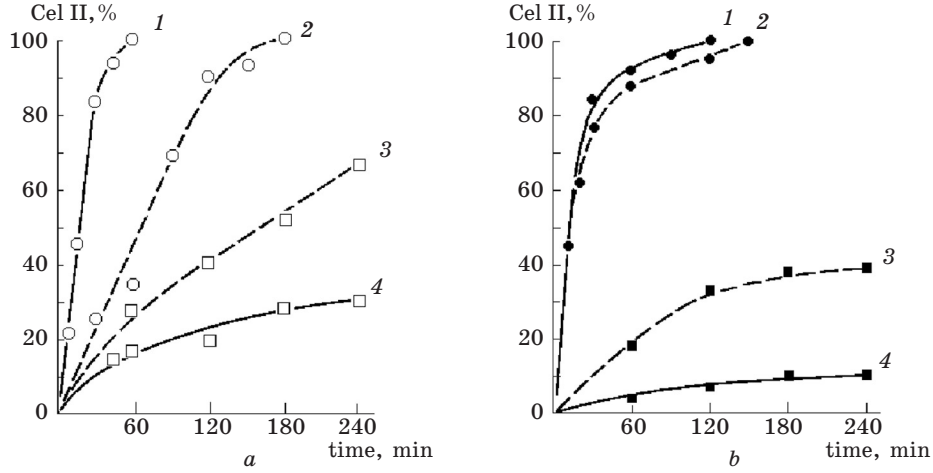

Fig. 2. Degree of transformation into polymorph-II of fibrous (*a*) and microcrystalline (*b*) form of WCel (*1*, *2*) and cotton Cel (*3*, *4*) as Function of interaction with 68.5 % HNO_3 at 20 °C (*1*, *4*) and 0 °C

transformations caused by hard pulping conditions used for the removal of large quantities of lignin and hemicelluloses from the wood tissue exert negative influence on porous capillary system and reactivity of the fibres being isolated. Dense deposits of unremoved low-molecular fractions (consisting mainly of hemicelluloses) prevent the reagent penetration through the capillary system and make diffusional mechanism prevail over the capillary one [20, 22]. Thus, there are reasons to think that the HNO_3 transfer towards WCel crystallites at lower temperatures occurs under conditions of larger diffusional inhibition than it is seen in the case of CCel. This can be associated with a decreased ability of the acid to overcome the hemicellulose deposits due to its weaker hydrolytic activity at lower temperatures. The crystallite transformation is 'retarded' correspondingly, and this is seen on the X-ray patterns. Sound confirmation of this point of view is the fact that WMCCel is 'mercerized' at 0 °C more rapidly than the initial Cel. The most probable cause of this acceleration is weakening of the diffusional factor influence on the process kinetics as a result of 'liberation' of crystallites from the structurally disordered binding material. In the traditional mercerization, the reagent penetration is favoured by the hemicellulose solubility in alkaline media. Furthermore, the swelling of Cel in 68–69 % HNO_3 is not so extensive as in NaOH solutions [17]. Microphotographs shown in Fig. 3 enable a comparison to be made between transversal dimensions of the cellulose fibre on swelling in 68.5 % HNO_3 with that swollen in 18 % NaOH. It is apparent that the alkaline medium caused a two-fold greater thickening of the fibre as compared with the nitric acid one.

The incapability of the two cotton Cel morphological forms to be «mercerized» completely under conditions providing complete «mercerization» of the corresponding WCel forms (Fig. 2) is in agreement with the idea [21] about the influence of crystallite dispersity and imperfectness on the depth of phase transformations associated with the formation of additive compounds. The crystallites of cotton Cel are considerably larger and more perfect than the crystallites of WCel, and this fact, together with a relatively small swelling of Cel in 68–69 % HNO_3, makes WCel more suitable for the nitric acid 'mercerization'.

During the nitric acid «mercerization», the conventional (amorpho-crystalline) Cel undergoes a considerable depolymerization (Fig. 4). A rapid decrease in DP of the initial Cel at the beginning of its interaction with 68.5 % HNO_3 is followed by a slow degradation of molecular chains. The rate of hydrolytic cleavage of the

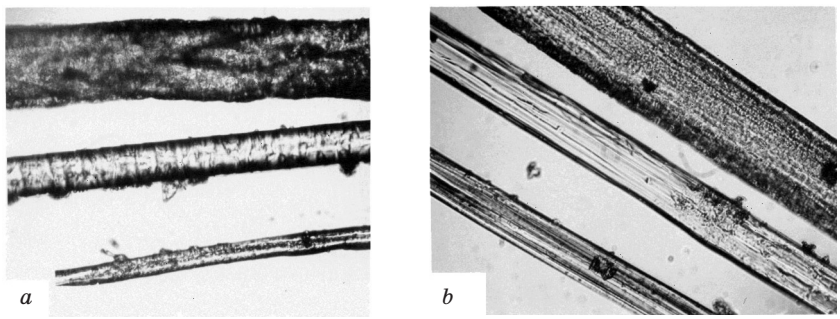

Fig. 3. Optical microphotographs of flax Cel (*a*) and Cel hydrate (*b*) fibres. From the bottom upwards: initial fibre swollen in 68.5 % HNO_3 solution; fibre swollen in 18.5 % NaOH solution

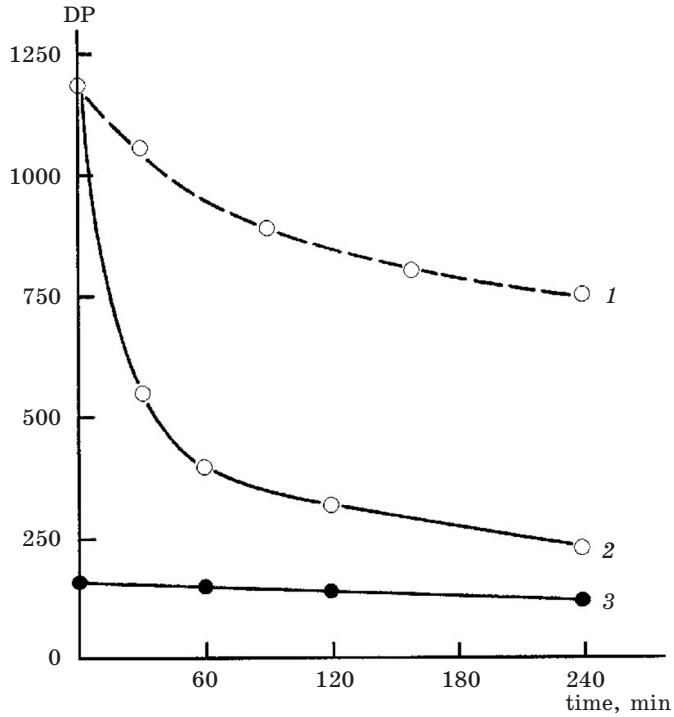

Fig. 4. Changes in DP of initial WCel (*1*, *2*) and WMCCel (3) during mercerization at 20 °C (*2*, *3*) and at 0 °C (*1*, *3*)

macromolecules strongly depends on the 'mercerization' temperature (Fig. 4). A complete polymorphous transformation of WCel at 20 °C (reaction with HNO_3 for 1 h) is accompanied by an about three-fold decrease in DP (that initially was ~1200), while at 0 °C (reaction with HNO_3 for 3 h) the DP value decreases 1.5 times only. Unlike the initial Cel, its microcrystalline form remains resistant to hydrolysis under conditions of intracrystallite swelling as well. As a probable cause of preventing from the development of destructive transformations, a high stoichiometry may be noted in the reaction of 68.5 % HNO_3 with Cel macromolecules organized into crystallites [14, 23].

According to [14], one molecule of HNO_3 falls to the share of two anhydroglucose units of Cel. During the period of complete 'mercerization' of WMCCel at both 20 °C and 0 °C, the initial DP value remains virtually invariable.

The IR spectra of 'mercerized' Cel reveal prominent features making the difference between the Cel-II polymorph and Cel-I polymorphs [24]. There are no signs of oxidative transformations (1700–1800 cm^{-1}), but characteristic bands of nitroester groups are present (1650, 1280, 850 and 750 cm^{-1}). The rate of bound nitrogen accumulation in Cel depends strongly on the temperature at which the reaction with HNO_3 takes place (Fig. 5). The effect of the initial material morphology on the esterification process is small. In the course of complete 'mercerization' at both 20 °C (reaction with HNO_3 for 1h) and 0 °C (reaction with HNO_3 for 3h), the ordinary Cel accumulates approximately equal amounts of nitrogen: 0.7 to 0.8 % (DS_{-ONO_2} = 0.08–0.09).

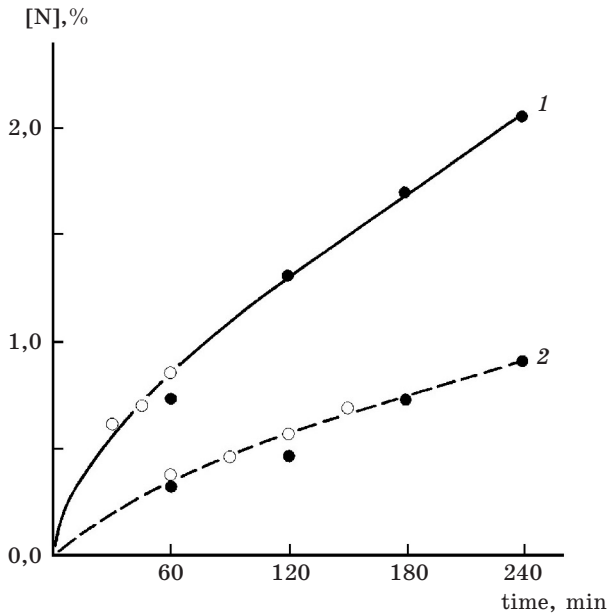

Fig. 5. Bound nitrogen accumulation kinetics reflecting the course of reaction of the initial WCel (o) and WMCCel (•) with 68.5 % HNO_3 at 20 °C (*1*) and 0 °C

In the case of nitric acid 'mercerization' of WMCCel, the influence of esterification on the physical structure of the products becomes appreciable. We noticed that WMCCel «mercerized» at 0 °C (interaction with HNO_3 for 2.5 h) is significantly superior in crystallinity to the same WMCCel «mercerized» at 20 °C (interaction with HNO_3 for 2 h) The latter one is notable for its two-fold higher bound nitrogen content (~ 1.3 %; $DS_{\text{-ONO}_2} = 0.15$). If the «mercerization» time is increased up to 4 h, the amount of bound nitrogen rises to ~ 2 % ($DS_{\text{-ONO}_2} = 0.25$).

In X-ray diffraction patterns of the products, a gradual «degeneration» of the crystallite scattering with increasing degree of esterification is observed, and it is hardly perceptible at $DS \geq 0.25$. At the same time, the X-ray diffraction pattern of WMCCel «mercerization» product obtained at 0 °C during 4 h displays a quite distinct crystallite scattering of Cel-II (Fig. 6), because the bound nitrogen content in this case does not exceed 0.9 % ($DS_{\text{-ONO}_2} = 0.1$). An obvious correlation can be discovered between the degree of esterification and the degree of decrystallization of the «mercerized» WMCCel. We think the main cause of structural disorganization of WMCCel during its nitric acid «mercerization» is associated with its partial esterification under conditions of intracrystallite swelling, which entails disturbance in structural regularity. It should be emphasized that a well-defined decrystallization effect can only be observed in the case of WMCCel, when the entire nitrating potential of HNO_3 is used up solely for the crystalline phase of Cel. Manifestation of this effect is favoured, in our opinion, by a relatively small chain length of WMCCel molecules, which is comparable in size with a segment of ordinary Cel.

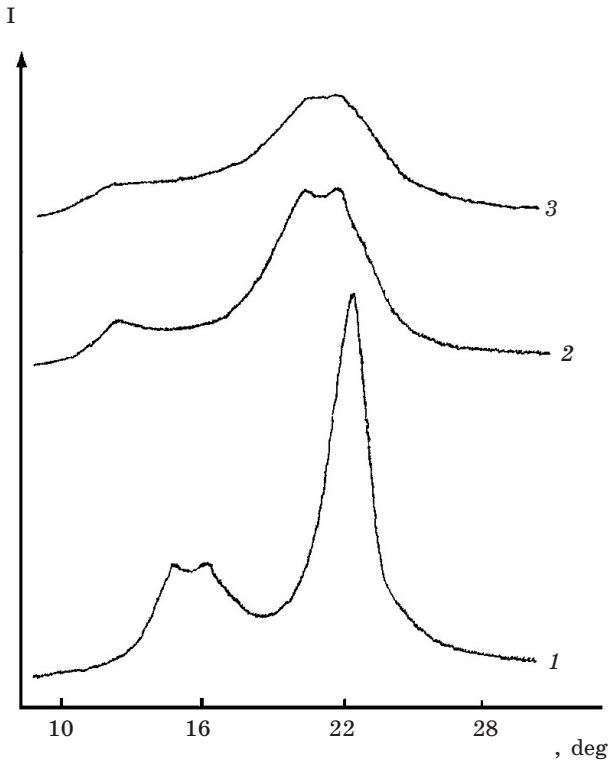

Fig. 6. X-ray diffractograms of WMCCel (*1*) and products of its «mercerization» during 4 h at 0 °C (*2*), and during 3 h at 20 °C (*3*)

It follows from the aforesaid that the combination of complex-forming and hydrolytic functions of HNO_3 makes it possible to realize a non-traditional, purely acidic WCel processing scheme to afford powder WCel-II forms having microcrystalline or amorpho-crystalline morphology [25–27].

During the non-traditional preparation of material with the microcrystalline morphology (WMCCel-IIn), WCel was first treated with nitric acid of concentration 68.5 % for 3 h at 0 °C and liquor ratio of 20 ml/g. The swollen Cel was then pressed off until a ca. 3-fold weight increase was reached. As a result of the press-off procedure, at least 60 % of initial acid volume is usually recovered. This acid, after appropriate fortification and compensation for losses, can be re-used for the polymorphic transformation of Cel. To the pressed-off fibrous mass, a quantity of water was added necessary to form 2.0 to 2.5 N HNO_3 solution from the concentrated acid absorbed by the fibres. As a result of the dilution procedure, the KC formed decomposes to yield Cel-II, which is then hydrolysed with boiling 2.0–2.5 N HNO_3 down to its «level-off DP» value (1 h, liquor ratio ca. 10 ml/g).

Samples of powder wood Cel-II (WPCel-IIn) having amorpho-crystalline morphology were prepared according to the purely acidic scheme from Cel previously hydrolysed down to the «level-off DP». The hydrolysis was carried out using boi-

ling 2.5 N HNO_3 at a liquor ratio of 10 ml/g during 1 h. The WMCCel-I thus obtained was converted into the Cel-II polymorph using 68,5 % HNO_3, as above.

In order to perform a comparative characterization of the Cel-II powder forms obtained by the purely acidic method, WMCCel-IIt and WPCel-IIt samples of similar structures have also been prepared according to the traditional scheme. In the traditional procedure, the polymorphic transformation was performed as a conventional mercerization of native Cel with 18 % NaOH solution during 1 h at 0 °C and at liquor ratio of 20 ml/g. The hydrolysis, washing and drying conditions were identical for all the samples prepared, the only difference being the way of converting native cellulose into hydrated cellulose.

The final powder product yield is mainly determined by the material mass loss during the hydrolysis of cellulose fibres down to the «level-off DP» value. Such losses are the most appreciable in the course of hydrolysis of Cel-II whose crystalline structure is less perfect than that of Cel-I. Accordingly, the WMCCel-IIn and WMCCel-IIt samples are obtained in yields of 72–75 %, with respect to the initial Cel mass, whereas the yields of WMCCel-I, WPCel-IIn and WPCel-IIt amount to 83–85 %.

Weak absorption bands characteristic of nitro ester groups were present in the spectrum of WPCel-IIn only, because 68.5 % HNO_3 which is known to possess a nitrating ability was used in the final preparation stage of this sample. According to the chemical analysis data, this preparation contains ca. 8 nitro ester groups per 100 cellulose elementary units. In the course of preparation of WMCCel-IIn, the treatment of cellulose fibres with 68.5 % HNO_3 is followed by the procedure of its hydrolytic cleavage, as a result of which the major part of nitro ester groups introduced during the first stage is removed from the fibre together with the amorphous binding component [25].

X-ray diffractograms of the prepared samples are shown in Fig. 7. When comparing angular positions of reflections in the X-ray diffractograms 2 and 4 with those in X-ray diffractograms of similar samples but prepared using a traditional mercerization procedure (3 and 5), it can be concluded that the action of 68.5 % HNO_3 results in a virtually complete polymorphic conversion of the native crystalline structure.

At the same time, however, there are reasons to suspect the presence of some «residual nativity» in WMCCel-IIn, because the most intense reflection in its diffractogram is (002), which is characteristic of Cel-I (curve *1*), and not of Cel-II (curves *3*, *5*). This is probably due to the fact that the polymorphic conversion occurs under conditions of a considerably less extensive swelling of Cel in the nitric acid medium as compared to the alkaline one. During the process of polymorphic transformation under the action of HNO_3, the Cel fibres undergo a significantly greater decrystallization than they do under common mercerization with a NaOH solution. This difference in crystallinity is retained also after the cellulose hydrolysis down to its «level-off DP». The crystallinity index of WMCCel-IIn is 0.44, whereas that of WMCCel-IIt amounts to 0.57 (Table 2). The polymorphic transformation of WMCCel-I under the action of HNO_3 is accompanied by the most profound decrystallization, the causes of which have been discussed above. The X-ray diffractogram of WPCel-IIn sample, curve 4, is typical of Cel-II with a very low degree of structural order: its crystallinity index is 0.23 against 0.45 for WPCel-IIt.

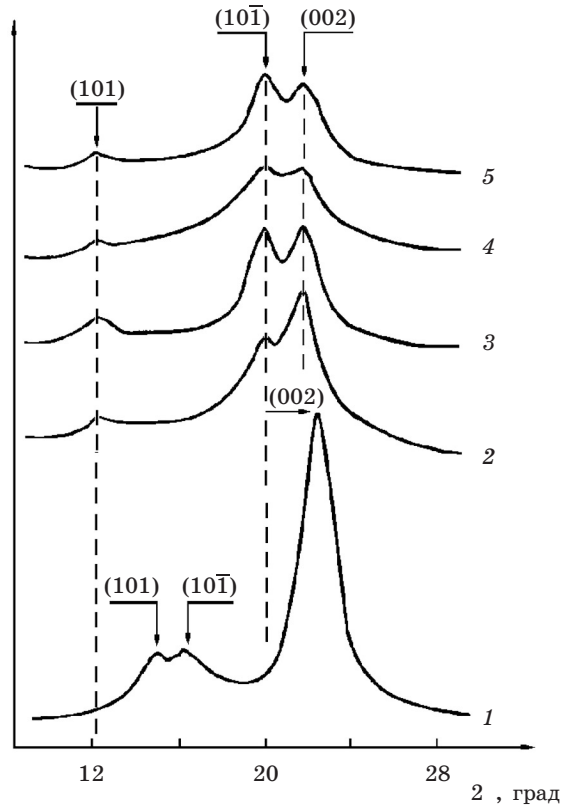

Fig. 7. X-ray diffraction pattern of Cel powder:
1 – WMCCel-I, *2* – WMCCel-IIn, *3* – WMCCel-IIt,
4 – WPCel-IIn; *5* – WPCel-IIt

Table 2

Some characteristics of cellulose powder forms

Sample	DP	Crystallinity index	WRV, %	I_2 sorption value, mg/g
WMCCel-I	170	0.67	58	19.9
WMCCel-IIn	50	0.44	107	76.3
WMCCel-IIt	50	0.57	105	27.0
WPCel-IIn	150	0.23	155	261.4
WPCel-IIt	160	0.45	208	119.1

Scanning electron microscopy photographs shown in Fig. 8 demonstrate particle dispersity and surface morphology of WMCCel-IIt and WMCCel-IIn. The observed particles represent aggregates of individual microcrystals. When comparing microphotographs *b* and *d*, it is seen that the way of polymorphic transformation of the initial Cel affects substantially the morphology of particles formed on

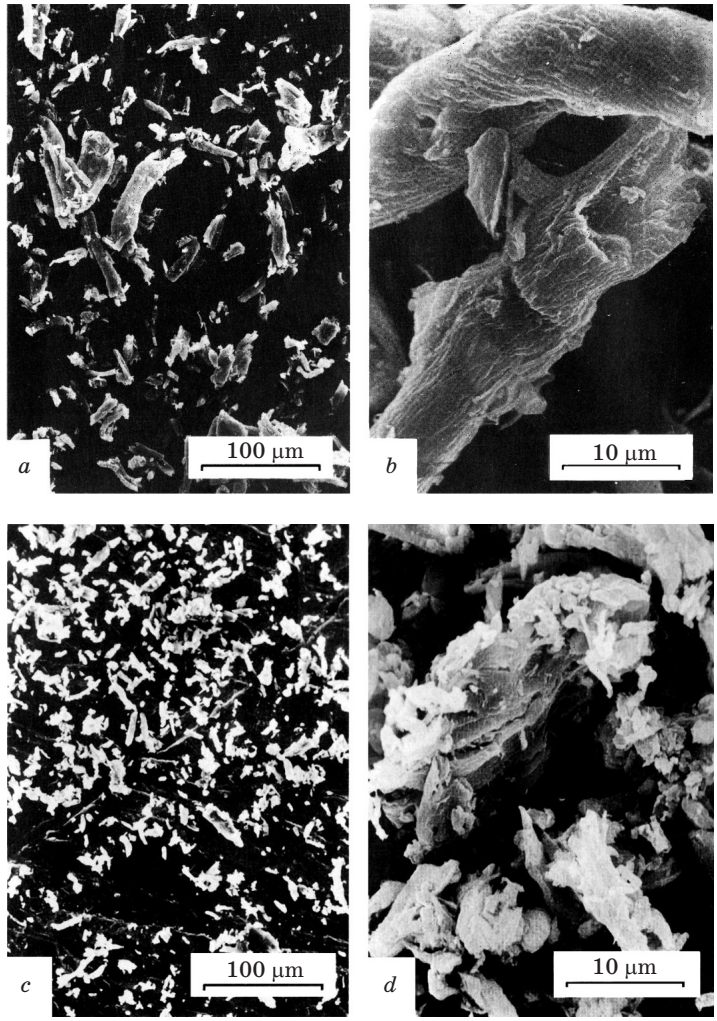

Fig. 8. Scanning electron microphotographs:
a, *b* – WMCCel-IIt; *c*, *d* – WMCCel-IIn

subsequent hydrolysis of the fibre down to the «level-off DP». The WMCCel-IIt particles obtained in the course of traditional mercerization of Cel retain a relatively «smooth» surface relief characteristic of the initial fibre. The particles of WMCCel-IIn obtained by purely acidic preparation technology are characterized by a developed surface relief reflecting the factors of not only transversal but also longitudinal cleavage of the fibre.

One can judge about dimensions of individual crystallites being constituents of samples with microcrystalline morphology from the value of «level-off DP» that is determined by longitudinal dimensions of the crystallites (Table 2). Based on the mean «level-off DP» value of 170 for WMCCel-I, the anhydroglucose unit length for Cel (5.15 Å), and the stretched conformation of macromolecules in mic-

rocrystals, the estimated mean longitudinal dimension of microcrystals of this native material is ca. 900 A. The conversion of Cel-I into Cel-II is accompanied by considerable changes in dispersity and morphology of crystallites [25, 27]. The «level-off DP» value of both WMCCel-IIn and WMCCel-IIt is ca. 50, which means a more than 3-fold decrease in crystallite length as compared to WMCCel-I.

In the course of preparation of both WPC-IIn and WPC-IIt by the polymorphic transformation of WMCCel-I using both alkaline and acidic reagents, the mean DP value of 170, that is characteristic of native microcrystals, remains almost unchanged, while the crystallite dimensions and crystallinity of the material as a whole decrease significantly (Table 2). The crystallite length is not determined by the DP value any more (the latter is greater). The microcrystalline structure of Cel-I transforms into a usual amorpho-crystalline structure of Cel-II with a small DP value.

We have found that the polymorphic transformation of Cel by the nitric acid method, unlike the traditional one, is accompanied by the appearance of numerous longitudinal microfissures in the fibre. The largest of these are visible quite well with the aid of a scanning electron microscope on both the side surfaces of WPCel-IIn particles and on the cross-sections of fibrous fragments (Fig. 9). Their formation must promote the enhancement of sorption properties of the material.

The prepared WCel-II powder forms differ from WMCCel-I by their considerably higher hydrophilicity and sorption activity (Table 2). The hydrophilic properties of Cel powders were evaluated according to their water-retaining value (WRV). This index reflects the water-retaining ability of a final product sample washed until neutral but not dried. Microcrystalline forms of Cel-II prepared by the both methods are characterized by comparable WRVs that are substantially inferior to those of the respective amorpho-crystalline forms. The most hydrophilic is the sample with an amorpho-crystalline morphology prepared by the traditional method (WPCel-IIt), in spite of the fact that its crystallinity index is higher

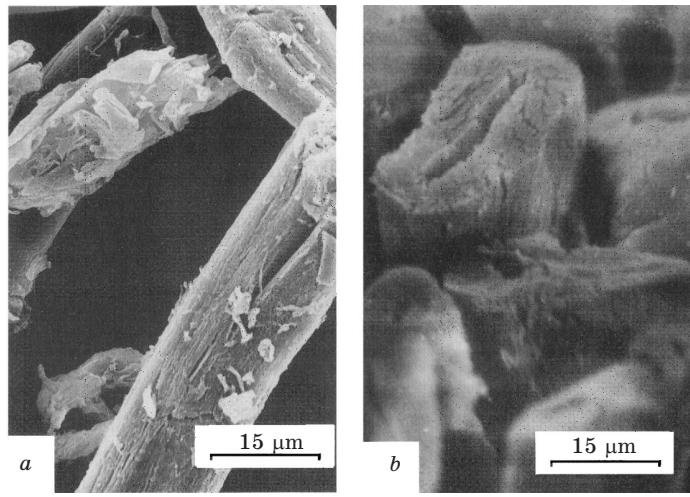

Fig. 9. Scanning electron microphotographs:
a – WPCel-IIn, *b* – cross-section of cotton Cel fibres treated with 68.5 % HNO_3

than that for the respective sample prepared by the purely acidic scheme (WPCel-IIn). There is no rigorous correlation between indices of crystallinity and those of hydrophilicity for the samples, whereas the influence of the morphological factor on the WRV is rather important.

The WCel-II powder forms prepared according to the purely acidic scheme manifest a more than two-fold superiority to their traditionally prepared analogues in sorption ability with respect to iodine (Table 2). Here too, the highest sorption activity is found for the samples possessing the amorpho-crystalline morphology. The iodine sorption values measured for these samples are 3–4 times higher as compared to the samples with microcrystalline morphology.

Similar effects are observed for Congo red dye sorption as well (Fig. 10). The Congo red sorption isotherms for WMCCel-I and WMCCel-II samples agree within experimental error (Fig. 10, curve *1*). It should be noted that the iodine sorption values for these samples are rather close too (Table 2). The sorption activity of the WMCCel-IIn sample towards the dye is somewhat higher than that for the two samples mentioned earlier, but the difference in the limit sorption values is small (curves *1* and *2*). Hence, with respect to voluminous molecules, the microcrystalline forms of Cel-I, as well as those of Cel-II of different preparation techniques, display similar li-

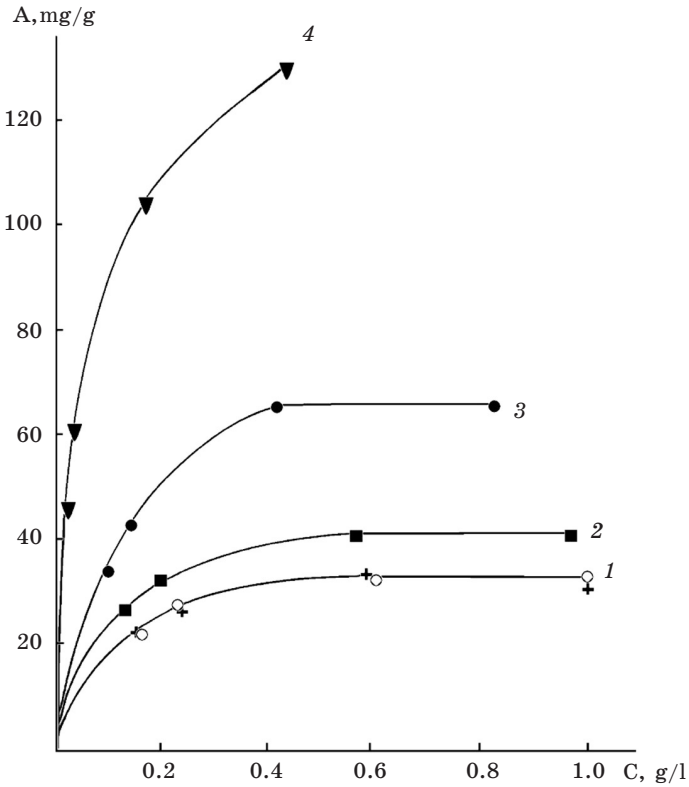

Fig. 10. Isotherms of Congo red sorption by Cel powder forms:
1 – WMCCel-I and WMCCel-IIt; *2* – WMCCel-IIn;
3 – WPCel-IIt; *4* – WPCel-IIn

mit sorption values. The most efficient sorption of Congo red (and that of iodine) is observed for the WPCel-IIn sample (curve *4*), being markedly superior to that for all the other samples in this respect. Within the same morphological form of powder material, an interrelation is observed between its crystallinity index and sorption ability with respect to both iodine and Congo red. The lower crystallinity of a sample, the more active it is as sorbent (Table 2 and Fig. 10). However, the superior sorption qualities of WPCel-IIn among all other samples are probably due to not only its low crystallinity, but to a more developed surface of its particles due to microfissure formation too. In the course of preparation of WMCCel-IIn samples, the micro-cracking effect is partially leveled during hydrolytic degradation of the fibre to form microcrystal aggregates in the final stage of the process. This effect is present in its most pronounced form in cases when the final stage is the polymorphic transformation of pre-dispersed fibres under the action of nitric acid (WPCel-IIn sample). In our opinion, just the micro-cracking effect, along with low crystallinity, provide the high sorption ability of this sample.

In the course of Cel oxidation with nitric acid, the KC adduct is capable of playing the role of a reactive «matrix» [28]. It is apparent that the structural state of Cel corresponding to KC should be superior to the initial one as regards activity and uniformity of reaction because the reagent taking part directly in oxidation of Cel is incorporated into crystal lattice of the latter.

The most rational method for obtaining carboxylated powder Cel (CPCel) based on the use of the same reagent for both oxidation and dispersion of the C fibre has been proposed in [29]. It consists in the treatment of Cel with 60 % HNO_3 in the presence of sodium nitrite that serves to generate nitrogen(IV) oxide acting as a catalyst of the oxidation process taking place in the system. In that way, a considerable oxidation degree (12 % to 14 % of COOH groups by mass)[1] can be obtained within 30 h at room temperature.

The oxidized fibres, after pressing-off the excess of the reaction medium and introducing the appropriate amount of water, are converted into a powder state by means of partial hydrolysis with diluted HNO_3 formed at the reflux temperature.

The course of oxidation of the KC obtained on the basis of flax Cel (97 % of α-Cel, DP=1800) under the stated conditions is depicted by the curve 1 in Fig. 11. Pre-activation of the initial Cel consisted in its treatment with 68.5 % HNO_3 for 1 h. After that, water was added to the system in a quantity necessary to form 60 % HNO_3, as well as $NaNO_2$ (1.4 g per 1 g of Cel). Except for the pre-activation stage, the reaction conditions were the same as in [29].

It is apparent that the carboxyl group accumulation occurs at a virtually constant rate throughout the whole time interval studied, suggesting a uniformity of oxidation within the bulk of the fibre. Appropriate conditions for a uniform reaction are created probably owing to a relatively high stability of KC towards 60 % HNO_3 at 18 °C. Within 10 h, 15.1 % of COOH groups are formed. According to [29], more than 30 h are needed to attain such level of oxidation. The material oxidized at 18 °C retains its initial fibrous form while somewhat increasing its mass due to the reaction. Just as in [29], an additional treatment is required to transform the fibres into a powder state.

[1] When the C-6 atoms of all anhydroglucose units are oxidized, the COOH group content is 25.57 %, by mass.

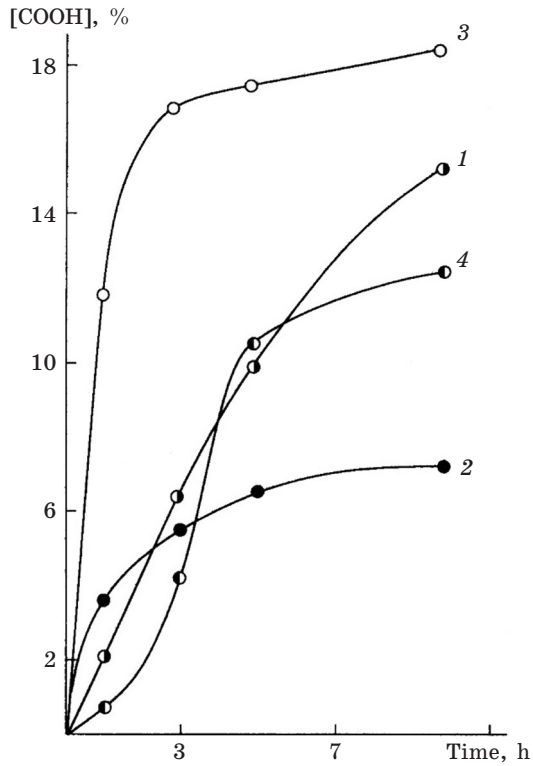

Fig. 11. Accumulation of carboxyl groups upon oxidation of (*1*) the KC with 60 % HNO_3 at 18 °Cel in the presence of $NaNO_2$; (*2*) Cel-I with 55 % HNO_3 at 70 °C; and the KC with 55 % HNO_3 at (*3*) 70 °C and (*4*) 50 °C

Initiation of the oxidative transformation by increasing the reaction temperature makes the use of $NaNO_2$ unnecessary, and allows the fibre oxidation and degradation processes to be combined into one, thus avoiding the separate stage of partial hydrolysis that involves a technologically complicated operation of pressing-off the oxidized fibrous mass from an excess of toxic and corrosive medium. In the single-stage version, the reaction temperature and acid concentration should be balanced in such a way that, while maintaining sufficiently high rates of Cel oxidation, excessive stimulation of hydrolysis and nitration be avoided, the latter being also very sensitive to the temperature and concentration factors.

In a series of experiments performed in order to find out acceptable conditions for a single-stage process for preparing CPCel from flax cellulose, the best results were obtained with 55 % HNO_3 at 70 °C and liquor ratio of 15 ml/g (Fig. 11, curve *2*). As one can see, the process character is typical for heterogeneous transformations of Cel, the depth of which is limited by the poor accessibility of the crystalline «component» of the fibre to the reagent. In this material, only 7.4 % of the COOH groups are accumulated after 10 h of reaction. The yield of oxidized powder mass is 80 %, which is equal to that of chemically unchanged microcrystalline Cel

(MCCel) obtained from the fibre by a usual hydrolysis procedure with boiling diluted mineral acid down to the «level-off» DP.

For the adduct of Cel with HNO_3, the rate and degree of oxidation increase sharply under these conditions (Fig. 11, curve *3*). After 1 h, the content of COOH groups is already 11.9 %; after 10 h, it reaches 18.3 %. However, the rate of hydrolysis is also high, hence an acceptable yield of CPCel cannot be obtained in this case; it amounts to 48 % after 1 h of reaction and is only 20 % after 10 h. The high rate and degree of hydrolytic degradation of the macromolecules promote oxidation because the hydrolysis products act as reducing agents, i.e. they assist (along with temperature) the formation of nitrogen oxide(IV) in the system. The major portion of the starting material undergoes deep hydrolysis and passes into solution already in the initial stages of the process, thus strongly promoting oxidation. As a result of this, the majority of COOH groups (about 17 %) is formed during the first 3 h at a nearly constant rate, and then the oxidation rate drops sharply, and only slight contribution is made to the development of oxidation process during the following 7 h of reaction. There is a synchronism in the decrease of oxidation and hydrolytic cleavage rates. The slow stage corresponds to after-oxidation of a relatively small amount of the material having structural organization that provides hydrolytic stability. As a whole, the increase in accessibility of the initial fibre structure due to pre-activation is so high that at 70 °C the major portion of the macromolecules undergoes a deep hydrolytic cleavage. The high rate and degree of oxidation of the activated Cel at 70 °C are achieved at the expense of the yield of the desired product.

The activation energy of heterogeneous acid hydrolysis of Cel is rather high (about 150 kJ [30]), therefore, the rate of this reaction stage is strongly temperature-dependent. For example, on decreasing the temperature by 20 °C, the yield of oxidized powder mass after treatment of KC for 10 h is 80 %. The rate and degree of oxidation decrease correspondingly because the factors that promote oxidation are weakened (Fig. 11, curve *4*). Oxidation is decelerated not only in the final stage, as it was seen in the cases discussed above, but also at the very beginning of oxidation. This is probably due to a slow accumulation of the required amount of nitrogen oxide(IV) in the system at 50 °C. Nonetheless, the degree of KC oxidation at 50 °C is much higher than that of common Cel at 70 °C. The content of COOH groups is 10.5 % after 5 h and 12.3 % after 10 h (cf. Curves *2* and *4*, Fig. 11). These reaction conditions are unlikely to be optimal, but it is apparently possible, by varying temperature and concentration, to select conditions that would provide a sufficiently high degree of oxidation of KC and a good yield of powdered oxidized Cel. According to chemical analysis data, the total carbonyl group content of the CPCel obtained on the basis of KC does not exceed 2 %, which is typical for the Cel oxidized at the 6-th carbon atom. The bound nitrogen content is also small (< 0.4 %).

The character of variation of the substrate accessibility during the reaction should also be considered as one of the major causes of different behaviour of KC in the experiments discussed. The KC oxidation proceeded in HNO_3 of lower concentration than that needed for this adduct to be formed. The concentration gradient alone would cause the KC to decompose gradually. Increasing the temperature, changing the chemical composition of macromolecules, their degradation, and other factors should also exert influence on this process. These circumstances affect the final product structure too.

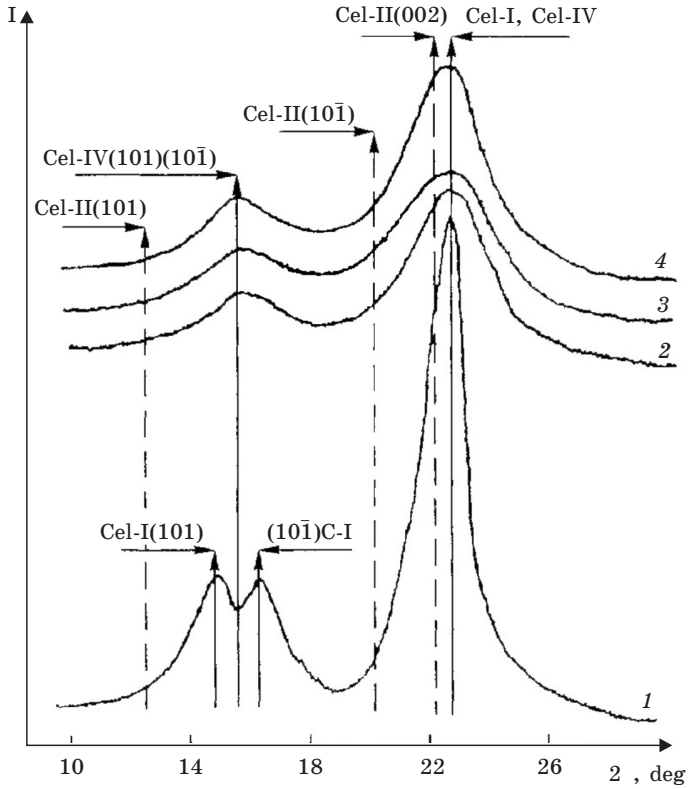

Fig. 12. X-ray diffraction pattern of the oxycellulose samples containing (*1*) 7.4, (*2*) 15.1, (*3*) 18.3 and (*4*) 12.3 % of carboxyl groups

The KC decomposition with water is known to involve a mercerization-like effect, i.e. the formation of Cel-II. In our case, the system where KC was formed (68.5 % HNO_3) was diluted with a relatively small amount of water, to reduce the acid concentration down to the level required (55–60 %), and thereafter the conditions promoting oxidation were created. In the diffractograms of CPCel obtained on the basis of KC (Fig. 12, curves *2–4*), there are no signs of reflections characteristic of Cel-II. According to angular positions of reflections, these diffractograms can be attributed to partially decrystallized Cel-I or Cel-IV. There are known examples of formation of Cel-IV in the systems given [31]. However, blurred appearance of diffractograms of the CPCel samples obtained on the basis of KC does not allow a specific Cel modification to be attributed to them.

The particles of CPCel samples thus obtained are characterized by low stability toward mechanical stress in either in dry or wet state. The latter circumstance allows a high degree of dispersity to be attained immediately after the powder wash-out from HNO_3, and, if necessary, the process could be ended with the formation of a uniform colloidal dispersion having consistency of a paste or ointment based on an aqueous-organic dispersion medium (ethanol, glycerol, acetone, etc.).

3. COMBINATION OF THE OXIDATIVE AND ACID-HYDROLYSING FUNCTIONS OF NITROGEN OXIDE(IV) AS A METHOD FOR PREPARING CARBOXYLATED MICROCRYSTALLINE CELLULOSE

Preparation of cation-exchanger enterosorbents based on carboxylated Cel capable, in particular, of binding and removing radionuclides and heavy metals from the human organism is a topical and promising trend in cellulose chemistry.

Of the cellulose-based sorbents, microcrystalline Cel (MCCel) deserves a particular attention in this respect. MCCel is a product of hydrolytic cleavage of cellulose down to the so-called «level-off DP» (150–220 monomer units, depending on the kind of initial cellulose). As a result of hydrolysis, the fibres are liberated from the structurally disordered component and impurities contained therein. A disruption of the fibrous structure of the material takes place, which is converted into a finely dispersed powder consisting of particles that are aggregates of microcrystals. The distinguishing features of MCCel are high degree of chemical purity, highly ordered supramolecular structure and a unique capability of forming stable tixotropic gels. Hydrogels are formed by applying hard shear stress conditions to 5–20 % aqueous dispersions of MCCel [32]. MCCel is widely used as filler or thickener substance in the manufacture of many medical products. It is used as a dietary additive, and as a means of removing sludge from the gastrointestinal tract; the latter application is due to high sorption capacity of MCCel in combination with some «abrasive» effect. A disadvantage of MCCel as enterosorbent is its lack of ionogenic groups present in such well-known enterosorbents as pectin or marine algae polysaccharides (laminarin, carrageenan).

Features of the proposed method for preparing carboxylated MCCel (CMCCel) are as follows [33]:

Air-dry Cel was treated with gaseous nitrogen(IV) oxide in a specially-made reactor. The process was conducted at room temperature during the time necessary for attaining the required degree of Cel oxidation. Then a calculated quantity of water was filled into the reactor fitted with a reflux condensor, and the reactor content was heated to boiling temperature to convert the carboxylated cellulose fibres into CMCCel. Reaction of water with the excess nitrogen oxides sorbed by Cel leads to formation of nitrous and nitric acids, which play the role of catalysts in the hydrolytic process of Cel destruction. Thus, nitrogen(IV) oxide is, in fact, fulfilling both oxidative and acid-hydrolyzing functions. Under conditions we used in our experiments, approximately 4 % HNO_3 was formed in the system. The hydrolysis process was continued until a complete conversion of the fibre into a uniform finely dispersed mass was attained. The latter was repeatedly pressed-out and washed with water on a Schott filter until complete removal of nitrate and nitrite ions, as checked by reaction with diphenylamine. A part of the obtained CMCCel was dried at 60 C, ground in a mortar, and fractions were taken out that passed through a 100 μm sieve. Another part of the wet CMCCel was used for hydrogel preparations.

Preparation of a material that possesses both ion-exchanger properties and the properties of MCCel imposes certain requirements on the first stage of the process: carboxylation of Cel fibres. The Cel fibre crystallinity, and consequently the CMCCel yield, depend on the degree of carboxylation. If the degree of oxidation is small (up to ca. 5 % w/w COOH groups, γ~18,3)[1], the Cel crystallinity incre-

[1] γ is the number of COOH groups per 100 anhydroglucose units

ases to some extent due, in particular, to the refining effect. The increase in crystallinity may be also caused by the removal of largely destroyed macromolecular fragments of Cel present in amorphous areas, together with hemicelluloses, during the wash-out procedure.

A deeper oxidation of Cel decreases its crystallinity owing to disruption in regularity of the macromolecules. The higher the degree of oxidation, the greater is the decrystallization, because the reaction acquires an intracrystallite character. The MCCel yield in the reaction of Cel hydrolysis down to the «level-off DP» is directly associated with crystallinity of the starting material. For this reason, it is always higher for cotton Cel than for WCel irrespective of its origin or method of manufacture. The CMCCel yield from oxidized Cel containing 5 % of COOH groups is ca. 80 %, i.e. it is virtually the same as the MCCel yield from WCel. From oxidized Cel containing 13.5 % of COOH groups (γ= 49.3), a powder material of low crystallinity is obtained in a yield of ca. 60 %. Thus, to obtain CMCCel, it is rational to oxidize the starting fibre to a relatively low carboxyl group content, e.g. 5 %, that is equal to the free carboxyl group content of pectins. In this case, the ion-exchanger properties, the properties due to the microcrystalline morphology, and the final product yield are well-balanced. It should be pointed out that the COOH group content in the oxidized Cel fibre and in the CMCCel prepared thereof agree within the error limits for the barium acetate analytical method, in spite of the fact that significant amounts of structurally disordered material were removed from the fibre in the course of hydrolysis. This observation can possibly be accounted for as follows:

As it has already been pointed out, the hydrolytic cleavage of oxidized Cel takes place in an oxidizing medium. In the initial stage of the hydrolytic process, evolution of brown vapours of NO_2 from the reaction mixture is observed. Under such hydrolysis conditions, «afteroxidation» of Cel is possible, in particular, of carbonyl groups present. This may be the cause of equal carboxyl group content in oxidized fibrous Cel and in the CMCCel prepared from it, and of enhanced stability of CMCCel. For example, the temperature at which thermal decomposition starts for CMCCel containing 3.5 % of COOH groups (γ = 12.7) is by 32 °C higher than the corresponding value (175 °C) for its precursor, fibrous Cel with the same degree of carboxylation. The observed difference in thermal stability (196 °C vs. 163 °C) remains after 4 h exposition of the samples to UV light, which causes the both starting decomposition temperatures to decrease by ca. 12 °C. Among factors that contribute to the enhanced stability of CMCCel, its content of nitroester groups should be mentioned, which is inferior as compared to its precursor, carboxylated fibrous Cel. Cel oxidation with nitrogen(IV) oxide is always accompanied by accumulation of nitroester groups in small amounts, which lower chemical stability of the material [34]. Unlike Cel oxidation, nitration of Cel depends substantially on the diffusion factor; therefore, the nitroester group accumulation takes place primarily in easily accessible areas of the fibre, which are then removed in the course of hydrolysis. It should be noted that nitrogen oxide compounds are capable of Cel bleaching [35]. Under the reaction conditions employed, the enhancement of bleaching after conversion of the starting Cel into CMCCel is seen quite distinctly.

Conversion of the acid CMCCel form (H-CMCC) into its sodium salt (Na-CMCCel) facilitates preparation of homogeneous, stable tixotropic hydrogels. To prepare similar gels from MCCel, special high-speed (ca. 20000 rpm) shear blendors are necessary. It is

only under severe shear stress conditions that the disaggregation of MCCel microcrystals is possible, which is necessary for a stable hydrogel to be formed. To facilitate gel formation, after Cel hydrolysis and washing the MCC obtained, addition of water-soluble Na-carboxymethylcellulose in amounts of 8–10 % w/w has been proposed [32]. Such an additive envelops the microcrystals, playing the role of a «barrier» compound.

To prepare Na-CMCCel gels, there is no need for high-speed blendors any more. It is noteworthy that, in the case of Na-CMCC salts, an easy gel formation occurs already with a ~2 % COOH group content ($\gamma = 7.2$). Under our experimental conditions, cream-like hydrogels with pH 6.5 to 7.0 were obtained containing 10 ± 0.5 % w/w of Na-CMCCel.

Convincing evidence of completeness of salt formation is obtained when comparing IR spectra of dry samples of H- and Na-CMCCel. On neutralization, an intense band at 1730 cm^{-1} in H-CMCCel spectrum due to the stretching C=O vibration of the carboxyl group disappears almost totally; instead, an intense band at 1610 cm^{-1} is seen, characteristic of carboxylate anion [34].

Na-CMCCel hydrogels have a distinctly marked tixotropy. After a certain time, they become structured and lose fluidity, which reappears on shaking. During two years of storage, we did not observe any signs of layer separation in the hydrogels. On drying thin layers of the hydrogels, brittle mat films are formed, easy to reduce into powder that we used in our experiments along with the hydrogels themselves.

In Fig. 13, curve *1*, X-ray diffractograms of H-CMCCel with carboxyl group contents of 2.5 % and 4.8 % ($\gamma = 9.1$ and 17.5) and of the respective Na salts (cur-

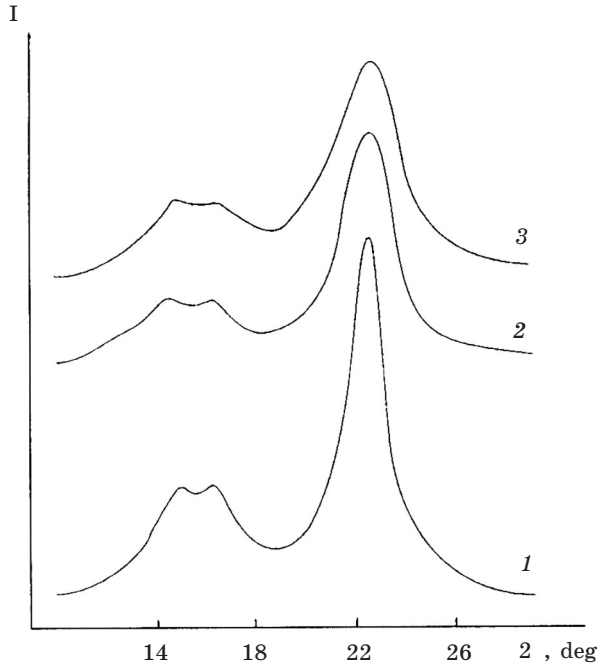

Fig. 13. X-ray diffraction pattern of CMCCel samples: *1* – H-CMCCel with 2.5 % and 4.8 % COOH group content; *2* – Na-CMCCel with 2.5 % COOH group content; *3* – Na-CMCCel with 4.8 % COOH group content

ves *2* and *3*) are shown. The X-ray patterns of the both samples containing the H-form are almost identical, and correspond to the native modification of Cel (Cel-I) with highly ordered supramolecular structure. The crystallinity index for H-CMCCel samples is 0.66, being somewhat higher than that for the starting cellulose (0.64). These data are convincing evidence of carboxyl group localization in the intercrystallite areas on the microcrystal surface.

Conversion of the H-form of CMCCel into the Na-form causes a significant decrease in size of microcrystals, which is the more pronounced, the higher is oxidation degree of CMCCel. This is seen from the broadening of reflections of Cel-I on X-ray patterns of Na-CMCCel, accompanied by a corresponding decrease in their intensities (Fig. 13, curves *2* and *3*). The crystallinity index for Na-CMCCel ($\gamma = 9.1$) goes down to 0.62, and that for Na-CMCCel ($\gamma = 17.5$) – to 0.60. Nevertheless, the core of particles forming the disperse phase of Na-CMCCel hydrogel remains crystalline.

The decrease in microcrystal size and crystallinity may be explained by a strong hydrophilization of the microcrystal surface as a result of salt formation, and by formation of a «water-soluble» fraction of Na-CMCCel from a certain part of oxidized molecules of the surface layer. Most probably, the fraction in question is a colloid-soluble, sol-like one. This fraction, playing the role of a «barrier» between microcrystals, assures the ease of their disaggregation on dispersing the aqueous suspension into the state of hydrogel. It should be noted that O. A. Battista, in his well-known monograph [32], pointed out prospective character and practical significance of topochemically modified MCCel.

Table 3

Sorption values (mg/g) measured for various sorbents and various periods of time using neutral 0,02 % solutions of methylene blue

Sorbent	Duration of sorption, hours	
	3	72
«Ankir» brand MCCel	~ 1.0	4.2
«Medetopect» brand pectin-containing product	24.0	26.5
CMCCel with 3.0 % COOH group content	31.6	32.6

To assess sorptive activity of various CMCCel samples as compared to one another and to commercial enterosorbents available, a bulky organic cation – methylene blue (MB) – was selected as the agent to be sorbed. Of commercially available enterosorbents of polysaccharide nature, «Ankir» brand (Russia) cotton MCCel, and «Medetopect» brand apple pectin-based product were tested. The sorption results are presented in Table 3. According to the experimental conditions, maximum sorption value for the dye from its 0.02 % solution should be 33.3 mg/g. Based on the average period of time that food stays in the stomach, we suggested that the results obtained after sorption period of 3 hours would be the most representative. As seen from Table 3, irrespective of sorption duration, MCCel binds the dye rather poorly, in spite of the fact that its surface is negatively charged [32]. Sorption ability of the acid form of CMCCel with 3 % COOH group contant ($\gamma = 10.9$) is distinctly higher than that of the pectin-based product. During 3 hours, it binds up 95 % of MB, whereas only 72 % binding could be achieved with the «Medetopect» product.

In the case of «Medetopect» product, about 20 % of non-bound dye are still present in solution after 72 h of sorption duration. This value is 10 times as high as the corresponding result obtained with a CMCCel sample.

In Fig. 14, dye sorption isotherms are shown for the samples of H- and Na-CMCCel taken in different forms (powder or hydrogel), and with different degree of carboxylation. All the sorption isotherms are described by the Langmuir equation. As seen, Na-CMCCel hydrogels have the highest sorptive ability, calculated on the basis of dried substance. This can be naturally explained by the maximum accessibility of active sorption centres in the hydrogels. The overwhelming part of the dye is sorbed according to the cation-exchange mechanism. An almost two-fold difference in the degree of oxidation (γ = 9.1 and 17.5) accounts for the corresponding two-fold difference in maximum MB sorption values measured for the two Na-CMCCel gels (195 and 390 mg/g). Maximum MB sorption value for the Na-CMCCel gel (γ = 9.1) makes 109 % of the total exchange capacity (TEC), and the respective value for the Na-CMCCel gel (γ = 17.5) makes 115 % of the TEC. The fact of exceeding the 100 % TEC value may be due to a contribution of physical sorption to the MB binding.

Powder Na-CMCCel samples have significantly lower sorptive ability as compared to gels because the active surface of the sorbent grains is not maximally exposed

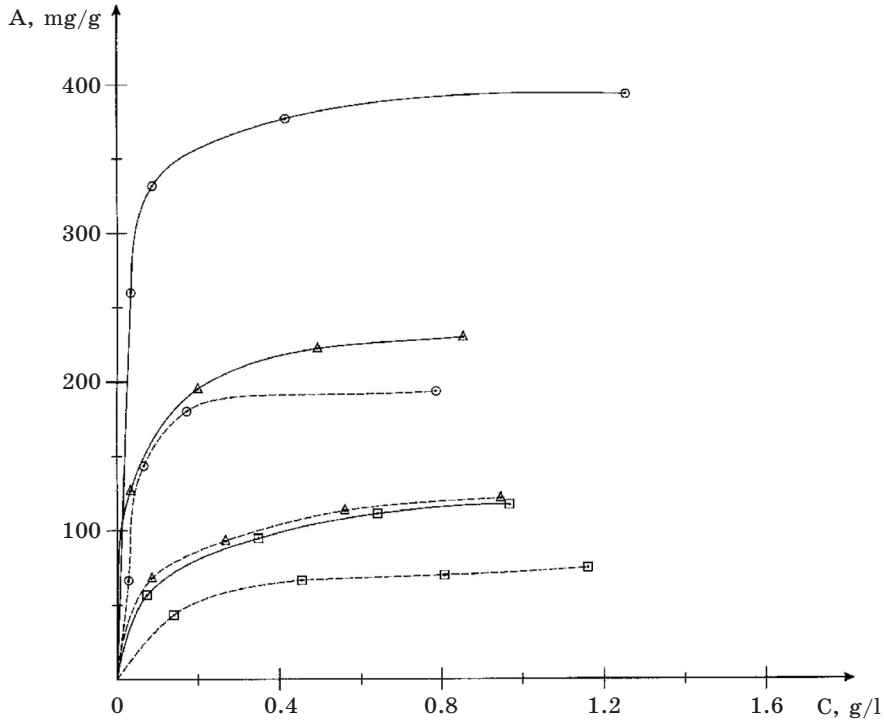

Fig. 14. Isotherms of methylene blue sorption by CMCCel samples containing 4.8 % of COOH groups (solid curves) and 2.5 % of COOH groups (dotted curves). □ – H-CMCCel in powder form; Δ – Na-CMCCel in powder form; o – Na-CMCCel in hydrogel form

in this case. It would be logical to assume the presence of shielding effects as well, exerted by bulky MB molecules already sorbed which prevent access of further molecules to many of the active centres available. The difference in carboxylation degree of powder Na-CMCCel samples (γ = 9.1 and 17.5) results in about two-fold difference in maximum sorption values, similarly to that observed in the case of gels. For these samples, the TEC is filled up to 69 % and 72 %, respectively.

As regards sorption capacity, the salt CMCCel forms have obvious advantages over the acid ones. This logically follows from their higher degree of ionization. It should also be taken into account that interaction of Na-CMCCel macroions with MB in its hydrochloride form results in formation of NaCl salt, whereas the reaction product in the case of H-CMCCel is HCl – a strong acid that shifts the ion exchange equilibrium toward the starting compounds.

The dependence of maximum sorption value on the degree of carboxylation is not so pronounced for H-CMCCel as it is in the case of Na-CMCCel. Maximum MB sorption values for the acid CMCCel forms with 2.5 % and 4.8 % COOH group content are 80 and 118 mg/g, respectively. The TEC fill is higher for the sample with lower degree of carboxylation (48 % vs. 34 %). This fact can be explained by higher degree of dissociation of the former.

In that way, the proposed method of structural chemical modification of cellulose using exclusively a «one-pot reagent» makes it possible to obtain practically valuable materials with microcrystalline morphology, enhanced stability, whiteness and gel-forming ability, and a marked ion-exchanger activity. The aforementioned properties are evidence of a promising character of these preparations as a basis for creation of sorbents for health care applications.

As a result of extended studies of combined oxidative-hydrolytic action of a number of nitrogen- and iodine-containing reagents (nitric acid, periodic acid, nitrogen oxides, etc.) on Cel and properties of the derivatives obtained, methods for preparation of novel Cel-based sorbents with a promising potential of application in medicine have been developed [33, 36]. The range of the sorbents being obtained covers both medications for emergency use as antidotes in cases of poisoning with heavy metals or radionuclides (mainly highly-carboxylated products) [36] and remedies for prevention of chronic intoxications, including the «drug diseases», capable of long-term removal of endogenous toxins or toxic substances from the human organism (mainly low- and medium-carboxylated Cel-based substrates) [37]. New C-based entersorbents in hydrogel form that have now passed clinical testing in gastroenterology and detoxication therapy possess ulcer-enveloping anti-ulcerogenous action superior to that of aluminium-based antacid medications. The latter have the disadvantage of containing aluminium that has undesirable side effects, particularly on long-term use, with a potential of developing «aluminium dementia», Alzheimer disease, etc. Studies of the named enterosorbent gels revealed their innocuous character and their ability to manifest the so-called «parachute effect» – a property highly appreciated by detoxication therapy clinicians. This effect consists in an increase of sorptional ability of a medication in distal areas of the gastrointestinal tract. Other advantages of the new enterosorbent gels include their compatibility with remedies used for similar purposes, e.g. with varous strains of useful microflora, activated carbon, etc. The stabilizing effect of Cel component contributes to increase the shelf life of the final products while significantly decreasing the side effects [37].

Furthermore, these products can be used not only as the main active components, but as a basis for creation of various sustained release drug forms containing other active agents, designed for either internal or external use. For example, cytarabine and its analogues used in ophtalmological practice proved to possess an enhanced efficacy in the form of CMCCel-based eye ointments that we have developed recently [38]. The modified Cel-based enterosorbents of this kind were shown to synergetically enhance the effects of lithium cations as applied in psychiatry, narcology, immunology and cardiology, while suppressing undesired side effects. Active component release studies performed with antibiotics encapsulated in granules of oxidized Cel suggest a potential for the development of corresponding *per os* forms with prolonged action [39].

4. NITRIC ACID DELIGNIFICATION AS A METHOD FOR OBTAINING RADIONUCLIDE-FREE CELLULOSE AND NITROLIGNIN FROM RADIONUCLIDE-CONTAMINATED VEGETAL MATERIAL

Over recent years, a major effort in scientific activity of the Laboratory of Physical Chemistry and Modification of Cellulose at the RIPhChP BSU is focused on the use of nitrogen oxide compounds to enhance efficacy of delignification of straw from various agrocultures. The Cel content of straw from such plants as cereals, rape, and soya is on the same level as that of wood of deciduous species (ca. 50 %). In the case of flax fibres, it attains the value of 80 %. An enormous interest in the low-cost and annually renewable raw materials for obtaining fibrous products is actually manifested worldwide [40–43]. Studies in this area are now on the upgrade. Straw Cel is now produced in thousands of industrial plants [41]. The worldwide consumption of non-wood materials for cellulose production has increased by more than 50 % from 1983 to 1994, and an increase by more than 120 % is forecasted for the year 2010 [43]. Currently, about 12 % of Cel produced worldwide are obtained from annual plants [42].

Owing to features of their morphological structure, the stems of annual plants are the best material for delignification involving HNO_3 [44]. High reactivity of HNO_3 toward lignin determines the main advantages of the process: high rate, moderate temperature, and atmospheric pressure. The two-stage nitric acid method for delignification of vegetal material is actually a modified version of the single-stage alkaline soda method that is widely used. The latter consists in treating the plant material with an alkali solution under relatively hard conditions, whereupon lignin is removed in the form of its soluble derivatives of phenolate type. A pre-treatment of the raw material with HNO_3 solution results in selective nitration and oxidation of lignin, which markedly enhance its solubility during the subsequent alkaline extraction in the second stage.

This has allowed, in particular, a chemical «cottonization» of flax raw material to be performed, rendering it suitable as a substitute for cotton in its conventional application areas (textile industry, etc.). The data obtained in the course of pilot trials of the fibrous product manufactured from this material provide evidence of its high quality and suitability for production of staple fibre yarn. This area of activity appears to be very topical for Belarus where shortages of cotton

raw material are now a problem. We have reported [45–47] the nitric acid delignification conditions for winter rye straw allowing Cel to be isolated in a high yield (up to 50 %), with low residual lignin content (1.7 % vs. 23.5 % in the starting raw material), pentosan content (up to 16.5 % vs. 22.2 % in the starting raw material) and high α-Cel content (up to 90 %). Physico-mechanical tests of the experimental samples have shown that the nitric acid straw Cel can be efficiently used in compositions with WCel for the manufacture of various kinds of paper and cardboard products.

The most significant and promising results have been obtained in experiments on nitric acid delignification of vegetal material grown on radionuclide-polluted territories [48, 49]. It has been discovered that during the delignification process carried out under specific conditions a most complete separation of radioactive mineral components from the plant tissue is achieved. A comparison of deactivating capability was made between the nitric acid method and the alkaline soda one that is most commonly used. The starting materal was winter rye straw from Khoyniki region that had suffered from the Chernobyl accident. Its contamination level for ^{137}Cs was 470 Bq/kg, and for ^{90}Sr – 25 Bq/kg. The final Cel half-product isolated from this raw material using the nitric acid method had the contamination level of 30 Bq/kg for ^{137}Cs and 2.5 Bq/kg for ^{90}Sr. The respective indices for the product treated according to the alkaline soda method were 282 Bq/kg and 15 Bq/kg. When comparing these results it becomes clear that, as regards deactivating ability, the nitric acid version of treatment is superior to the alkaline soda one by an order of magnitude. The high deactivating capability of the nitric acid method was confirmed in experiments with model highly-contaminated raw material – meadow grasses (65500 Bq/kg in ^{137}Cs and 3790 Bq/kg in ^{90}Sr). Treatment of these under conditions of nitric acid delignification allows the radioactivity level of the final solid residue to be reduced more than 200 times for ^{137}Cs and more than 250 times – for ^{90}Sr, with respect to the initial values. Along with this, it is important to note that the major part of radionuclides is extracted, in a practically selective manner,in the first stage of acid treatment, and the lignin extracts obtained in the second stage are of a relatively low activity. The high selectivity of radionuclide extraction is probably due to good solubility of nitric salts being formed. Liquid radioactive waste will be localized in the initial stage of the process. Then, they can be concentrated, converted into some solid state form using one of the known technologies and safely disposed of. In this connection, the technology of extracting radionuclides from liquids by means of widely used industrial sorbents (ceolites) appears to be acceptable. The nitric acid delignification can be performed using both commercial and the so-called «missile» nitric acid that contains such additives as N_2O_4, I_2, HF and H_3PO_4 and is the main component of missile fuel. After nuclear missile disarmament of Republics of the former USSR, large quantities of unclaimed 'missile' nitric acid were left on their territories. Storage of this material in concentrated form in the absence of special conditions is rather dangerous, whereas its utilization is problematic and expensive. In the periodic press, there were several communications about leakage of this oxidant from depositories in the Far East of Russia. Even these relatively minor episodes of leakage involved human casualties and pollution of air and water resources over large territories. The proposed version of utilization of nitric acid solutions in a diluted form will not entail technological or environmental problems.

The obtained results are in direct relation to the development of rational technologies for rehabilitation and deactivation of territories polluted with radionuclides and heavy metals as a result of technogenous accidents, military tests or hostilities, and terrorist attacks.

The post-Chernobyl experience has shown that essentially two types of agricultural technologies are acceptable on polluted territories.

The first one, the so-called agrotechnical or agrochemical counter-measures, is based on a regular heavy application of various fertilizers into the soil. This promotes competitive absorption of cations – analogues of radionuclides – by the plants, leaving radionuclides themselves in the soil and decreasing thereby the radionuclide uptake by the plants being used as fodder or for food production [50, 51]. However, the costs required are quite high, and no soil deactivation is achieved According to [52], any counter-measures undertaken at present, i.e. after a long time after the Chernobyl disaster has broken out, are economically unjustified in ^{137}Cs pollution zones with less than 370 kBq.m^{-2}.

Technologies of the second type, which are less studied but very promising, are based on cultivation of technical (non-nutritional) plants whose seeds are raw material for obtaining radionuclide-free products. In Belarus, on territories with pollution density of 370 to 555 kBq.m^{-2} of ^{137}Cs, and 37 to 55 kBq.m^{-2} of ^{90}Sr, the culture of rape has already been introduced, and radionuclide-free oil was extracted from its seeds [51, 53]. Average accumulated radionuclide level of the rape seeds as compared to the rape straw is 1.5 times lower for ^{137}Cs, and 2.6 times lower for ^{90}Sr [53]. After oil extraction, the radionuclide content of the oilcake becomes doubled whereas almost none is found in the rape oil [53]. In an effort to recover for rural economy 500,000 ha of soil contaminated with strontium and caesium, sowing all these territories with rape is planned in Belarus. Studies are also underway aimed at improvement of soya and flax cultivation technologies on these territories with a view to obtain competitive products from the respective seeds. Along with obtaining radionuclide-free products, a phytodeactivation of contaminated soil, i.e. progressive purification due to radionuclide uptake by the plants, is achieved using this technology [54]. A large interest in phytodeactivation technologies is actually manifested in many countries.

Agrotechnical products are not intended for nutritional purposes. Therefore, the efficiency of technologies of the second type should be evaluated primarily from the point of view of economical and environmental expediency, and not using directly the deactivation coefficient, as is generally done in the case of the first type technologies [51]. One can admit an arbitrarily high deactivation coefficient value provided that radionuclides cannot come into a human organism some other way, say, by inhalation of contaminated smoke. Nevertheless, the production residues in the form of straw where the major part of radionuclides is accumulated are disposed of by incineration. In the course of this procedure, certain amounts of radionuclides are usually dispersed into the environment with the smoke particles, even if special equipment is used [55]. Thus, a problem of utilization of contaminated straw from the technical agriculture plants does exist. For example, after harvesting rape seeds, up to 5 t of contaminated straw per hectare is left as residues.

Obtaining radionuclide-free Cel and nitrolignin from the straw of technical agrociltures is profitable from economical and ecological point of view. This ap-

proach opens additional possibilities in reducing costs for rehabilitation and deactivation of polluted territories by increasing the range of commercial products being in a stable demand on the market. Cel value is 4–5 times higher than that of the energy obtained on combustion of the same quantity of Cel-containing material. Bringing nitrolignin into contaminated soil will enrich it with humin-like substances and prevent wind erosion and radionuclide transportation with the dust. It will reduce to a minimum the secondary contamination, prevent radionuclide transportation through the «nutritional chain» and provide a progressive deactivation of the soil.

The research work in this area is conducted in the framework of a project approved by the International Science and Technology Center (ISTC) financially supported by EC.

REFERENCES

1. *Gert E. V.* // Russian Chem. Reviews. 1997. Vol. 66. №. 1. P. 73–92.
2. *Socarras-Morales A., Bobrovskii A. P., Gert E.V.* and *Kaputskii F. N.* // Zh. prikl. khimii. 1982. Vol. 55. №. 10. P. 2364–2365.
3. *Gert E. V., Socarras-Morales A., Makarenko M. V.* and *Kaputskii F. N.* USSR Author's Certificate №. 1035030 (1983).
4. *Philipp B., Lukonoff B., Schleicher H.* and *Wagenknecht W.* // Z. Chem. 1986. Bd. 26Jg. S. 50–58.
5. *Komarova Z. B., Averyanova V. M., Efremova O. G* and *Kaybusheva R. Kh.* // Khim. volokna. 1979. №. 4. P. 31–34.
6. *Batura L. I., Vichoreva G. A.* and *Noreika R. M.* // Cellulose Chem. Technol. 1981. Vol. 15. P. 487–492.
7. *Torgashov V. I., Bil'dyukevich A. V., Gert E. V., Kaputskii F. N., Syatkovskii V. A.* and *Vasilenko L. P.* // USSR Author's Certificate №. 1244151 (1986).
8. *Torgashov V. I., Bil'dyukevich A. V., Gert E. V.* and *Kaputskii F. N.* // USSR Author's Certificate №. 1381118 (1987).
9. *Torgaschow W. I., Gert E.W., Bildjukewitsch A. W., Kaputskii F. N.* // Angew. Makromol. Chem. 1996. Bd. 234. S. 31–38.
10. *Torgashov V. I., Bil'dyukevich A. V., Gert E. V.* and *Kaputskii F. N.* // Report at the II USSR Conference on Microbial Polysaccharides. Leningrad. 1984. P. 59.
11. *Torgashov V. I., Gert E. V.* and *Tyurin V. I.* // Report at the USSR Conference «Application of Cellulose and Derivatives in Health Care and Microbiology Industry». Moscow. 1989. P. 54.
12. *Atroshchenko V. E.* and *Kargin S. I.* Nitric acid technology (Russ.) 3-th ed. Moscow. 1970. 496 p.
13. *Knecht E.* // Berichte. 1904. Bd. 37. S. 549–552.
14. *Andress, K. R.* // Z. Phys. Chem. 1928. B. 136. S. 279–288.
15. *Goikhman A. Sh.* and *Solomko V. P.* Macromolecular inclusion compounds (Russ.). Kiev. 1982. 192 p.
16. *Gess K.* Chemistry of cellulose and its concomitant compounds. (Russ.) Leningrad. 1934. 620 p.
17. *Gert E. V., Socarras-Morales A., Zubets O. V.* and *Kaputskii F. N.* // Cellulose. 2000. Vol. 7. P. 57–66.
18. *Gert E. V., Zubets O.V., Shishonok M. V., Torgashov V. I.* and *Kaputskii F. N.* // Zh. prikl. Khimii. 2003. Vol. 76. №. 4. P. 616–620.

19. *Shishonok M. V., Gert E. V., Filanchuk T. I.* and *Kaputskii F. N.* // Zh. prikl. Khimii. 1987. Vol. 60. №. 5. P. 1153–1157.
20. *Nikitin N. I.* Wood and cellulose chemistry (Russ.). Moscow-Leningrad. 1962. 706 p.
21. *Ioelovich M. Ya.* and *Veveris G. P.* Delignification and cellulose chemistry (Russ.). Riga. 1991. 176 p.
22. *Papkov S. P.* and *Fainberg E. Z.* Interaction of cellulose and cellulosic materials with water (Russ.). Moscow. 1976. 232 p.
23. *Gert E. V., Shishonok M. V., Torgashov V. I. and Kaputskii F. N.* // J. Polym. Sci. Part C: Polym. Letters. 1990. Vol. 28. P. 163–166.
24. *Nelson M. L.* and *O'Connor R. T.* // J. Appl. Polym. Sci. 1964. Vol. 8. P. 1311–1324.
25. *Gert E. V.* // Cellulose. 1996. Vol. 3. №. 4. P. 217–228.
26. *Gert E. V., Socarras-Morales A., Zubets O. V., Matyul'ko A. V., Shishonok M. V., Torgashov V. I.* and *Kaputskii F. N.* // Report at the II Kargin Symposium «Polymer Chemistry and Physics at the Beginning of XXI Century» Chernogolovka (Russia). 2000. Pt. 1. P. 1–82.
27. *Gert E. V., Socarras-Morales A., Matyul'ko A. V., Shishonok M. V., Zubets O. V., Torgashov V. I.* and *Kaputskii F. N.* // Vestnik Belorus. Univ. 2000. Ser. 2. №. 2. P. 7–15.
28. *Gert E. V., Shishonok M. V., Zubets O. V., Torgashov V. I.* and *Kaputskii F. N.* // Polymer Science. 1995. Ser. A. Vol. 37. №. 7. P. 1137–1144.
29. *Blazicek I., Cerny P., Langr S.* and *Uhlir J. A. O.* 221227. CSSR (1986).
30. *Korol'kov I. I.* Percolation hydrolysis of vegetal raw material (Russ.) 2-nd ed. Moscow. 1978. P. 41.
31. *Gert E. V., Torgashov V. I., Shishonok M. V., Sinyak S. I.* and *Kaputskii F. N.* // J. Polym. Sci. Part B: Polym. Physics. 1993. Vol. 31. P. 567–574.
32. *Battista O.A.* Microcrystal Polymer Science. New York. 1975. 208 p.
33. *Gert E. V., Zubets O. V., Shishonok M. V., Torgashov V. I.* and *Kaputskii F. N.* // Vestnik Belorus. Univ. 2003. Ser. 2. №. 1. P. 3–9.
34. *Ermolenko I. N.* Spectroscopy in oxidized cellulose chemistry (Russ.). Minsk. 1959. 291 p.
35. Rutkowski J., Perlinska-Sipa. // Cellulose Chem. Technol. 1994. Vol. 28. P.35–42.
36. *Torgashov V.I., Zubets O.V., Socarras-Morales A., Gert E.V., Shishonok M.V.* and *Kaputskii F. N.* // Report at the II Kargin Symposium «Polymer Chemistry and Physics at the Beginning of XXI Century» Chernogolovka (Russia). 2000. Pt. 2. P. 4–47.
37. *Torgashov V. I., Gert E. V., Zubets O. V., Kaputskii F. N., Plenina L. V., Khl'ustov S. V.* and *Derevnina O. N.* // Report at the International conference «New medications: synthesis, technology, pharmacology and clinics» Minsk. 2001. P. 148–149.
38. *Zubets O. V., Torgashov V. I., Larchenko L. V., Kaputskii F. N., Gert E. V., Kalinichenko E. N.* and *Girina O. E.* // Report at the International conference «New medications: synthesis, technology, pharmacology and clinics» Minsk. 2001. P. 53–54.
39. *Torgashov, V. I., Zubets O. V., Kaputskii F. N.* and *Gert E. V.* // Report at the International conference «New medications: synthesis, technology, pharmacology and clinics» Minsk. 2001. P. 147–148.
40. *Atchison J.* // Tappi. 1996. Vol. 79. №. 10. P. 87–95.
41. *Van Roekel G. J.* // J. Int. Hemp Assoc. 1994. Vol. 1. №.1. P. 12–15.
42. *Bowyer J. L., Stockmann V. E.* // Forest Product Journal. 2001. Vol. 51. №. 1. P. 10–21.
43. *Pande H.* // Unasylva. 1998. Vol. 49. №. 193. P. 44–49.
44. *Nipenin N.N.* and *Nipenin Yu.N.* Cellulose technology. Vol. III. Purification, drying and bleaching of cellulose. Other methods of cellulose production. (Russ.) Moscow. 1994. 590 p.
45. *Shishonok M. V., Torgashov V. I., Zubets O. V., Gert E. V.* and *Kaputskii F. N.* // Vestnik Belorus. Univ. 1996. Ser. 2. №. 2. P. 3–9.
46. *Shishonok M. V., Torgashov V. I., Gert E. V., Zubets O. V.* and *Kaputskii F. N.* // Materialy, technologii, instrument. Minsk. 1996. №. 3. P. 67–72.

47. *Shishonok M. V., Torgashov V. I., Gert E.V., Zubets O. V.* and *Kaputskii F. N.* // Cellulose Chem. Technol. 1997. Vol. 31. P. 425–438.
48. *Torgashov V. I., Zubets O. V., Shishonok M. V., Gert E. V.* and *Kaputskii F. N.* // Materialy, technologii, instrument. Minsk. 1996. №. 2. P. 103–104.
49. *Torgashov, V. I., Gert, E. V., Zubets, O. V., Shishonok, M. V., Kaputsky, F. N.* // International Ecological Congress. Voronezh. Russia. September 22 – 28. 1996. Proceedings and Abstracts. Section: Technology and the Environment. Korenman M.Y. ed. Kansas State University. Manhattan. Kansas. U.S.A. 1996. P. 37.
50. *Aleksakhin, R. M., Fesenko, S. V., Sanzharova, N. I.* // Proceedings of International Radiological Post-Emergency Response Issues Conference. Washington. 1998. P. 113.
51. Strategies of Decontamination. Final report by the project ECP-4: EUR 16530 EN. Brussels-Luxembourg. 1996. 174 p.
52. *Fesenko S.V., Sanzharova N.I. and Aleksakhin R.M.* // Radiation Biology. Radioecology. 1998. Vol. 38. №. 3. P. 354–366.
53. *Putyatin Yu.* // XXIX ESNA Annual Meeting and International Union of Radioecology (IUR) Working Group Soil-to-Plant Transfer Annual Meeting. September 7 – 12. 1999. WYE College. University of London. UK. P. 17.
54. *Raskin I.* // Environm. Sci. and Technol. 1995. Vol. 29. P. 1239–1245.
55. Report at the International Conference «Science and Medicine for Chernobyl». Minsk. 1993. 184 p.

CHEMICAL PROBLEMS OF THE DEVELOPMENT OF NEW MATERIALS AND TECHNOLOGIES
Minsk 2003

**D. D. Grinshpan, T. A. Savitskaya,
N. G. Tsygankova**

NON-TRADITIONAL SOLUTIONS OF CELLULOSE AND ITS DERIVATIVES AND PRODUCTS OF THEIR TREATMENT

The main achievements of the Laboratory of cellulose solutions and products of their treatment lie in the following fields:

1) the elaboration of new cellulose dissolving processes;

2) the homogeneous synthesis of cellulose derivatives;

3) the elaboration of the incompatible polymer solutions stabilization method;

4) the creation of new film – fabric materials and filtering equipment on their base;

5) the preparation of solid quickly disintegrated drug forms (tablets, granules) using new water soluble cellulose derivative.

1. NEW PROCESS FOR THE PREPARATION OF HYDROCELLULOSE FIBRES WITHOUT CARBON DISULFIDE

For the purpose of cardinal protecting the environment while producing hydrocellulose fibres and films it is necessary to create a new process allowing for the transmission of cellulose into a dissolved condition without using of carbon disulfide. One of the alternatives suggested herein is to use the $ZnCI_2$–H_2O dissolving system, according to which concentrated solutions of cellulose have been recently received. They are suitable for forming of fibres and films with satisfactory physico-mechanical characteristics [1–4].

The Dissolving of Cellulose in Aqueous Zinc Chloride Solutions

It is known that 62–65 % aqueous zinc chloride solutions at the temperature of 65 °C and more dissolve cellulose. When dropping the concentration or temperature of the zinc chloride solution, or increasing the content of salt in the solution more than 70 % (mass), there is only a swelling of cellulose [5]. These properties of concentrated zinc chloride solutions that under certain conditions cause either swelling or dissolving of cellulose, discovered in 1850, served as a basis for a set of practical proposals for their use, namely: for mercerization of cotton, receiving of vulcanized fibre, preparation of spinning solutions, and forming of rayons [6, 7]. But numerous attempts to produce the fibre and film from cellulose solutions in zinc chloride failed because of the strong destructive action of the solvent, that is why zinc chloride aqueous solutions found industrial application in the production of fibre [8]. In 1984 it was announced in Japan that it was possible to

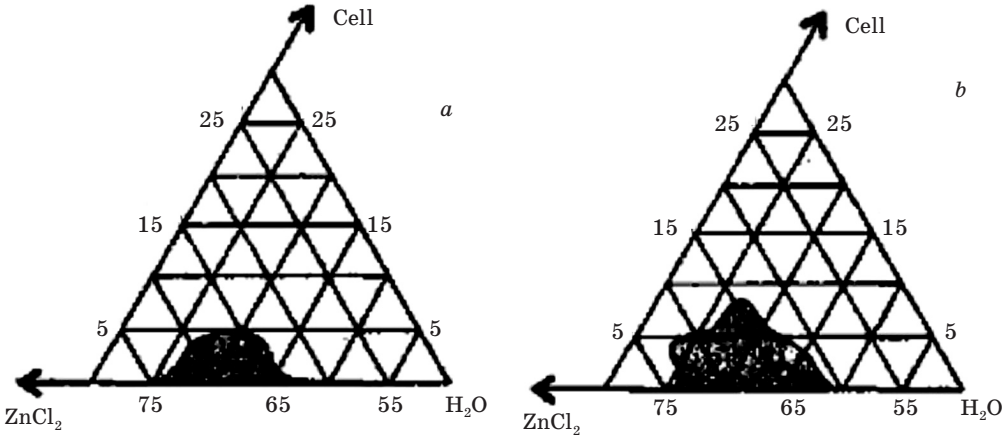

Fig. 1. The diagrams of dissolubility of sulphate cellulose (DP 740) in the following dissolution conditions:
a) the «direct» method of dissolution: in 65 % $ZnCl_2$ at the temperature of 75 °C;
b) our method [9]: swelling in 80 % $ZnCl_2$ at the temperature of 75 °C for an hour, dissolution – in 65 % $ZnCl_2$ for 4 hours.

obtain cellulose spinning solutions using cotton from a 67 % $ZnCl_2$ aqueous solution at temperature of 80–105 °C by means of preliminary treatment of the initial material for 5 minutes with zinc chloride solutions concentration being equal or greater than to 79 %. Fibres from the obtained solutions were formed by dry-wet method into the spirituous bath with tensile strength of 13,5 cN/tex and elongation of 18 %.

The suggested method was used for dissolving of high-molecular cotton cellulose and at the time appeared to be worthless for dissolving of wood cellulose, that was widely used in xanthate spinning solution production.

All this predetermined the necessity of carrying out of further experiments in order to find optimal conditions of different kinds of celluloses dissolving in zinc chloride aqueous solutions. The data obtained indicated that, as regards to the immediate influence upon the cellulose of zinc chloride hot aqueous solutions (T > 50 °C), only a limited range of aqueous solutions composition ($ZnCl_2$– 60–73 %) can be considered as the solvent of cellulose. Maximum dissolving capability in regard to cellulose are possessed by 65–68 % zinc chloride solutions at a temperature of 75 °C. But the dissolving of cellulose in them is rather limited and composed, for sulphate cellulose (DP 740), less than 5 % (Fig. la), which is not sufficient for use as a spinning material. Increasing the dissolving time up to 8 or more hours or increasing the temperature of process more than 75 °C brings about a sudden reduction of cellulose DP, but does not allow for increasing the concentration of cellulose in solution. We prepared more concentrated solutions (more or equal to 6 %) by reproducing the method [2], but they did not possess spinning quality due to significant destruction.

For example, the DP of sulphate cellulose (DP 740) precipitated from a 6 % solution was 210. By modifying the conditions of influence of zinc chloride depending on the type of cellulose (cotton, sulphate, hydro-cellulose) we established that the pure cellulose concentrated solutions (C = 6–12 %), keeping DP equal or

greater than 300, can only be obtained by means of preliminary treatment by solutions $ZnCl_2$ of non-dissolved composition which allow for implementation of a steady distribution of zinc chloride into the volume of cellulose material. This method was used as a base for all the methods that we suggested for dissolving cellulose [9, 10]. For example, one of the methods [9] provides the activation of cellulose by highly concentrated solutions (the concentration $ZnC1_2$ being greater or equal to 75 %) and consists of following stages: the preparation of a 75–84 % zinc chloride aqueous solution and heating it up to a temperature of 70–80 °C. The insertion of grinded cellulose into the prepared zinc chloride aqueous solution and conducting the process of cellulose swelling for 0.5–2.0 hours at a temperature of 70–80 °C;

Addition of water into the received homogeneous fibrous mass which is necessary for diluting the 75 – 84 % zinc chloride solution to a dissolving composition (63–67 %), reducing the temperature of treatment to 65–75 °C and intense mixing of this mass until it forms a homogeneous viscose-flow solution are the stages of cellulose solution preparation.

For this method of cellulose solution preparation, the diagram of dissolving-sulphate cellulose (DP 740) is given at Fig. 1b. From this diagram it follows that in this case the maximum dissolubility of cellulose is 8,5 %. This 2.0–2.5 times higher than under the direct dissolution of cellulose in 65–68 % $ZnCl_2$ (Fig.la). The importance of using the developed method with regard to different kinds of cellulose is illustrated by the data (Table 1), which show that the maximum concentration of cellulose in the system $ZnCl_2 – H_2O$ defines not only its DP but a set of other factors, including: the origin of cellulose; conditions of delignification; and the degree of structural heterogeneity. The wood celluloses received according to sulphite and sulphate methods possess the best dissolubility in zinc chloride.

Table 1

Several characteristics of the solutions of different kinds of cellulose in zinc chloride and the DP of the fibres moulded from them

Type of cellulose	Max concentration of the cellulose in the solution [%]	Viscosity of 5% solution at 70 °C [Pa/s]	DP initial	DP of the fibre
Sulphate of the Priosersky CPP	8.5	20	740	340
Sulphate Cord	7,0	90	1150	400
Sulphite of the Priosersky CPP	8,0	60	1070	380
Sulphite of the Priosersky CPP	8,0	32	1280	390
Cotton of the Bratsk CPP	7,0	100	1350	390
Cotton of the Svetlogorsk CPP	5,0	110	1000	420
Hydrocellulose	12,0	48	400	300

Table 2

Dependence of DP and viscosity of 7 % sulphate cellulose solution (DP 1070) from duration (F) of storage and temperature (T)

T	F	η	DP	T	F	1	DP
°C	h	Pa·s	–	°C	h	Pa·s	–
70	0	100	380	70	12	12	270
70	0.5	90	370	55	1	210	370
70	1	80	370	39	2	jelly	380
70	2	45	360	20	3	jelly	380
70	3	30	350	20	72	jelly	370
70	8	25	300	20	150	jelly	
70	10	20	280				

Table 3

The influence of calcium chloride on changing the viscosity of 5 % sulphate cellulose solution and its DP in the process of thermostatory solutions at the temperature 75 °C

The time of the thermostatory h	The quantity of calcium chloride (% from mass $ZnCl_2$)					
	0		0.2		0.5	
	DP	η [Pa·s]	DP	η [Pa·s]	DP	η [Pa·s]
0	410	80	440	90	465	105
1	320	26	410	30	420	33
2	300	8	290	14	300	15
4	250	3	260	5	260	5

Their spinning solutions present transparent, viscous liquids. When considering them under a microscope in polarized light it is determined to be no more than 2–3 cellulose fragment and they are according to the main indexes of viscosity, DP cellulose, and concentration of solutions, suitable for further processing into hydrocellulose goods.

The Properties of Spinning Cellulose Solutions in Aqueous Zinc Chloride

Spinning cellulose solutions in zinc chloride with a temperature of preparation of 70 - 75 °C have significantly high viscosity 50–100 Pa s, which is rapidly increased when cooling (Table 2). At 18–20 °C 6–9 % cellulose solutions in zinc chloride are converted into transparent thermo-convertible jellies, which after 20–40 hours of storage become dimmed and form regulated supermolecular structures – crystal/solvates with spherulite dimensions from a dozen micrometers up to 1–2 mm. Spherulites have a legibly expressed ring structure, crossed by a cross (Fig. 2). When heating spherulites separated from the original solution in the temperature interval of 45–50 °C, their congrugated melting occurs with a homogeneous transparent solution at which the concentration of cellulose reaches 10 %.

Fig. 2. Spherulites, produced from 5 % solution of sulphite cellulose in aqueous solutions of zinc chloride (x 290)

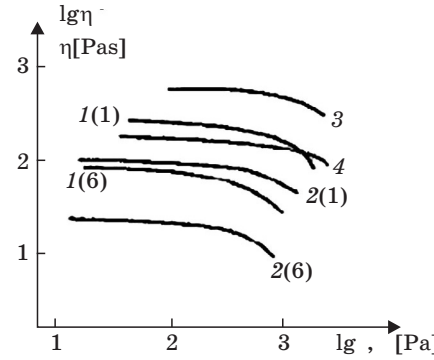

Fig. 3. The flow curves of 5 % solutions of sulphate cellulose in zinc chloride at 50 °C (*1*) and 70 °C (*2*) an the first and sixth days (they are figured in brackets) of their keeping at 20 °C and of 7 % solutions of cotton cellulose at 50 °C (*3*) and 70 °C (*4*).

Research into the stability of spinning cellulose solutions in zinc chloride demonstrated that at temperatures exceeding 70 °C there is a rapid decrease in viscosity. In spite of this, the spinning solution can not, depending on the kind of cellulose, remain in the increased temperatures for more than 3–8 hours. Otherwise the DP of the cellulose in the solution falls (due to 1, the destruction processes which are especially intensive if the temperature is above 50 °C) to a value lower than 300. This brings about a loss of the fibre - and film - making properties of the solutions. The experiments we have carried out show that the degree of cellulose destruction may be lowered, by the addition to the solution some amount of calcium chloride – about 0.2–0.5 % of the mass of the zinc chloride (Table 3). But at the same time a supplementary rise of the cellulose solution's viscosity takes place, and this is not desirable.

The solution's «life» can be increased owing to a more simple method by keeping the solution made at a reduced temperature (10–20 °C), which delays the destruction processes considerably, and when it is time to mould, by heating the solution to the temperature of viscose-flow condition ($T > 50$ °C).

The cellulose solutions in zinc chloride are not sensitive to shear deformations and in the area of displacement tensions from 4 to 200 Pa conduct oneself as Newton's liquids (Fig. 3). The rising of the temperature from 50 to 70 °C or maintaining at 18–20 °C practically speaking doesn't influence the flow of the solution.

Taking into consideration these peculiarities of cellulose solutions' conduct in zinc chloride, we determined conditions for moulding fibres and films.

The Moulding of the Hydrocellulose Fibres

The remaking of cellulose solutions into rayons was carried out at the spinning-plants by the wet and dry-wet methods of moulding. The most stable results were carried out by the wet shallow-bath method of moulding using horizontal spinning units.

Table 4

The influence of the coagulation medium composition on the fibres' physical-mechanical characteristics, moulded from 7 % solutions of sulphite cellulose in zinc chloride

Coagulation medium	Temperature of the coagulation medium °C	Tensile strength cN/tex	Elongation %
Ethanol	20	15.8 ± 1,1	7.9 ± 1.7
Ethanol – Water	20	13.2 ± 0.6	10.4 ± 1.3
Ethanol – Water – Zinc Chloride	20	13.6 ± 0.9	12.1 ± 1.1
Isopropanol	35	11.9 ± 0.4	7.5 ± 1.1
Isopropanol – Water	35	14.6 ± 0.7	10.8 ± 0.8
Isopropanol – Water – Zinc Chloride	35	16.8 ± 0.6	13.4 ± 0.5
Ethylene – Glycol – Water	40	14.7 ± 0.5	5.9 ± 0.8
Ethylene – Glycol – Water – Zinc Chloride	40	18.4 ± 1.4	6.0 ± 1.2
Glycerin – Water – Zinc Chloride	40	15.6 ± 0.3	12.8 ± 0.6

It was determined that water-alcohol mixtures have the best coagulation ability for cellulose solutions in zinc chloride. In place of alcohol, ethyl, isopropyl, ethyleneglycol, and glycerine were substituted. The results obtained regarding the influence of the coagulation medium on the properties of the hydrocellulose fibres are set forth in the Table 4. From the data given in the table it follows that both the kind of spirits and their amount in the coagulation bath influence the physical-mechanical characteristics of the fibres. Comparing the properties of the fibres formed in a coagulation medium, which contains ethanol, isopropanol, and ethyleneglycol, one can see that the fibres which were moulded in the water-isopropanol coagulation medium have a better complex of physical- mechanical characteristics (tensile strength and elongation). The pure spirits (ethanol and isopropanol) are sufficient hard precipitates for the cellulose solutions in zinc chloride, and addition to water, which is one of the components of the cellulose solvent, lead to a softening of the coagulation conditions and to the improvement of the entire complex of the fibre's characteristics (strength and elongation). The fibres which were moulded in the coagulation medium containing zinc chloride have much better results as regards physical-mechanical characteristics.

The Table 4 shows that, besides ethanol and isopropanol, the water solutions of ethyleneglycol and glycerin were used, and while moulding into these solutions hydrocellulose fibres were obtained, whose physical-mechanical characteristics are not worse than the those of the viscose fibres.

The analyses carried out regarding the main factors which determine the process of the mould (the speed of the supply of the spinning solution, the speed of receiving, the temperature, and composition of the coagulation medium, etc.) and determination of the parameters of the orientational elongation of the fibre allowed for obtaining hydrocellulose fibres, which are close in their physical-mechanical properties to ordinary viscose fibres of the wool type, and in some characteristics even exceed them. From Table 5, which illustrates a comparison of the properties of the experimental fibres with different types of viscose fibres produced by

Fig. 4. The cros-ssection of the experimental fibre moulded from 6 % solution of sulphate cellulose in zinc chloride (x 730)

industry, one can see that the moulded fibres in the standard conditions have tensile strength from 15 to 25 cN/tex with elongation from 15 to 25 %. The experimental fibres have more strength in the loop (10–13 cN/tex), and are characterized by a high elasticity modulus both when dry and wet (4500–1300 MPa). The diametrical cut of the experimental fibres has a correct round form such as is typical of the diametrical cuts of viscose high modulus and polynose fibres (Fig. 4).

Table 5

The comparative properties of the experimental and different types of viscose fibres

Characterization		Experimental fibre	The viscose fibres			
			Ordinary of the		High Modules	Polynose
			Wool type	Cotton type		
Linear density, tex		0.36–1.1	0.32–0.55	0.17–0.2	0.13–0.17	0.13–0.17
Strength, cN/tex		15–25	16–20	22–25	32–34	36–38
Elongation, %		15–25	21–30	19–24	16–20	3–13
Elasticity modulus, cN/tex		450–1100	150–200	280–300	240–260	–
Strength, cN/tex	when wet	7–10	8–10	11–12	20–22	26–28
	in the loop	12.0–16.0	5.0–6.0	7.0 – 8.0	9.0–9.5	4.5–5.5
Elongation when wet, %		18–27	24–28	24–27	18–24	10–15
Elasticity when wet, cN/tex		45–130	20–30	30–40	80–120	200–250
Solubility in the 6% of NaOH, %		14–16	20–22	20–22	4–8	1,5–3,0
Steadiness to the double pends, thousands of cycles		1.0–2.0	3.0–3.5	30–40	3,0–4,0	–
Swelling in the water, %		110–140	110–120	100–110	65–75	55–65
Water sorption, %		12.5–13.0	12.0–13.5	7.5–8.5	12.5–13.0	11.0–12.0
DP		300–450	280–320	280–320	350–400	450–550

The change of the dissolution and precipitation conditions helped to simplify moulding of the fibres in comparison with method [2], i.e. to exclude the using of the air streak, and to improve the properties of the moulded fibres.

The Production of the Hydrocellulose Films

The production of the hydrocellulose films was realised by sprinkling the cellulose solution in the zinc chloride either on a smooth polished surface or on the reinforced paper layer (in the case of production of reinforced films) with the future regeneration into the coagulation mediums of the different compositions. Table 6 shows that the composition of the medium greatly influences the physical-mechanical characteristics of the films formed, especially their tensile strength. For example, during moulding into an acid coagutation medium, which is also used with the viscose process in the production of cellophane, the tensile strength of the films which are produced by the cellulose solution in zinc chloride is greatly reduced.

The highest tensile strength of hydro - cellulose films is attained when water-spirit mixtures, which contain zinc chloride, are used in the coagulation medium. By means of changing the composition of the mixture «water-spirit-zinc chloride» and the type of the spirits used films were produced which have a strength from 60 to 100 MPa and an elongation from 6 to 9 % without any plastification.

At the same time in the laboratory conditions we have obtained hydro-cellulose films (sausage wrappers) reinforced by paper with a tensile strength of 35 to 60 MPa, moulded in various coagulation mediums. It was established that physico-mechanical properties of reinforced films are determined not only by the composition of the coagulation medium, but also to a considerable degree depend on the properties of the reinforcing material. Sanitary and hygienic tests indicated the nontoxicity of the reinforced films obtained from the aqueous solutions of cellulose in zinc chloride and their applicability for the manufacture or sausage wrappers.

Table 6

The mechanical properties of the films moulded from solutions of sulphate cellulose in zinc chloride

Coagulation medium	Tensile strength MPa	Elongation %
Sulphuric acid – Water	62 ± 8	7.7 ± 0.4
Sulphuric acid – Sulphate of Zinc – Water	33 ± 2	7.3 ± 0.5
Sulphuric acid – Sulphate of Zinc – Sulphate of Sodium – Water	49 ± 3	7.3 ± 0.4
Ethanol	58 ± 18	7.4 ± 1.0
Ethanol – Water	87 ± 13	6.6 ± 0.2
Isopropanol	70 ± 5	7.8 ± 0.5
Isopropanol – Water	80 ±13	8.2 ± 1.2
Isopropanol – Water – Chloride of zinc	96 ± 4	8.4 ± 0.2

The Compatibility of Cellulose and Its Derivatives with Synthetic Polymers in Aqueous Solutions of Zinc Chloride

The use of aqueous solutions of zinc chloride as dissolvent opens up wide-ranging possibilities for the compatibility of cellulose with many synthetic high molecular compounds dissoluble in $ZnCl_2$, as well as for the manufacture of composites possessing the properties of both mixed polymers. We have obtained compatible solutions of cellulose which possess a high kinetic stability with polyvinyl alcohol, polyacrylonitrile and its copolymers, diacetyl-, methoxypropyl, oxyethyl-, diethylaminoethyl-, and phosphate cellulose, Besides, the real dissolubility of polymers in each other is a rather small percentage. For the system of cellulose-alcohol it is, for example, not more than 3–5 %.

We have studied the cellulose - polyacrylonitrile system over a wide scope of compositions (of 5 : 95 to 95 : 5) and have found the order and optimal conditions for the manufacture of compatible solutions. We have also taken rheograms of their viscosity and examined stability of the solutions at various temperatures and time conditions. It was established that a small addition of PAN (5–20 %) to cellulose or, vice versa, an addition of cellulose to PAN, causes a diminution in the first case and an increase in the second of the solutions' viscosity of corresponding initial polymers.

A 1–30 day observation of the solutions of cellulose – PAN, at a temperature of 20–25 °C and in composition 50 : 50 (which is the least acceptable for compatibility) did not reveal any efficient indications of stratification; this fact proves rather kinetic stability of the compatible solutions of cellulose – PAN in zinc chloride. Concentrated compatible solutions, as well as those of cellulose only, were manufactured in laboratory conditions with the use of a spinner. It was established that for solutions with 50 or more percent of cellulose the best coagulation conditions are the following: the coagulation medium - water-isopropyl alcohol-zinc chloride; temperature of coagulation – 35–40 °C. For solutions with a considerable PAN concentration the conditions are as follows: coagulation medium – water – zinc chloride; temperature – 10–15 °C. The fibre moulded in these conditions in the composition of cellulose-PAN with the ratio of 90 : 10 and 10 : 90 has tensile strength and elongation of 15.6 cN/tex, 14 % and 25,2 cN/tex, 32 %, which makes it possible to produce cellulose fabrics modified by PAN addings and polyacrylonitrile fabrics modified by cellulose in the $ZnCl_2 – H_2O$ dissolving system.

A Schematic Diagram of the Process of Obtaining Hydrocellulose Fabrics from Cellulose Solutions in Zinc Chloride

As a result of our comparative examination of concrete technological stages of the viscose and experimental methods, we have proposed a diagram of the process of obtaining hydrocellulose fabrics from cellulose solutions in zinc chloride (Fig. 5). In comparison with the viscose process, the experimental one consists of far fewer technological cycles. It elliminates the stages analogous to those of the first ripening, xanthation, and second ripening; and when finishing the fabric some stages may also be omitted, for example, distillation of carbon disulfide, acidification, and desulphuration. Besides, there is no need of viscose and alkaline drains or damping pits. It makes it possible to considerably diminish the industrial areas and the labor-consuming character of the process. Moreover, the established process is expected to be less harmful owing to a large reduction of toxic fallout in the atmosphere and water basins, due to the exemption of high toxic, in-

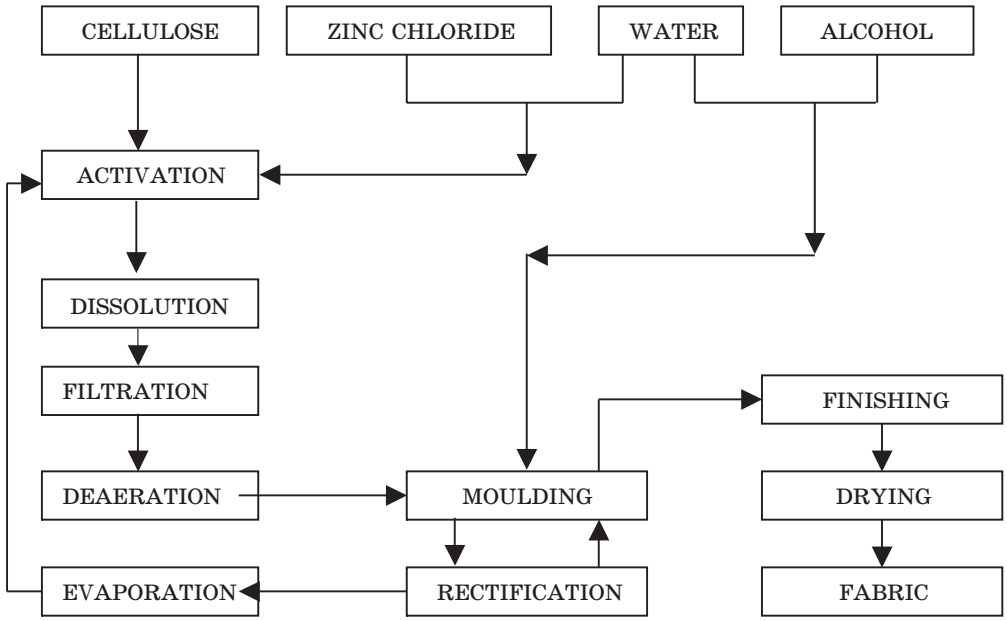

Fig. 5. Schematic diagram of the process of obtaining hydrocellulose fabrics from cellulose solutions in zinc chloride

flammable and explosive carbon disulfide from the practice scheme. The process is also expected to be more economical because of the use of the cheap materials - zinc chloride, alcohols – and due to a reduction of capital equipment expenses and expenditures on environment protection.

A detailed examination of the technological process of regeneration of the primary reagents – which are components of the dissolvent and of the coagulation, - as well as a calculation of the economy of the established process (taking into account the necessity for corrosion-proof equipment usage) reveal the possibility of its industrial implementation and its potential ability to compete with the viscose process.

2. LIQUID CRYSTALLINE PROPERTIES OF HOMOGENEOUSLY SYNTHESIZED NEW CELLULOSE DERIVATIVE

Cellulose derivatives such as hydroxypropyl cellulose; cellulose diacetate, triacetate, and acetate butyrate; etc. are shown to experience the development of an LC order in the arrangement of the anisometric macromolecules in the presence of a relevant solvent when a certain critical polymer concentration is attained; specific values of these concentrations were estimated in [10–17]. Water-soluble sodium salt of cellulose acetate sulfate (Na-CAS) was synthesized via a homogeneous synthesis and prepared as solid transparent and semitransparent plates [18]. The as-prepared Na-CAS is characterized by an exceptionally high water solubility (up to 58 wt %). Highly concentrated aqueous solutions of Na-CAS show stable birefringence. In a stationary state and upon flow, these solutions opalesce, changing

their color from yellow-red to violet, which is indicative of the formation of the cholesteric mesophase [11]. To reveal LC ordering in aqueous solutions of the sodium salt of cellulose acetate sulfate we first time performed polarizing microscopic examinations and rheological measurements over its wide concentration range.

As a subject of study we used Na-CAS synthesized according to the procedure described in [18]. The viscosity-average molecular mass M_h of Na-CAS was determined according to the formula [19]

$$[\eta] \quad 2.1 \cdot 10^{-3} \overline{M}_{\eta}^{0.95}$$

and appeared to be equal $40.5 \cdot 10^3$.

Aqueous Na-CAS solutions with different concentrations varying from 1 to 58 wt. % were prepared at 293 K, taking weighed portions of the compound; the swollen substance was carefully agitated until full homogenization of the system was attained. Dissolution is considered to be complete when the optical observations with a light microscope showed no fragments of non-dissolved Na-CAS. When the dissolution was accomplished, the resultant Na-CAS solutions (c = 42–58 wt %) were deaerated by evacuation for 2 days. The concentration of the solutions prepared was determined more precisely by the gravimetric method [20]. To detect the isotropic phase-anisotropic phase transition, a drop of the as-prepared solution was placed on a slide and pressed with a cover glass and the thin layer of the solution obtained was examined in a polarized light with an Amplival optical microscope equipped with two polarizers. The structural changes observed were recorded on a photographic film using a photocamera. Rheological studies of aqueous Na-CAS solutions were performed on a Rheotest rotary coaxial-cylinder viscometer (Germany) at temperatures varying from 293 to 323 K at shear rates of (1.6–3.0) 10^3 Pa.

As we found, the aqueous Na-CAS solutions are visually transparent and isotropic at concentrations below 2 wt. % and also isotropic but not transparent in the concentration range 2–42 wt. %, thus indicating the association of macromolecules without any ordering in their arrangement. The fact that the association of macromolecules starts at concentrations above 2 wt. % is also proved by the results of the determination of the crossover concentration in the Na-CAS solutions, which appeared to be equal to 1.93 g/dl.

At a concentration of 42 wt. %, the first indications of the development of ordered supramolecular structures as individual spherulites (Fig. 6*a*) appear; as the concentration is increased to 49 wt. %, these spherulites are organized into spherulite ribbons and more complex structural aggregates. The spherulites formed are characterized by a well-pronounced annular structure cut by a Maltese cross. Upon prolonged staying (for one month) at 278 K, the above solutions experience well-defined separation into transparent and opaque phases. According to the published data [21], these phases may be structurally identified as isotropic and anisotropic phases. The appearance of the two-phase region in the Na-CAS solutions suggests that, first, the development of the Na-CAS mesophase is related to geometric anisotropy of the polymer chain as such, rather than to its conformational changes during concentrating the solution. Second, the transition to the LC state in this concentration range takes place only partially [17]. At higher concentrations (above 52 wt. %), the Na-CAS solution in a structural respect represents an LC matrix which contains small-sized regions of isotropic inclusions (Fig. 6*b*) that completely disappear upon a further inc-

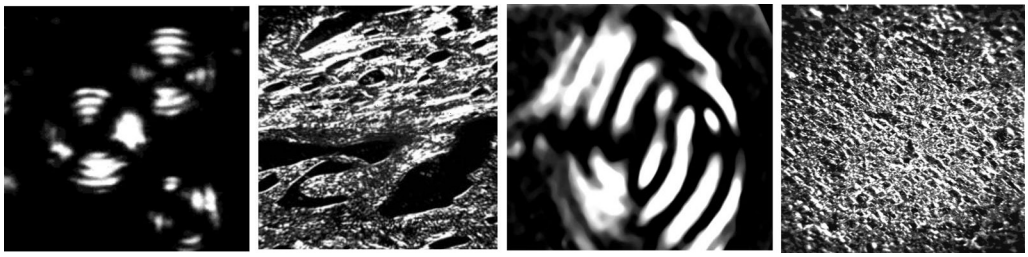

a *b* *c* *d*

Fig. 6. Microphotographs of structures in aqueous Na-CAS solutions with a concentration of (*a*) – 42, (*b*) – 50, (*c*) – 52, and (*d*) – 58 wt. %

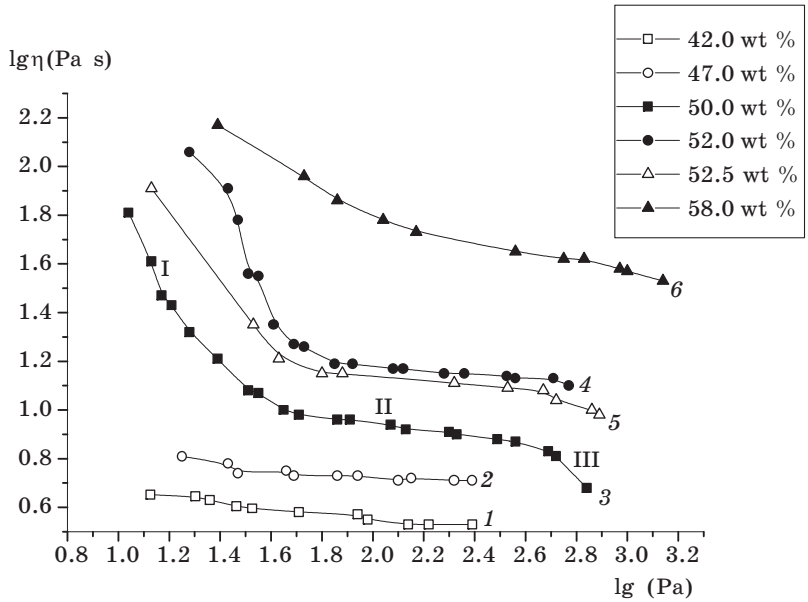

Fig. 7. Viscosity vs. shear stress for aqueous Na-CAS solutions with a concentration of 42.0 – (*1*), 48.0 – (*2*), 50.0 – (*3*), 52.0 – (*4*), 52.5 – (*5*), and 5.08 – (*6*)

rease in the concentration of the solution up to its maximum attainable level (to 58 wt %), the above inclusions. In this case, the corresponding microscopic images of the solution show a confocal texture (Fig. 6*d*) which, upon shearing of the cover glass, is transformed into a planar structure. Furthermore, a specific fingerprint texture typical of cholesteric liquid crystals is observed in the concentration range 50–52 wt. % (Fig. 6*c*).

It is known [21] that the LC nature of polymer solutions is also proved, in addition to their optical properties, by characteristic rheological properties, such as the existence of the yield point and by the absence of the region of constant viscosity in rheological curves.

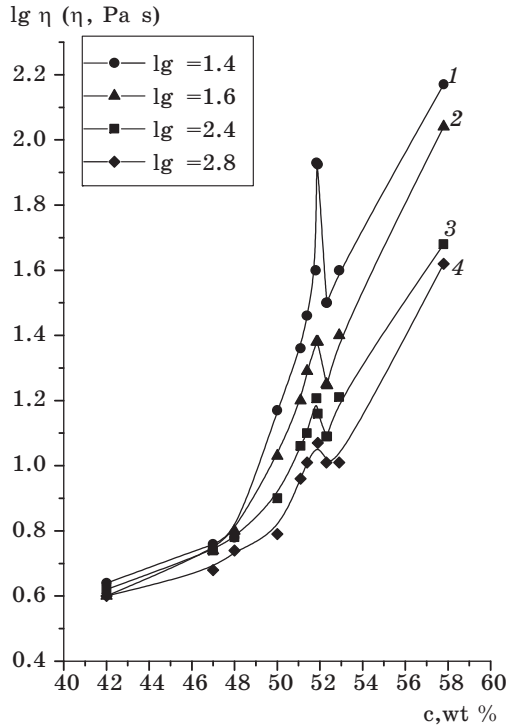

Fig. 8. Viscosity vs. concentration for aqueous Na-CAS solutions at 293 K and at a shear rate of 25 – (*1*), 40 – (*2*), 250 – (*3*), and 660 – (*4*) Pa

For the Na-CAS solutions at the concentrations corresponding to the development of an LC phase, the rheological curves (Fig. 7) show all the aforementioned specific features of LC systems: the region of a marked decrease in the viscosity at low shear stresses (I), a quasi-Newtonian region (II), and the structural wing (III) corresponding to a molecular flow with flow orientation (curves 3–6). The transition to the fully anisotropic solution (c = 58 wt. %) is accompanied by the disappearance of the third region in the flow curve, that is, the structural wing is absent. At the same time, as follows from Fig. 2, the Na-CAS solutions with a concentration of 42 or 47 wt. % show anomalous viscous behavior upon shear deformation, which is typical of structured systems.

The concentration dependence constructed for the viscosity of the Na-CAS solutions from the rheological data shows a maximum typical of LC systems, at a concentration of 52 wt. % (Fig. 8). As the temperature increased from 293 to 323 K, this maximum was shifted to 52.5 wt %. The height of the maximum tends to decrease with increasing the shear deformation rate, thus suggesting the breakdown of LC domains in the Na-CAS system under such external action on the system and the spontaneous ordering of Na-CAS macromolecules in the solutions in the absence of the external action. The ascending branch of the log η = f(c) plot corresponds to isotropic solutions in which the nucleation of ordered structures commences. The maxi-

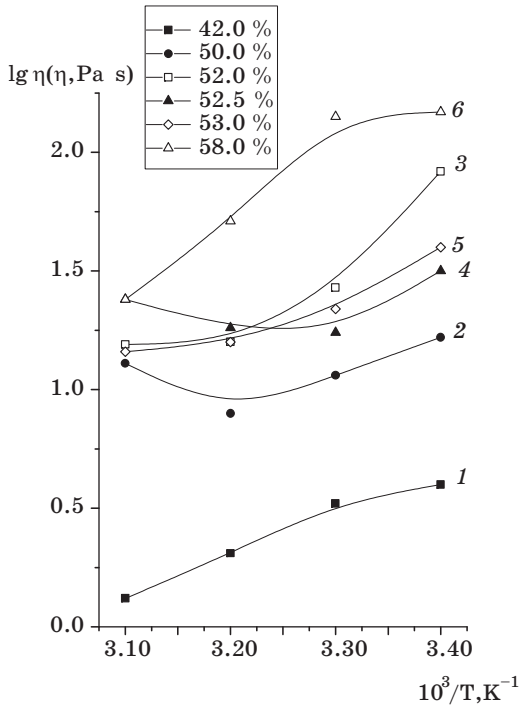

Fig. 9. The effect of temperature on the viscosity of aqueous Na-CAS solutions with the concentration of 42.0 – (*1*), 50.0 – (*2*), 52.0 – (*3*), 52.5 – (*4*), 53.0 – (*5*) and 58.0 – (*6*) wt. %

mum viscosity characterizes the point when the inversion of isotropic and anisotropic phases takes place. The descending branch of the concentration dependence of viscosity describes the behavior of the solutions in which the volume fraction of the isotropic phase dramatically decreases. At a concentration of 52.5 wt % and higher, the solution is fully anisotropic, and viscosity again increases.

Figure 9 presents the temperature dependence of viscosity for the Na-CAS solutions of different concentrations. In a single-phase system, the viscosity monotonically decreases with increasing the temperature; however the temperature dependence shows an extremum for the two-phase solutions (c = 50 – 52.5 wt. %), a this nonmonotonic pattern was also reported for other LC systems [21]. The minimum in the temperature dependence of viscosity may be explained as follows. As temperature increases, the two competing processes take place, a decrease in the viscosity due to the enhancement of thermal motion and a decrease in the viscosity caused by an increase in the volume fraction of the isotropic phase in the system. When the second process starts to dominate, the viscosity increases again after passing through the minimum.

In summary, the parallel investigation of structural transformations and rheological properties of aqueous Na-CAS solutions over a wide concentration range shows that the new cellulose derivative exhibits spontaneous LC ordering which is realized to the maximum extent at 293–323K at a polymer concentration in the solutions higher than 52–52.5 wt. %.

3. NEW METHOD FOR THE STABILIZATION OF CELLULOSE ACETATE – SYNTHETIC POLYMER BLENDS IN SOLUTION

It is generally known that the incompatibility of most polymer pairs in the solution is rather a rule than an exception. For this reason polymer blends solutions in the common solvent are colloid systems like emulsions but not the real solutions. Two layers are formed as a result of a long storage in such systems after a period of time. The segregation of the polymers in polymer blends solutions on a long storage makes their processing practically impossible with standard equipment and it negatively influences the product properties. Consequently the elevation of polymer 1-polymer 2- solvent systems stability is an urgent issue. The elevation of the kinetic stability by means of modification some physical and chemical characteristics of the systems (temperature, viscosity, copolymer adding and so on) has already been mentioned [22].

A new approach to the problem of the stabilization of incompatible polymer blends solutions is suggested as the result of our investigations [22]. This paper studies some novel experimental results on the stabilization of cellulose acetate (CA) solutions containing synthetic polymers. Polymer blend precipitated from a solution of two polymers in the common solvent is taken as a stabilizing agent. The composition of the solution used for the preparation of the precipitated polymer blend and the composition of the stabilized solution are identical. Then the part of the initial polymers in the stabilized solution is changed by the same quantity of precipitated product. It is possible because the ratio of polymers in the solution is the same as in the precipitated product. The main principles of the stabilization of CA solutions which contain chlorinated poly(vinyl chloride) (cPVC), butadiene-acrylonitrile rubber (BAR) and poly(methylmethacrylate) (PMMA) are discussed. The questions addressed are: is the stabilization realized and what is it affected by? For we understand that the real reason of this phenomenon is not common.

The stabilization effect has been found most conspicuous in the case of 50% content of precipitated blend (PB). There is no elevation of stability in the solution with less than 20 % of PB. Table 7 lists the composition and the kinetic stability of the investigated systems. This data shows that a 50 % increment in PB contents leads to a 2–2.5 time increase in kinetic stability.

Any further increase in PB content decreases the stability of the solution. The most pronounced manifestation of the stabilization effect is observed in solutions containing CA or cellulose, these are polymers with H-bond system.

Apart from kinetics separation we have studied the PB influence on the concentration limit of separation (i.e. total polymer concentration in the solution below which there is no phase separation). The substitution of 50 % of initial polymers by their PB contributes to the increase of concentration limit of separation (Fig. 10).

Table 7

Kinetic stability of polymer blends solutions contained stabilizing agent

Polymer ratio, wt. %	Total polymers concentration, g per 100g of solution	Solvent	Quantity of stabilizing agent, % from total content of polymers	The time it takes for solution to be separated into layers, h
CA-cPVC 70 : 30	6	acetone	0	20 ± 2
			50	42 ± 2
CA-cPVC 50 : 50	12	acetone	0	6 ± 0,5
			10	6 ± 0,5
			25	8 ± 0,5
			35	11 ± 0,5
			50	13 ± 0,5
			70	8 ± 0,5
CA: cPVC 30: 70	12	acetone	0	3 ± 0,2
			50	5 ± 0,2
C: cPVC 50 : 50	6	DMF: N_2O_4 (19:1)	0	24 ± 2
			20	30 ± 2
			50	48 ± 2
CA:BAR 50 : 50	8	DMF	0	33 ± 2
			20	40 ± 2
			40	51 ± 2
			50	57 ± 2
CA:PMMA 50 : 50	15	DMF	0	48 ± 2
			30	56 ± 2
			50	62 ± 2
PMMA:BAR 50 : 50	8	DMF	0	3 ± 0,2
			50	4 ± 0,2

In order to determine the reasons of the observed phenomenon we have studied the influence of individually precipitated polymer (IPP) on the kinetic stability of polymer blends solutions. The total polymer concentration in the investigated solution was 6 % , the percentage of CA and cPVC equaled 50:50 (acetone was taken as a solvent). Four variants of making stabilized solutions have been sampled:

1. 25 % (of total content of polymers in the solution) of individually precipitated CA was taken instead of 25 % of initial (i. e. nonprecipitated) CA.

2. 25 % of individually precipitated cPVC - instead of 25 % of initial cPVC.

3. All amount of CA was taken in the form of individually precipitated CA.

4. All amount of cPVC was taken in the form of individually precipitated cPVC.

The effect of kinetic stability elevation has been found to take place only with the introduction of 25 % of individually precipitated CA (Case 1). If introduced in different quantities, individually precipitated cPVC does not have any pronounced effect on the kinetic stability of solution. Complete substitution of the initial CA for the precipitated CA failed to increase the stability.

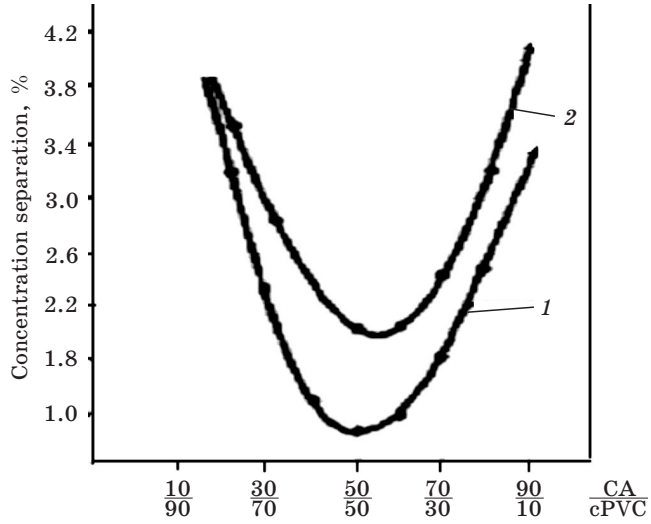

Fig. 10. Concentration separation limit versus polymer relation for the CAcPVC – acetone system. The region above and under the curse is the region of colloid and true solutions, correspondingly. *1* – initial polemer solution, *2* – solution containing 50 % (by wt.) PB

Three model systems were therefore used for further investigation. These systems were identical as for chemical nature and quantity of polymers (CA : cPVC = 50 : 50 wt. %): 1 – solution of initial polymers blend; 2 – solution containing 25 % of individually precipitated CA; 3 – solution containing 50 % of precipitated CA/cPVC blend.

Influence of Polymers and Solvents Characteristics

The stability of the solutions on the basis of CA with one degree of substitution (DS) but different molecular weights as well as with different DS but the same molecular weight has been studied. Stabilization efficiency was expressed as the ratio of separation time of the stabilized solution to that of the non-stabilized solution. It turned out that the stabilizing effect of CA practically does not depend on the molecular mass but correlates with degree of substitution (DS) for the CA with different molecular weights. It was found that DS increase leads to a lower CA stabilizing effect both in the case of individually precipitated CA and CA simultaneously precipitated with cPVC. By the increment of DS from 2.34 to 2.55 the ratio of separation time decreases from 1.5 to 0.8 in the case of individually precipitated CA and from 1.7 to 1.1 in the case of CA simultaneously precipitated with cPVC.

We have found out that the stabilizing efficiency of CA also varies with the solvent quality (Table 8).

Table 8

The influence of the solvent quality characteristics on kinetic stability of CA:cPVC=50:50 acetone solutions containing 25 % of precipitated CA

The time it takes for the solution (total polymer content is 12 g per 100g of solution) to be separated into layers, h*	Solvent used for CA precipitation	The second virial coefficient A_2 10^{-4} cm^2 mol g^{-2}	Intrinsic viscosity of initial CA in corresponding solvent, dL/g
14 ± 1	acetic acid	9,0	2,15
16 ± 1	DMF	2,7	2,11
18 ± 1	methyl acetate	-	1,97
26 ± 2	dioxan	2,4	1,94
40 ± 2	acetone	0,9	1,84

Thus, the kinetic stability of CA and cPVC blend in acetone did not increase with the introduction of the CA precipitated from the solvent with good thermodynamic quality (acetic acid, DMF, methyl acetate) [24]. However CA precipitated from the worse quality solvents (dioxan, acetone) acts as an efficient stabilizing agent. The worse the solvent quality is, the higher the CA stabilizing efficiency gets (see the correlation between the second virial coefficient A2 and the time of solution separation into layers). From this point of view it becomes clear that the action of simultaneously precipitated blend CA/cPVC is more effective than individually precipitated CA in this case. The solvent quality (in addition to CA) is expected to deteriorate because of the second polymer (cPVC) presence in the solution [25]. As for solvent we also observed the following:

1) The kinetic stability increases when CA precipitated from the solution in DMF added into CA – PMMA blend in DMF and it decreases when the same CA is added into the same blend but in acetone; 2) The stabilizing effect of CA precipitated from the acetone solution disappears when added to the blend of CA-PMMA in DMF, however takes place when added to this blend but in acetone.

We have also established a number of other factors affecting the velocity of solution separation into layers. All these factors have to do with the preparation conditions of the solutions that were used for making the precipitated product. Thus, the elevation of the solution preparation temperature causes the significant lowering of separation velocity. At the same time the elevation of the precipitator temperature acts diametrically opposite. The increase in the polymer concentration in the solution leads to the increase in velocity. To understand the observed phenomenon one has to answer the question: what happens with the polymer during the precipitation from the solution?

It may be expected that the elimination of impurities from the polymer and changing of its chemical composition take place in the precipitation process. However the results of our chemical and spectral analysis showed the identical composition of the initial and the precipitated CA (it is not surprising because of the indifferent character of the used solvent and precipitator). There was no change in the molecular weight distribution of above mentioned CA examples. Thus, Fig. 11 shows the curves of turbidimetric titration of the solutions of the initial and precipitated CA that can give qualitative characteristic of CA polydispersivity.

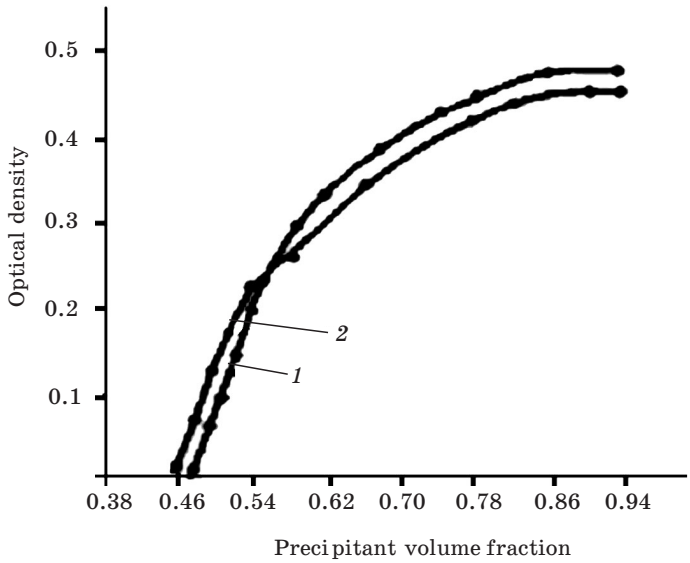

Fig. 11. Turbidimetric titration curves of the initial and precipitated CA solutions. Epichlorohydrin and n – butanol were used as solvent and precipiant

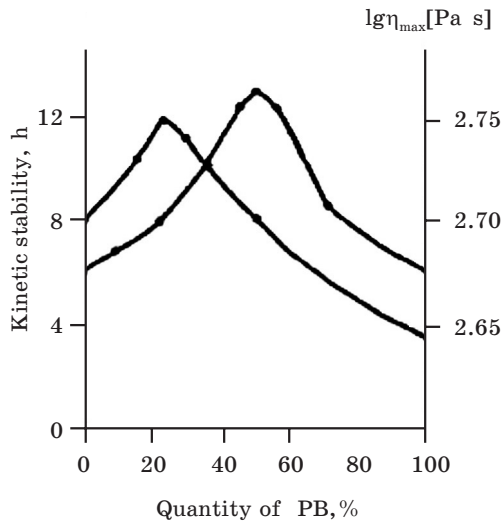

Fig. 12. Kinetic stability (1) and maximum Newtonian viscosity (2) versus PB.

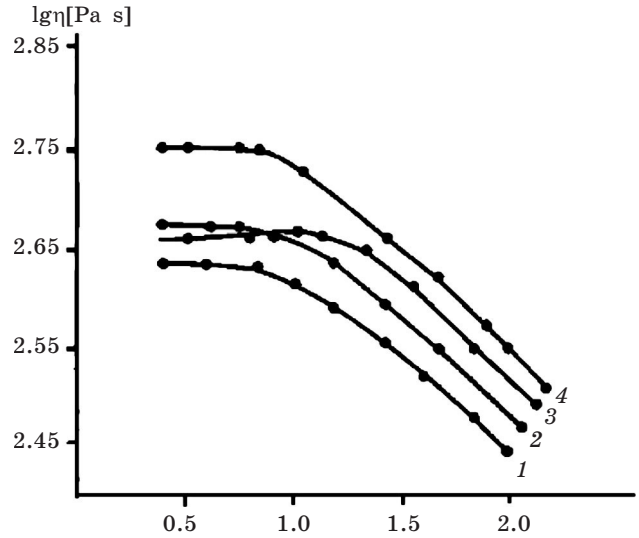

Fig. 13. Viscosity rheograms of CA – cPVC 12 % (total polymer concentration); acetone solutions contained 0 % (*2*), 25 % (*4*), 50 % (*3*) and 100 % (*1*) PB

Moreover, we have attempted to establish the impact of the elimination of different fractions from CA on its stabilizing action. CA without low or high molecular weight fractions has been shown not to demonstrate the stabilizing action. When added to CA/cPVC solution these two samples of CA hasten the separation. Different kinds of CA added to CA : cPVC=50 : 50 solution in DMF could be arranged in sequence according to their capacity to elevate the solutions kinetic stability: $CA_{\text{without low molecular weight fractions}} < CA_{\text{without high molecular weight fractions}} < CA_{\text{simply precipitated}}$.

Solutions Rheological Behavior

Our rheological investigations indicated that there is no correlation between the viscosity and kinetic stability of solutions containing different quantities of PB (Fig. 12). The main difference between the rheogram of investigated solution is in the larger extent of maximum Newtonian viscosity region for the solution containing 50 % of precipitated mixture (Fig. 13, curve 3). This fact suggests the change of the solution structure and the parameters of its fluctuated space network. It is to be noted that the increased PB content in the solution leads to the increased activation enthalpy of viscous flow (from 34 to 38 kJ/mol), which presumably implies an increase of intermolecular contact's number.

To establish the correlation between structure and stability of solutions, we have also carried out the work revealing the reasons of solution structure strengthening in the presence of precipitated polymers.

Macromolecules characteristics of precipitated polymers

The results of viscometric investigation of hydrodynamic polymer's characteristics are given in table 3. As follows from these data the decrease of intrinsic viscosity ([h]) and Huggin's constant (kH) of CA takes place during the precipitation process. The characteristics of CA (substitution degree) as well as of the solution, which was used for precipitated products preparation (total polymer concentration, nature of the solvent) influence the value of [h] and kH. There is a corre-

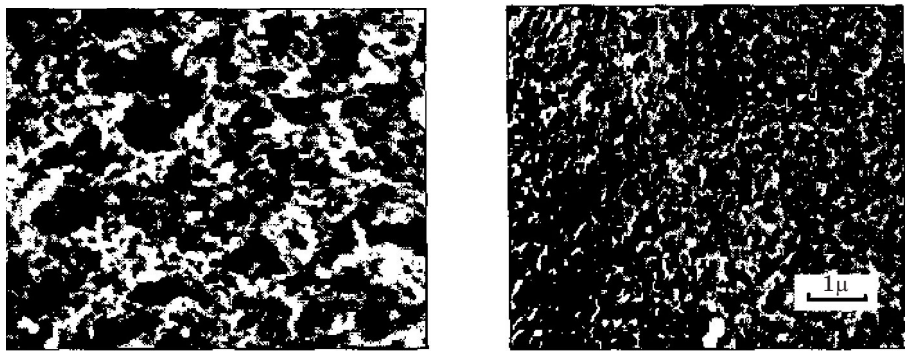

a *b*

Fig. 14. Scanning electron microphotographs of films surface:
a – based on two initial CA solution with different DS;
b – based on the same CA blend + 50% of PB

lation between the hydrodynamic characteristics of macromolecule in dilute solutions and stabilizing action of precipitated polymers in concentrated solutions. Namely the larger the difference between the value of [h] and kH of the initial and precipitated polymer, the more effective the stabilization is.

If it is possible to imagine dissolution of polymer and its subsequent precipitation as inter-and intramolecular bonds «destruction-reduction» process, then the change of temperature, CA substitution degree, solvent nature, second polymer adding into the solution can be considered as factors having affect on the degree of change of hydrogen bonds system.

This is especially true for CA, that has a large number of hydrogen bonds. In particular, the decrease of precipitated polymer [η] is attributable to the fact that macromolecule undergoes destruction or changes the conformation. Since destruction is excluded, we may suggest conformation changing. During the dissolution of CA the solvent destroys part of the hydrogen bonds including intramolecular. This contributes to the increment of the macromolecular flexibility. In this case, macromolecule conforms to a more compact shape. This conformation is fixed during the precipitation. When the precipitated CA is dissolved, macromolecular reproduces this conformation. As seen from the Fig. 14 the morphological structure of the initial and precipitated CA is different. Investigated synthetic polymers (cPVC, PMMA) have not extensive hydrogen bonds system. For this reason, the dissolution and the following precipitation may not practically cause the molecular characteristics change.

IR-spectroscopic Investigation of Solutions

The IR-spectra of initial and precipitated CA powders and solutions, CA-cPVC solutions were recorded in the structure-sensitive region (450……650 cm^{-1}) [26]. As follows from the data (Fig. 15 *a*), the IR-spectra of the powders of the original and precipitated CA have essential distinctions: in the spectrum of precipitated CA the band 432 cm^{-1} vanishes, but the bands 498 cm^{-1} and 455 cm^{-1} shift to 495 cm^{-1} and 450 cm^{-1} respectively. In the IR-spectrum of precipitated CA solution in dimethylformamide (Fig. 15 *b*) the 483 cm^{-1} band vanishes and two bands appear at 495 cm^{-1} and 480 cm^{-1} in the form of two small juts.

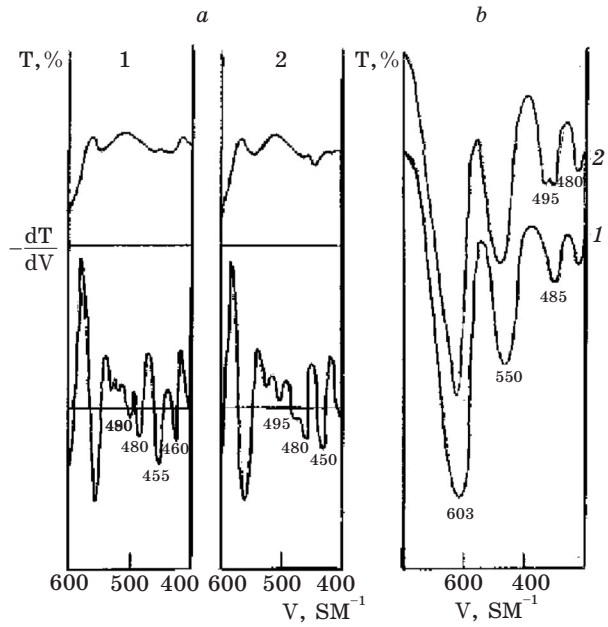

Fig. 15. IR – spectra of the powders (*a*) and solutions (*b*) of the initial CA (*1*) and precipitated CA (*2*)

Though to carry on the assignment of the bands in this area is rather difficult, observed distinctions can be unambiguously connected with the conformation changes of macromolecules.

The results of the theoretical calculations indicate that the oscillation frequency with the participation of acetic groups angles and bonds C – O, C – C, OCO, OCC and also OCO, COC and OCC angles of anhydroglucopyranose links with the participation of oxygen atoms 0 (1), 0 (5) and 0 (4) are exhibited in this region. The considerable mobility of these angles is justified by the significant freedom of the rotation around the C – O bonds compared to C – C bonds and also by the fact that the most mobile atom in the ring is the oxygen atom that has the lowest number of bonds with other atoms. We can assume that in our case the differences between the spectra of original and precipitated cellulose are associated exactly with this phenomenon. The variations of absorption intensity in the pointed region are caused by the variation of relative spatial position of elementary links. In this way, the conformations of precipitated macromolecules turn out to be modified in comparison with conformations of the initial ones. Conformation variations take place obviously on the level of links attachment.

We believe that these conformational changes are induced by the glucopyranosic cycles turning which is caused by the changes intra- and intermolecular hydrogen bonds system of initial CA. All of the preceding makes it possible to assume the macromolecules of initial and precipitated CA differ in hydrodynamic size in the solution. The stabilized solution may be thought of as containing three polymers: initial CA, precipitated CA, which are not conformationally isomorphic and cPVC. We think that this explains the increase of the time of phase separation in the investigated polymer 1 – polymer 2 – solvent systems.

4. NEW FILM – FABRIC MATERIALS AND HIGHLY EFFICIENT FILTERING SYSTEMS ON THEIR BASE

New film-fabric materials, filtering elements and systems produced on their basis are designed for application in food, medical, microbiological, perfumery, cosmetic, chemical, electronic and other industries, besides they can be widely used in agriculture and housing public services.

The materials and filtering systems on their base are necessary for purification of large volumes of water and gas from mechanical impurities.

The original technology of production of high-strength film-fabric materials with fixed pore sizes (Fig. 16) hag been developed. Cartridge filtering elements (Fig. 17) with large filtration areas were made up on their basis. Large areas are obtained due to the ability of film-fabric materials for corrugation. Highly efficient filtering systems (Fig. 18) with the capacity of water passage in-between 0.1–40.0 m^3/h were assembled of filtering cartridges. They ensure water purification from sand, mechanical suspended matters and iron oxides (rust) insoluble in water. That is why filters can be used for finishing purification of cold and hot water running along «black» tubes of communal water supply, from artesian wells and other sources. Besides they can be efficiently used in processes of filtration of milk, juices, syrups, drinks, beer, wine materials, liqueurs, vodkas, perfumery and cosmetic liquids, culture media, waste, processing solutions, organic solvents, acids and bases of low and mean concentrations, for gas purification. Filtering systems being offered can be placed on inlet taps of a dwelling-house, porch, fiat, cottage, hospital, kindergarten, canteen, photolaboratory; just before heat meters, meters of cold and hot water, bottle washing machines; bottling lines of liqueurs, vodkas, drinks; milk separators; in systems of preparation of isotonic and hemodialysis solutions; in cooling systems of X-ray apparatuses, etc. New film-fabric materials are applicable for manufacturing of multi-used bag filters for machine milking, fitters for coffee-pots, filters for domestic funnels, filtering sheets in filter presses to keep the washed in layer during beer filtration, etc. In all cases the recovery of initial water passing capacity of filtering sheets and systems is easily achieved by their washing with reverse water flow under pressure.

Unlike the traditionally used filtering fabrics, papers, boards, nonwoven sheets, film membranes, metal nets, ceramic filters etc. new materials posess a unique property – high water permeability and at the same time high retentivity. They are easily regenerated with the recovery of the initial filtering ability. For example, polyether filtering sheet passes through itself more than 180 m^3/sq.m.h of water under the pressure of 0,05 MPa, the effect is 95 % of retained particles with the size of more than 10 micrometres.

New filtering materials are stable to microorganisms, disinfecting solutions, hot water, organic solvents, diluted acids and acids of mean concentration, diluted alkalies: they can stand chemical and temperature sterilization, are easily washed up by water and other detergents – that is why they are reusable.

Both firms-consumers and firms-producers of traditional fitters and filtering elements can be interested in this project.

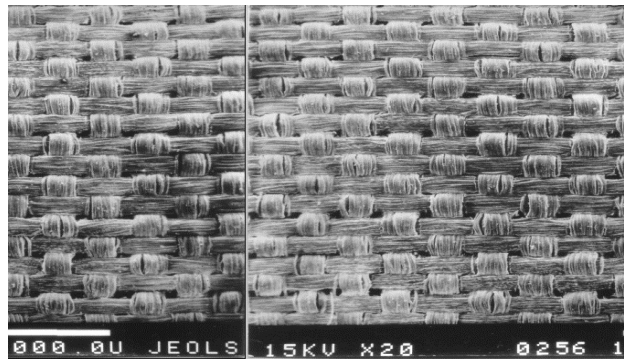

a

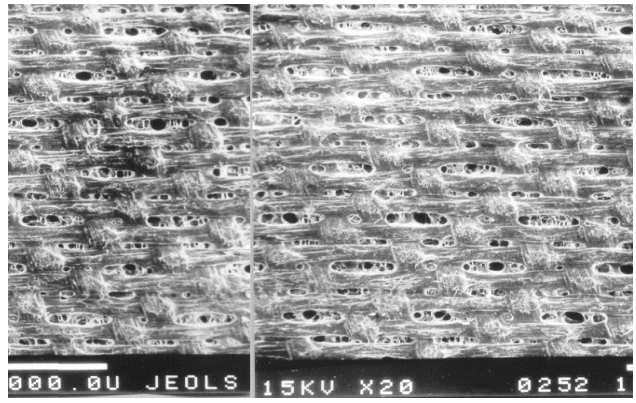

b

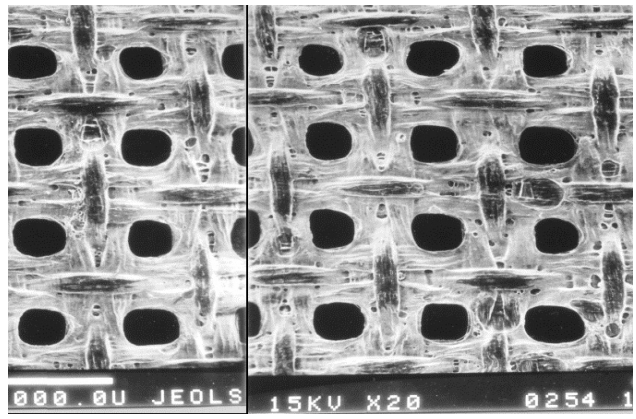

c

Fig. 16. Microfotographies of N°TECHMA filtering fabrics: *a* – viscose; *b*, *c* – polyester

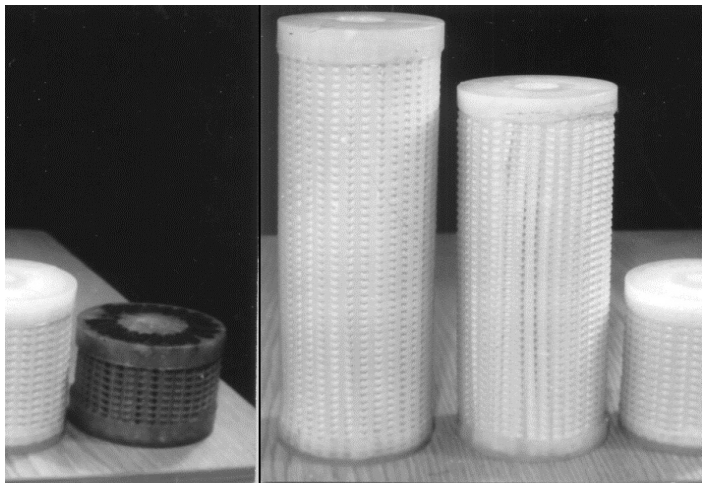

Fig. 17. Filter cartridges

a

b

Fig. 18. N°TECHMA filtering units
of cartridge type (*a*, *b*)

The industrial operation practice for the production of film-fabric materials with specified porosity has been developed. Prototypes of filtering cartridges (filtering elements) and filtering systems with different number of filtering elements (from 1 to 23) have been manufactured and then their approbation in real processes was carried out. There are prototypes for demonstration.

Materials have certificates and resolutions of Belarussian Ministry of Public Health to use them in food industry.

5. NEW ACTIVATED CARBON DRUGS

The reason why active carbon in the form of tablets, granules and capsules cannot be efficiently used as enterosorbent lies within the low stability and flowability of suspensions generated in the gastrointestinal tract of a patient. The nature of the polymer used as a binder while preparing tablets or material for capsule coating should be particularly set off from other factors responsible for the stability and rheology of such suspensions.

The intent of this work was to study the impact of high molecular compounds on the aggregative and sedimentation stability, rheological properties of carbon suspensions in water. Our objective was also to evaluate the possibility of using different polymers for producing drug forms of activated carbon capable of quick disintegration in aqueous media.

The fibrous activated carbon of AUT-MI type was used as activated carbon. Activated carbon was taken in the form of powder, granules or tablets. Industrially produced polyvinylalcohol (PVA) with a molecular mass of $M\mu = 4.4 \cdot 10^6$, polyvinylpyrrolidone (PVP) with $M\mu = 3.0 \cdot 10^5$, starch (S), containing 25 % of amilose and 75 % of amilopectine, polyacrylamide (PAAm) – $M\mu = 4 \cdot 10^6$, polyacrylic acid (PAAc) – $M\mu = 5.0 \cdot 10^5$, carboxylmethyl cellulose sodium salt (NA-CMC) – $M\mu = 5.5 \cdot 10^5$, oxypropylmethyl cellulose (OPMC) – $M\mu = 1.4 \cdot 10^5$, and our new synthesized water-soluble cellulose derivative (WSCD) of polyelectrolyte nature – $M\mu = 3.4 \cdot 10^4$ were used as a binder while making granules and tablets.

Granulates and tablets were prepared on special equipment (mixers, granulators, presses) by mixing the components in the given ratios. The suspensions studied had a dispersed phase concentration of 5–37 mass % and polymer concentration of 8–12 %. Only distilled water was employed as a dispersing liquid since it had earlier been established [27] that aggregative stability and sedimentation velocity are significantly higher in acid (pH 1.6) and alkaline media (pH 8) resembling those of stomach and intestines.

The sedimentation analysis was carried out in compliance with the methods [28]. Rheological studies were conducted using concentric cylinder viscometer Rheotest – 2 with the shearing stress of 1–200 Pa. The concentration of colloid dispersity degree particles that do not form sediment in the period of 30 or more days was determined gravimetrically. The volume of sediments was estimated for the 5 % suspensions (vol. $25 \cdot 10^{-4}$ m^3) in graduated tubes with $1{,}4 \cdot 10^{-2}$ m in diameter after 30 days.

The adsorption activity of carbon drugs in relation to methylene blue that models the class of low molecular toxins with the molecular mass up to 500 Д, was

determined by the value of specific adsorption by the procedure [29]. Vitamin B12 adsorption was evaluated by the same procedure.

The interaction velocity of antacid and hydrochloric acid was determined in the following way: 50 mL of 0,1 M HCl solutions were thermostated at 37 °C within 0.5h, then 0,5g of antacid were added and pH was checked with the help of Thermo Orion PerpHecT Meter (Model 310).

The results of the visual observation and sedimentation analysis showed that the most stable suspensions are formed in the presence of the following polymers WSCD, PVP, Na - CMC, and OPMC.

However the full phase separation, i.e. the formation of transparent water layer and flaky carbon particle sediment, was noted only for suspensions containing PAAm, PAAc, PVA and starch. As for the rest of the suspensions there were sediments on tube bottoms and above there was a fine dispersion of carbon particles. At the same time it turned out that polymers can be arranged according to the value of sediments: WSCD < PVP < Na – CMC ≈ OPMC ≈ carbon suspension < starch < PAAc < PVA < PAAm. The sediment volume changes can be attributed to the change in particle size distribution character in the suspensions. Therefore the increase of sediment volume points at the merger of particles into bigger sets, forming loose flaky residuum, and the decrease indicates the dissociation of particle sets that are generated in the original carbon suspension, and the buildup of thicker sediment. This can also be attested by the results of the sedimentation analysis of granules and tablets suspensions. In the general case WSCD, Na – CMC and OPMC constrict the particle size distribution (PSD), whereas PAAc, PAAm, starch and PVP expand it. Derived curves of particle size distribution for several systems are shown in the Fig. 19. The narrower PSD is achieved through the presence of WSCD in the carbon suspension. The rheological study of features peculiar to aqueous carbon dispersions obtained on the basis of different carbon granulates and original carbon powder showed that dispersions with WSCD as opposed to other polymers behave like a Newtonian fluid. They are also characterized by the absence of structuring in the whole range of the studied dispersed phase concentrations.

In any case, up to the point of 36 % concentration (the further increase of concentration is limited by viscosity growth), structuring is not observed and the dispersions flow evenly (Fig. 20). At the same time structure formation in the dispersion of carbon powder and granules with other polymers starts already in the range of concentrations (Ccr) from 11 % (PAAm) to 21 % (pure carbon). Sudden drop in the viscosity due to the shearing stress increase is evidence to it (Fig. 21, 22). The correlation of Ccr with sedimentation stability allowed to conclude that polymers with Ccr being higher than by pure carbon suspension appear to be flocculants (PAAm, PVA, PAAc, S, MC). Polymers with lower Ccr serve as stabilizers (PVP, WSCD). Whereas with the same polymer content in the suspension the amount of particles incapable of gravity sedimentation is higher in the case of WSCD as compared to PVP. It constitutes 8–9 % and 4–5 % respectively. This implies the bigger specific surface of such suspension and higher adsorption activity of its particles correspondingly.

The obtained results enabled recommendation of WSCD as a unique polymer for creation of different drug forms on the basis of activated carbon.

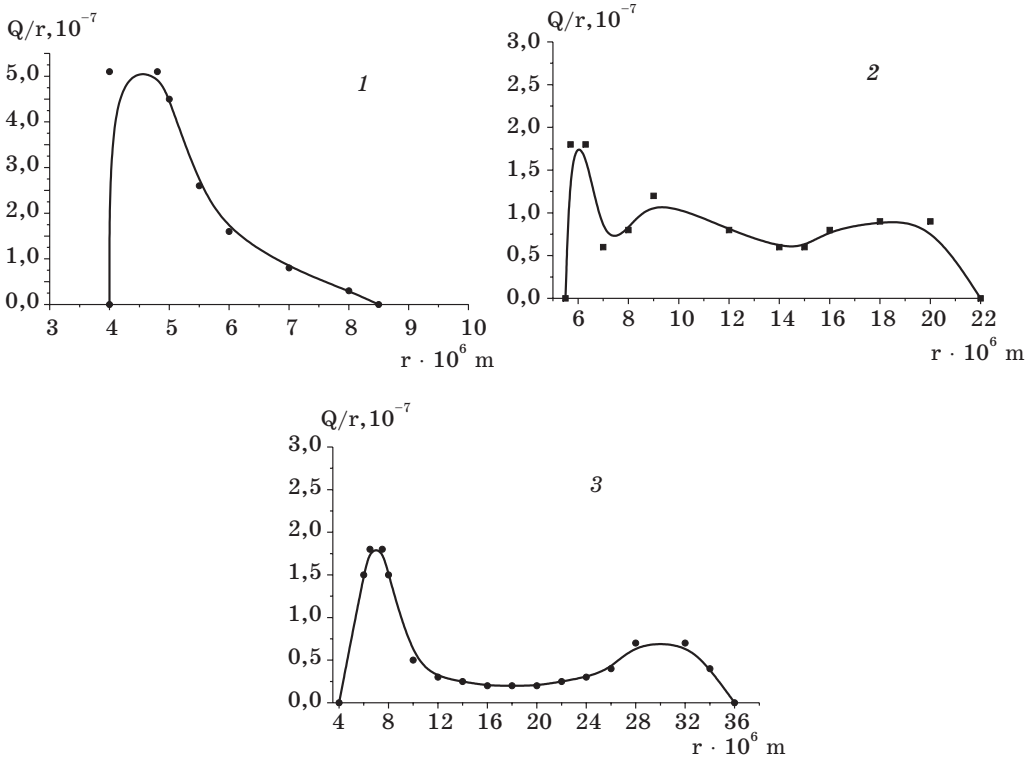

Fig. 19. Derived curves of particle size distribution for the tablets containing WSCD (*1*), starch (*2*) and PVP (*3*)

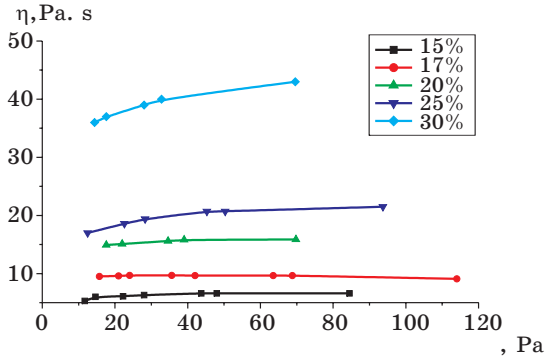

Fig. 20. Viscosity rheograms of aqueous AUT-MI carbon dispersions stabilized by WSCD with different concentrations of the dispersed phase at 37 °C

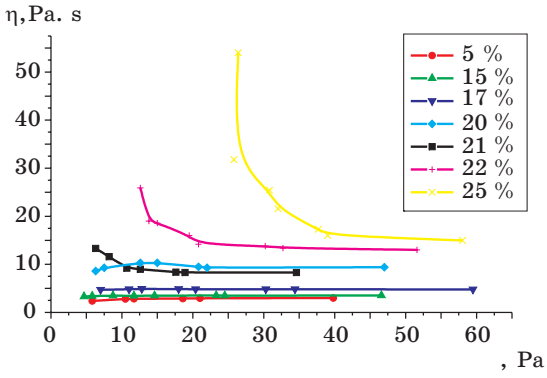

Fig. 21. Viscosity rheograms of aqueous AUT-MI carbon dispersions with different concentrations of the dispersed phase at 37 °C

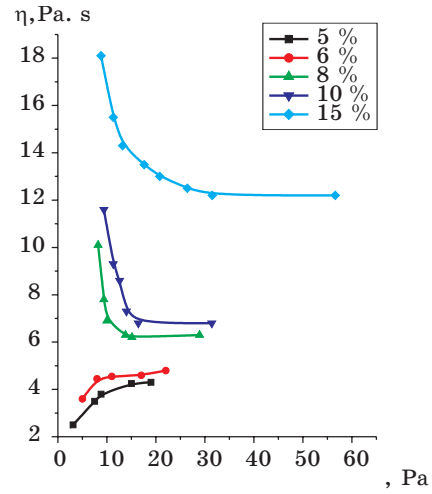

Fig. 22. Viscosity rheograms of aqueous AUT-MI carbon dispersions stabilized by PAA with different concentrations of the dispersed phase at 37 °C

New quickly – disintegrated tablets, new hydrophilic ointments and gels «Carbon-Levomycetin»

«Carbon- Valerian »
«Carbon-Aspirin-Vitamin C»
«Carbon-Aspirin- Vitamin C- Valerian »
«Carbon-Phenygedin »
«Carbon-Nicotinic Acid»
«Carbon-Sodium Nucleinat»
«Carbon-Calcium Carbonate»
«Carbon-Calcium Carbonate-Magnesium Carbonate»
«Carbon-Pectin-Vitamin C-Sweet»
«Calcium Carbonate»
hydrocortisone ointment 1 %
lincomycine ointment 2 %
prednisolone ointment 0,5%
prednisolone gel 0,5 %
dexamethasone gel 0,1 %

Chief distinctions of new tabletted drug forms from the well-known

- the disintegration takes several seconds;
- they do not contain citric add and sodium bicarbonate; while dissolved in water do not carbonate it;
- absence of irritating effect on mucous of gastrointestinal tract and toxic effect on kidneys and liver;
- significant reduction of the administrated dose (in 3–5 times) with the perseverance of the drug efficiency;
- can be used:

– in the form of water solutions for the treatment of children under 4, including infants;

– for bed-patients with the peristaltic dysfunction;

– for patients with stomach and duodenum ulcer.

Main advatages

«Ultrasorb» tablets

«Ultrasorb» tablets disintegrate 10–100 times quicker in contrast to the well-known carbon pills manufactured by Russia, Ukraine, Holland and France. Their sorption capacity is considerably higher regarding harmful substances and their decay products - toxins. This is because of the high specific surface and dispersion degree of the carbon in water solutions of «Ultrasorb» These tablets are suitable for administration: there is no need in chewing, they can be swallowed, taken with water or dissolved in water beforehand. The drug, dissolved in water, is good for the treatment of children including infants. As against powder-like forms of activated carbon like «Belosorb», given tablets do not cause tickles in the throat, belching, retching etc. The course of treatment and the taken dose are decreased several times owing to the high efficiency of the drug- it is also virtual when treating food or medicine allergies, food poisoning. Moreover, what is very important, its high capacity towards the lowering of radio nuclide level in the organism has been revealed (one tablet reduces specific radiation activity by 20 Bq/kg). As compared with such drugs as «Spirulin», «Jablopect», «Medetopect», «Vitus-iodine» traditionally used for these purposes, tablets «Ultrasorb» in terms of mass are several times more active.

«Uglepect» tablets

The combined form of activated carbon and apple pectin is meant to decrease the specific radiation activity of people with advanced radiation dose. It is especially commendable for the children's rehabilitation, as it appears to be a sa vory pastille, containing vitamin C and sweet. What concerns the efficiency of the drug it is comparable with that of the «Ultrasorb».

«Carbon-Aspirin-Vitamin C» («Black Aspirin») tablets

This is a fundamentally new form of soluble aspirin without side effects regarding GIT. Unlike Bayer and UPSA aspirin this one does not contain filling agents such as sodium bicarbonate and citric acid which constitute more than 80 % of the tablet's mass, consequently it doesn't affect stomach and duodenum mucous membrane and the activity of digestive ferments. «Black Aspirin» tablets are 20 times lighter than soluble aspirin.

While using «Black Aspirin» contra-indications are apparently not likely to appear due to the fact that its dissolution does not induce the irritation of stomach mucous membrane, there is no gassing. Children under 4, patients with stomach or duodenum ulcer, can administrate it. Obviously the tablets containing valerian, that reduces GIT spasms, will be particularly beneficial for these kinds of patients.

As opposed to Bayer aspirin, «Black Aspirin» has the same anti-fever effect as the insoluble aspirin. The distinguished advantages of «Black Aspirin» are retained in comparison with traditionally insoluble aspirin tablets, produced by countries here and abroad.

«Carbon-Valerian» tablets

In «Carbon-Valerian» tablets the original valerian extract activity is preserved as against to ordinary 'Valerian extract" tablets. This determines the high efficiency of their usage as a sedative.

«Carbon-Calcium Carbonate-Magnesium Carbonate», «Carbon-Calcium Carbonate» tablets

Calcium and magnesium carbonates are the main representatives of the antacid agents employed to decrease high acidity of gastric juice (under gastritis, stomach and duodenum ulcer). Thanks to the new cohesive used in the tablets, insoluble calcium and magnesium carbonates transfer into fine-dispersed suspension.

They quickly neutralize hydrochloric acid of the stomach contents. By comparison with well-known drugs («Vicair», «Vicalin», «RENNIE») the application of calcium and magnesium carbonates in the combination with carbon allows to sorb carbonic add, evolved during the neutralization of the stomach acid-

This does not evoke stimulating effect on the receptors of the stomach mucous membrane. This also doesn't intensify the secretion of the gastrin and doesn't cause the intensification of the secretion for the second time. They do not contain aluminates.

Main advantages of new ointments and gels

Very high distribution singularity of the acting substance in the volume of the ointment. The degree of dispersion is 15 - 80 mm, that is approximately 5 times higher than in the similar ointments on the fat basis. Ointment-solutions can be made in the number of cases with water-soluble drug substances (lincomycine, prednisolone) or substances that are dissolved in the gel components.

Their penetrating capacity is considerably higher than of those traditional heavy ointments, by reason of their higher compatibility with the organic tissues.

In individual cases when conducting a test of prednisolone ointment it has been found out that its efficacy is so high that there is no need in intra-articuiar injections of prednisolone suspension for the patients with rheumatic arthritis. In addition The new cellulose derivative can be used in order to receipt quick-dissolving tablets that form fine suspensions in the liquid phase without the application of carbon. This is extremely important in the case of receiving quick-acting drug forms, produced from sparingly soluble substances, e. g. «Calcium carbonate».

REFERENCES

1. *Grinshpan D. D., Tsygankova N. G.* et al. // Fibres and Textiles in Eastern Europe. 1994. October/December. P. 35-39.
2. Japan Ahhlication 58 – 151217 (1983).
3. US Patent 4999149 (1991).
4. US Application W 0922/09726 (1992).
5. Baykalz N., Segal L. Cellulose and Cellulose Manufacture. Vol. 1. 1974. P. 505.
6. Greate Britain Patent 13296 (1859).
7. *Suvern E.* // Die Kunstliche Seide Berline 1921. S. 294-300.
8. *Belonogov K. N., Starostina V. D.* et al. // Papers of the Ivanovo Technological Chemical Institute . 1988. P. 56.
9. I.C. 1548283 (USSR), 1989.
10. I.C.1582711 (USSR), 1990

11. *Werbowij, R. S. and Gray D. G.* // Mol. Cryst. Liq. Cryst., Lett. Sect. 1976. Vol. 34. P. 97.
12. *Dayan S., Gill J. M., Sixou P.* // J. Appl. Polym. Sci. 1983. Vol. 28. P. 1527.
13. *Aharoni S. M.* // Mol. Cryst. Liq. Cryst., Lett. Sect. 1980. Vol. 56. P. 237.
14. *Savchenko N. A., Khanchich O. A., Dibrova A K.* and *Gul' V. E.* // Khim. Volokna 1997. № 5. P. 25.
15. *Iovleva M. M.* and *Banduryan S. N.* // Khim. Volokna 1995. № 2. P. 9.
16. *Dave V., Wang J. Z., Glasser W. G.,* and *Dillard D. A.* // J. Polym. Sci. Part B: Polym. Phys. 1994. Vol. 32. P. 1105.
17. *Kulichikhin V. G.* and *Golova L. K.* // Khim. Drev. 1985. № 3. P. 9.
18. *Grinshpan D. D., Emel'yanov Yu G.,* and *Kaputskii F. N.* // Khim. Drev. 1987. № 1. P. 30.
19. *Pavlov G. N., Grinshpan D. D., Pavlov A. N., Stepchenkova T. A.*, and *Makarevich S. E.* // Khim. Drev. 1992. № 4. P. 12.
20. Analiticheskii kontrol' proizvodstva iskusstvennykh volokon: spravochnoe posobie (Analytical Monitoring of Synthetic Fiber Production: A Handbook), Moscow: Khimiya, 1986.
21. *Papkov S. P.* and K*ulichikhin V. G.* Zhidkokristallicheskoe sostoyanie polimerov (Liquid Crystalline Polymers), Moscow: Khimiya, 1977.
22. *Curbanaliev M., Tager F.* and *Dreval V.* // Mechanika polimerov. 1973. Vol. 2. P. 360.
23. *Savitskaya T. A., Knypikova L. A., Grinshpan D. D.* et al. // Khimia Drevesiny. 1988.№ 4. P. 24–28.
24. *Budtov V., Monakov Yu., Geller B.* // Vysokomol. soed. 1974. № 7. P. 1587.
25. Mysaev H., Tashmychamedov S. // Khim. Volokna. 1978. № 1. P. 28-29.
26. *Zhbankov R. G.* Infrared Spectra of Cellulose and its Derivatives. N. Y.: Pergamon Press, 1966.
27. *Nevar T. N., Grinshpan D. D., Savitskaya T. A., Lazarev P. M.* // Vesci NAN B. 200l. Ser. Khim. № 4. P. 5–8.
28. *Khodakov U. S., Udkin U. P.* Sedimentation analysis of high dispersed systems. Chemistry. M. 1981. P. 10–23.
29. *Grigorov O. N., Karpova I. P., Kuzmina Z. P.* Guide for practical works on colloid chemistry. M. 1964. P. 30–35.

CHEMICAL PROBLEMS OF THE DEVELOPMENT OF NEW MATERIALS AND TECHNOLOGIES
Minsk 2003

**S. V. Kostyuk, V. P Lesnyak., L. V. Gaponik,
V. P. Mardykin, F. N. Kaputskii**

LEWIS ACID COMPLEXES: SYNTHESIS AND APPLICATION IN POLYMERIZATION PROCESSES

INTRODUCTION

Organoaluminium compounds (OAC) are characterized by various types of reactivity, catalytic activity, and a wide spectrum of synthetic applications. Their high reactivity towards oxygen and water creates numerous difficulties in handling them and limits considerably their use, especially in polymerization processes. Using OAC complexes with electron donor compounds (etherates) removes the above named difficulties because these complexes are more stable while manifesting high activity in many reactions, and displaying specific properties in a number of cases [1–4].

Systematic work performed in the area of synthesis and investigation of properties of OAC and their complexes have made it possible to develop simple and convenient synthetic methods for the named compounds, along with studying their physicochemical properties and catalytic activity in polymerization processes [1–10].

Mechanistic studies performed on the reaction of aluminium, magnesium and alkyl halides in paraffine hydrocarbon medium, both in the presence of an ether and without it, have shown that this complex heterogeneous process occurs via intermediate formation of dialkylmagnesium compounds, their complexes with alkylaluminium species, as well as alkylmagnesium and alkylaluminium halides [11]. The overall process mechanism depends on not only the electron transfer from the metal surface to alkyl halide but on subsequent alkylation reactions of alkylaluminum halides as well, which proceed easier with higher alkyl halides due to better hydrocarbon solubility of higher alkylmagnesium compounds [12]. The data obtained offered the possibility of targeted syntheses of AlR_3 [2, 11–14], of the respective etherates [11, 12, 15, 16] and of $Mg_mAl_nR_{2m+3n}$ [3, 12, 17, 18] to be performed according to the following scheme 1.

Many etherates of OAC and their derivatives were obtained by direct reactions between the components [1, 4]. It is noteworthy that, in a number of cases, these apparently simple reactions are complicated by disproportionation processes, radical exchange, etc. For separation of alkylaluminium halide mixtures, a method has been developed based on formation of solid alkylaluminium dihalide complexes with 1,4-dioxane, 2,2'-dipyridyl, 1(2)-alkyltetrazoles or 2,5-disubstituted tetrazoles [1, 4, 19].

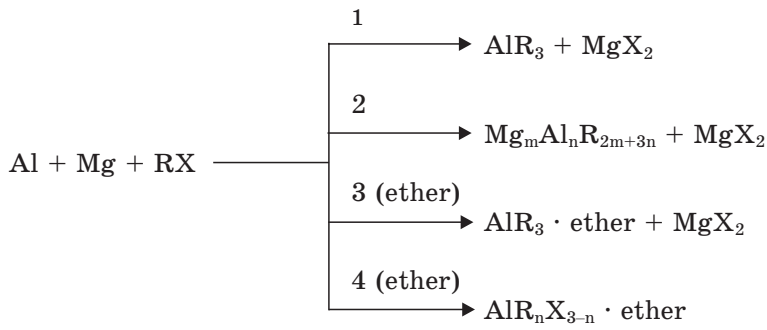

1 – R = n-C_5H_{11} – n-$C_{10}H_{21}$;
2 – R = n-C_4H_9 – n-$C_{10}H_{21}$, n/m = 0.5–30 ;
3 – R = C_2H_5 – n-$C_{10}H_{21}$;
4 – R = i-C_3H_7, i-C_4H_9, cyclic-C_6H_{11}.

Scheme 1. Synthesis of aluminium alkyls, aluminium alkyls etherates and magnesium aluminium alkyls

Studies of physicochemical properties of OAC and their complexes made it possible to forecast the behavior of these compounds in their most important application area – as catalysts in polymerization and co-polymerization of α-olefines, dienes, and other monomers [1–9, 20–45].

AOC complexes with dialkylmagnesium compounds, in combination with $TiCl_4$, possess high catalytic activity in styrene and ethylene polymerization and also in copolymerization of ethylene with higher α-olefins [6, 26, 28, 30, 31, 33]. The mentioned catalytic systems have been found to be effective in the synthesis in super high molecular weight isotactic polystyrene [6]. We have recently shown [46, 47] that the catalytic system on the basis of the complexes of higher OAC with dialkylmagnesium compounds promotes the obtaining of high molecular weight poly(1-hexene) with considerable percentage of isotactic polymer. Alkylaluminium halides and their etherates are efficient complex forming species in alternating copolymerization of styrene or pentadiene-1,3 with methylmetacrylate or acrylonitrile [35–38]. Complexes of chlorine-containing aluminium compounds with diphenyl ether are highly active catalysts of cationic preparation procedures of liquid rubbers [8, 42, 43, 48, 49], polymeric petroleum resins (PPRs) and petroleum polymerizate (PP), used for production of paintwork materials and in construction sector [50–57].

Investigations of trans-pentadiene-1,3 oligomerization under the action of isobutylaluminium dichloride etherate have shown that these processes possess features characteristic of «living» polymerization [24]. The interest towards the «living» and controlled polymerization is due primarily to the possibility of obtaining polymers with a well-defined structure, molecular weight, molecular weight distribution (MWD) and functionality, or block copolymers with pre-determined length and block sequence, without admixture of homopolymers. During the last years, we made considerable efforts in studying the «living» polymerization of

styrene, aimed at the search for new initiating systems suitable for industrial use to perform controlled cationic polymerization of industrial C_9 fraction of liquid products of gasoline pyrolysis.

1. THE «LIVING» CATIONIC POLYMERIZATION OF STYRENE

1.1. Polymerization in the system 1-chloro-1-phenylethane/$TiCl_4$/Bu_2O

In this paper, the results of studies of styrene polymerization in the system 1-phenylethyl chloride/$TiCl_4$/Bu_2O at -15 °C are presented. It is known that tertiary alkyl and aryl halides in combination with $TiCl_4$ and in the presence of strong electron donors (ED) ([$TiCl_4$] >> [ED]) are often used for initiation of the «living» cationic polymerization of styrene at low temperatures (– 80 °C). The initiator we have chosen belongs also to this compound class but is characterized by greater stability under usual conditions. Introduction of a weak ED in excess with respect to the Lewis acid (LA) into the system studied has been shown to promote the controlled polymerization [58]. For realization of the «living» cationic polymerization of styrene, dibutyl ether (Bu_2O) has proved to be the most suitable system component; therefore, the system 1-phenylethyl chloride/$TiCl_4$/Bu_2O was studied in more detail.

Controlled polymerization in the named system was found to proceed in media of low polarity (mixture of 1,2-dichloroethane (DCE) with hexane). With all this going on, a decrease in solvent polarity leads to a substantial narrowing in molecular weight distribution of the polymer obtained: from $M_w/M_n = 2.14$ to ~ 1.75 at DCE : hexane = 2:1 and DCE : hexane = 1:1, respectively [59]. Investigation of styrene polymerization at various Bu_2O concentrations has shown that the optimal [$TiCl_4$] : [Bu_2O] ratio was 1:2. Further increase in the ether content led to a conventional (non-controlled) polymerization, as evidenced by a decrease in M_n with increasing monomer conversion, whereas MWD retained its quite narrow value ($M_w/M_n = 1.88$) [60].

The results obtained allowed optimal conditions and reagent ratios to be found and the «living» polymerization of styrene to be performed in the system 1-phenylethyl chloride/$TiCl_4$/Bu_2O. Thus, M_n of the polymer increases with increasing monomer conversion, the straight line of the «M_n-conversion» relationship passes through the origin, and the experimental data correlate well with those calculated (solid line in Fig. 1). This evidences the absence of a chain transfer reaction in the system. It is noteworthy, that MWDs for the polymers synthesized ($M_w/M_n = 1.46 – 1.56$) are more narrow as compared with those for other polystyrenes obtained in other systems based on $TiCl_4$.

The second relationship shown in Fig. 1 (dotted line) indicates that the chain growth is a first order reaction with respect to the monomer, i.e. the concentration of active species remains constant in the course of reaction. This is evidence of the absence of an irreversible chain termination.

The data presented above are evidence of «living» character of styrene polymerization under the conditions studied. Earlier we have found that the lifetime of active species is longer than the time of complete conversion of the monomer [59]. This fact is an indication of a prevailing role of chain growth processes over those of irreversible chain termination.

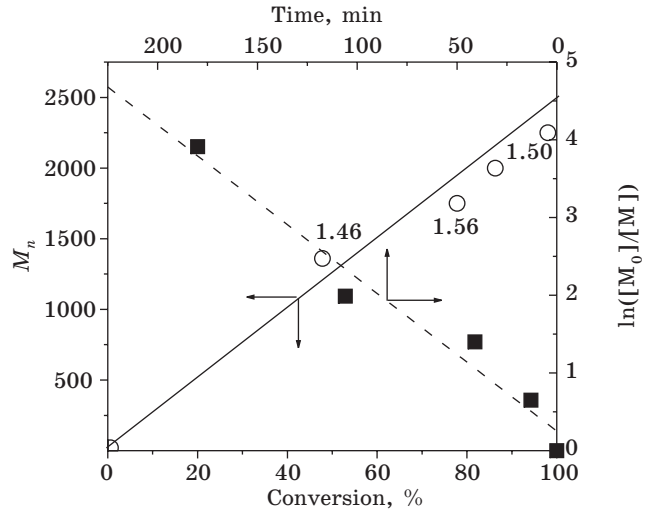

Fig. 1. Molecular weights as function of monomer conversion, and $\ln([M]_0/[M])$ versus time in the polymerization of styrene with 1-phenylethyl chloride/$TiCl_4$/Bu_2O/ –15 °C; $[M]_0$ 0.82 M; $[I]_0$ $3.5 \cdot 10^{-2}$ M; $[TiCl_4]$ 0.14 M; $[Bu_2O]$ 0.28. Numbers are MWD values. The straight line corresponds to theoretically calculated M_n values

^{1}H NMR spectroscopy data indicate the presence of only chlorine terminal groups in the macromolecules. The number-average molecular weight (M_n = 1760) calculated from the ^{1}H NMR spectrum is virtually the same as the M_n value measured using gel permeation chromatography (GPC) (M_n = 1720), and is quite close to that determined from the relationship $[M_0]/[I] \cdot 104$, where $[M_0]$ and [I] are concentrations of the monomer and the initiator (M_n = 1600) [60].

The first-order (with respect to the monomer) relationship for styrene polymerization in the system 1-phenylethyl chloride/$TiCl_4$/Bu_2O at various $TiCl_4$ concentrations is shown in Fig. 2. The values for apparent rate constants (k_{papp}) determined from the slopes of straight line plots of $\ln([M_0]/[M])$ vs. polymerization time were $1.1 \cdot 10^{-2}$, $2.1 \cdot 10^{-2}$ and $3.9 \cdot 10^{-2}$ min^{-1}, for $TiCl_4$ concentrations of 0.07, 0.14 and 0.21 M, respectively [61].

As is seen from Fig. 3, the reaction order with respect to $TiCl_4$ for styrene polymerization in the system 1-phenylethyl chloride/$TiCl_4$/Bu_2O is 1.09, that is very close to 1. Taking into account that the first order in isobutylene polymerization is observed when [initiator] ≥ $[TiCl_4]$ [62], we have suggested that initiation of polymerization in the system 1-phenylethyl chloride/$TiCl_4$/Bu_2O is performed by means of a small amount of $TiCl_4$ resulting from dissociation of its complex with Bu_2O. In this case, the instantaneous concentration of $TiCl_4$ < [initiator] and, according to [62], the reaction order with respect to $TiCl_4$ should be equal to 1. On the other hand, the free ether formed as a result of dissociation of the complex can interact with the growing species by solvation. This leads to both decrease in the overall polymerization rate and suppression of side reactions. The suggested reaction mechanism is presented in the scheme 2 [61].

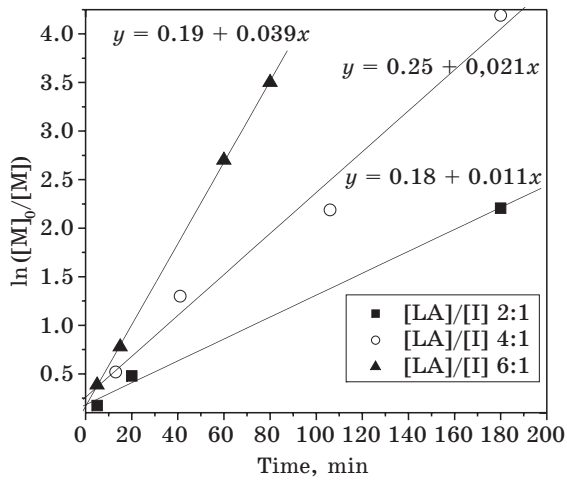

Fig. 2. The plot of ln([M_0]/[M]) vs. polymerization time in the system 1-phenylethyl chloride/$TiCl_4$/Bu_2O at –15 °C using various $TiCl_4$ concentrations; [M_0] = 0.82 M; [I] = $3.5 \cdot 10^{-2}$ M; [$TiCl_4$] = 2 [Bu_2O]

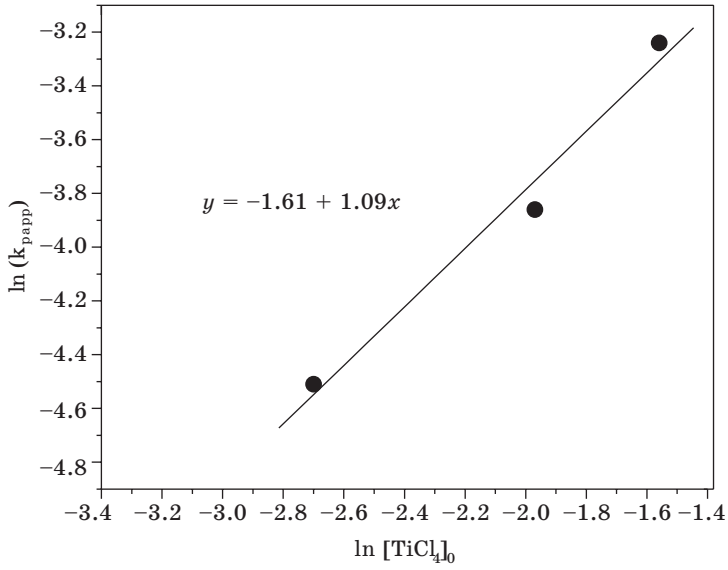

Fig. 3. Reaction order of [$TiCl_4$] for styrene polymerization with 1-phenylethyl chloride/$TiCl_4$/Bu_2O/ –15 °C; $[M]_0$ 0.82 M; $[I]_0$ $3.5 \cdot 10^{-2}$ M; [$TiCl_4$]=2[Bu_2O]

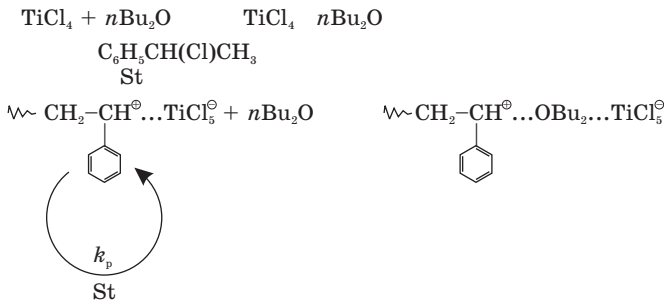

Scheme 2. Styrene polymerization mechanism
in the system 1-phenylethyl chloride/$TiCl_4$/Bu_2O

In that way, the studies performed made it possible to avoid low temperatures used to obtain «living» polymerization of styrene in systems based on $TiCl_4$, and to develop initiator systems with a potential of industrial use.

1.2. Polymerization in systems based on $AlCl_3$ etherates

It is known that aluminium trichloride is quite widely used in industrial practice as a co-initiator in cationic polymerization of styrene and other monomers. However, it is characterized by a rather low selectivity with respect to the chain growth reaction, and causes a number of side reactions to proceed. For the time being, there are no reports in the literature about realization of the «living» polymerization of styrene in the presence of aluminium trichloride.

At the same time, preliminary studies have revealed that when styrene polymerization is performed in the systems $H_2O/AlCl_3 \cdot O(C_6H_5)_2$ [63] and $H_2O/AlCl_3 \cdot O(C_4H_9)_2$, [64], no irreversible chain termination is seen, and M_n of the polymer increases with increasing its yield. However, lower M_n value as compared to that calculated indicates that a chain transfer reaction is involved in the named systems. A more detailed study of the system based on $AlCl_3 \cdot O(C_4H_9)_2$ has shown that, depending on polymerization conditions, the experimental M_n values for the polymer either exceed the calculated values (which is evidence of a slow or incomplete initiation) or are lower than the latter, which points to a chain transfer reaction present in the system (Fig. 4*a*) [65].

It is important to note that a polymer with a more narrow MWD is formed in styrene polymerization in the system $H_2O/AlCl_3 \cdot O(C_4H_9)_2$ than in the 1-phenylethyl chloride/$AlCl_3 \cdot OBu_2$ (Fig. 4b). The molecular weight distribution curve is unimodal in the case of styrene polymerization in the system $H_2O/AlCl_3 \cdot OBu_2$, i.e. the process takes place involving only one type of active species – ion pairs. At the same time, a small peak in the area of high molecular weights (at low V_R values) observed in the polymerization using the 1-phenylethyl chloride/$AlCl_3 \cdot OBu_2$ system is an indication of participation of free ions, along with ion pairs, in the chain propagation process.

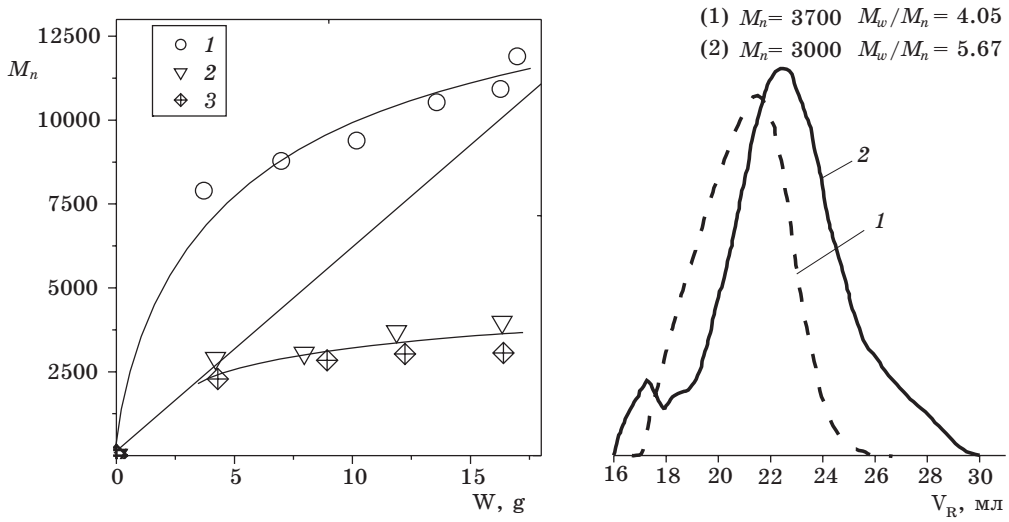

Fig. 4. Molecular weights as function of polymer yield in the polymerization of styrene with $AlCl_3 \cdot OBu_2$ at –15 °C; [$AlCl_3 \cdot OBu_2$] = 0.03 M; [H_2O] = 0.023 M (1, 2); [1-phenylethyl chloride] = 0.023 M (3). The straight line corresponds to theoretically calculated M_n values (a). GPC traces of polystyrene obtained by the $H_2O/AlCl_3 \cdot OBu_2$ (1) and 1-phenylethyl chloride/$AlCl_3 \cdot OBu_2$ (2) (b)

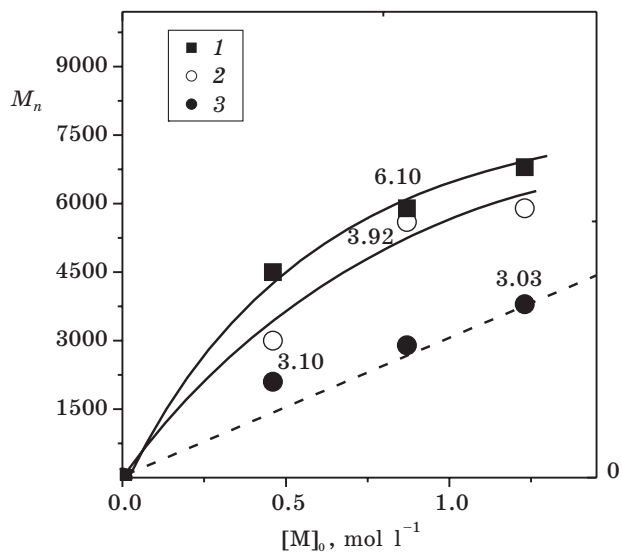

Fig. 5. Molecular weights as function of monomer concentration in the polymerization of styrene in the presence of $AlCl_3 \cdot OBu_2$: [$AlCl_3 \cdot OBu_2$] 0.05 M, [I] 0.04 M; [I]= 1-phenylethyl chloride (1), 1-phenylethanol (2), 2-phenyl-2-propanol (3). T= –15 °C. The dotted line corresponds to theoretically calculated M_n values

Within the framework of these studies, the effects of initiator structure on molecular weight distribution characteristics of polymers obtained in the presence of $AlCl_3 \cdot OBu_2$ were investigated. It has been found that initiators containing donor groups (–OH) promoted the controlled polymerization of styrene and led to polymers with a more narrow MWDs (Fig. 5). In the system 2-hydroxy-2-phenylpropane/$AlCl_3 \cdot OBu_2$, a «living» polymerization of styrene takes place: molecular weight of the polymer increases with the monomer concentration, and a good correlation of experimental data with the respective calculated values is observed. The polymer MWD decreases with increasing conversion of the monomer (Fig. 5) [66, 67].

In our opinion, the controlled polymerization of styrene in the system 2-hydroxy-2-phenylpropane/$AlCl_3 \cdot OBu_2$ is due to the formation *in situ* of a weaker Lewis acid ($AlCl_2OH$). This leads to a shift in the equilibrium between active and «dormant» species towards formation of the latter, as well as to acceleration of exchange reactions between them, which favors the control of M_n and narrowing its MWD. At the same time, the fact that dibutyl ether forms a fairly stable complex with the Lewis acid ($\Delta H \sim -36.5$ kcal/mol) favors a decrease in momentary concentration of the acid, which leads to suppression of side processes involving the latter. On the other hand, the ether may participate in stabilization of growing chains of polymerization by solvating them or forming donor-acceptor compounds.

Thus, the studies we have performed made it possible for the first time to realize a «living» cationic polymerization of styrene in the presence of a common industrial Lewis acid.

2. SYNTHESIS AND MODIFICATION OF PETROLEUM POLYMERIC RESINS

The intense development of petrochemical industry promoted the creation of a new group of synthetic film-forming substances for the manufacture of paintwork materials – the petroleum polymeric resins. The PPRs are also widely used as binding, plasticizing or dispersing additives in various composite materials employed as substitutes for products of natural and synthetic origin, while maintaining, and sometimes improving their physicochemical and performance characteristics. The use of PPRs is promising due to a broad-range and inexpensive raw material source (waste and side products of industrial-scale syntheses of ethylene and propylene, mainly the C_9 fraction). Furthermore, the manufacture of PPRs and their attendant compounds is one of the trends in profound integrated processing of oil stock [54, 55].

Fundamental investigations of the cationic polymerization mechanism of styrene [63–67], which is one of the major monomers of the C_9 fraction, have shown that the most promising method for preparation of PPRs is cationic polymerization. This is mainly due to the fact that the major monomers contained in the C_9 fraction – styrene, vinyltoluenes, dicyclopentadiene, indene, α-methylstyrene – are quantitatively polymerized by cationic mechanism only. Moreover, under certain conditions, the polymer yield may exceed the one theoretically calculated on the basis of monomer content, which may be explained by the inclusion of aromatic solvent molecules into the polymer chain owing to reactions of chain transfer to the solvent [63].

While performing cationic polymerization experiments with the C_9 fraction, donor-acceptor complexes of $AlCl_3$ with dibutyl and diphenyl ethers, ethyl acetate and carbamide were investigated [54]. It has been found that the most suitable catalyst for industrial use is aluminium trichloride diphenyl etherate, which is characterized by a relatively simple preparation procedure and high stability; the cationic polymerization proceeds rapidly in its presence (1–2 h) and the yields are quantitative [55, 68–70].

Properties of PPRs are known to depend directly on composition of the fractions used for synthesis. At the same time, the contents of hydrocarbon components in the industrial fractions are different. They are determined by composition of the starting raw materials and by pyrolysis conditions. So, depending of monomer composition of the fractions, the resulting PPRs may differ in melting points (60-140 °C) and M_n (350-850). The quantity and ratio of monomers in a fraction determines not only the PPR yields but, to a significant extent, their properties as well. On oligomerization of a fraction containing a large quantity of dicyclopentadiene (30 %), resins with low softening temperatures are formed. An increase of styrene content in the fraction leads to increase in T_{soft}. High content of dicyclopentadiene units in the oligomer chains imparts high elasticity and good adhesive properties to the paintwork materials (films) obtained on their basis. In that way, by varying relative contents of these monomers in a fraction, one can obtain various properties of coatings prepared on their basis, in accordance with their intended use [54, 55, 68].

Besides the fraction composition, other parameters of the oligomerization process, such as temperature, catalyst quantity, modifier and deacfivator nature, exert significant influence on properties of the resins obtained. Optimal concentration of the catalytic complex has been found to be 1–1.5 % (w/w) in a fraction. Introduction of small amounts of maleic anhydride (up to 2 % in a fraction) increases adhesive properties and melting point of the PPRs, which contributes to improvement of quality of the PPR-based films [55].

A significant disadvantage of the PPRs obtained by cationic polymerization is their darker colour as compared to resins synthesized by procedures based on the radical mechanism. It has been found that the colour of resins obtained is significantly affected in the stage of catalyst deactivation. The brightest resins were obtained when using ethylene oxide, propylene oxide, or mixtures of acetone or ethyl alcohol with water as deactivators [54]. The regularities in oligomerization reaction found in these experiments allowed wasteless technologies to be developed for synthesis of PPRs and of an analogue of petroleum polymer-based drying oil [68-70].

The wide range of application areas of PPRs is due, first of all, to their availability and the ability to replace many expensive compounds of natural origin. On the other hand, modification of PPRs by imparting to them hydrophilic properties would make it possible to extend significantly their application areas. Sulphonation and maleinization are the most efficient modification methods for hydrocarbon polymers.

We have performed preliminary studies of sulphonation of polystyrene having molecular weight of up to 3000, which is comparable to that of PPRs obtained by cationic polymerization. The obtained results allowed the reaction conditions, solvent and sulphonating agents to be selected for the synthesis of water-soluble polystyre-

ne. Taking into account the fact that PPRs represent a multicomponent system involving various monomer units, the C_9 fraction that contains the largest quantities of styrene-containing monomers has been selected for the study. The nature of sulphonating agent and the starting reagent ratio have been found to affect significantly both the yields of water soluble resins and content of sulpho-groups introduced. For PPRs sulphonation, chlorosulphonic acid, oleum, and sulphur trioxide complexes with dioxane proved to be the most suitable agents. The studies we have performed made it possible to develop optimal sulphonation parameters for PPRs and PP to prepare modified polymers with various degrees of sulphonation [71]. Some of the sulphonated resin samples (sulpho-PPRs) were tested as concrete plasticizers. Preliminary results have shown that concrete sorts of greater density and enhanced homogeneity as compared with unplasticized ones could be obtained using these samples. Moreover, application of sulpho-PPRs as concrete plasticizers allowed the deformation of autogenic shrinkage to be reduced [72].

In that way, the possibility of using sulphonated polymeric resins as concrete plasticizers has been demonstrated. Sulpho-PPRs are also promising agents for obtaining water-dilutable paints on their basis.

CONCLUSION

As a result of systematic studies on synthesis and properties of OAC and their complexes, easy preparative methods of synthesis for a number of compounds have been developed, and their physicochemical properties and catalytic activity in polymerization processes have been studied. The detailed investigation of the properties of the OAC complexes with ethers allowed working out a range of effective initiating system in cationic polymerization using etherates of $AlCl_3$ and $TiCl_4$. New catalytic systems capable of initiating styrene «living» cationic polymerization were established. These systems being suitable for synthesis of polystyrene with controlled molecular weight, as well as molecular weight distribution and quantitative functionality, are perspective to use in industry. The results obtained in these studies allowed targeted synthesis to be performed of PPRs and PP with pre-determined physicochemical and technical indices, which could be used as film-forming agents in paintwork materials and as concrete plasicizers, as well as for obtaining water-dilutable paints.

Based on the catalytic technology for preparation of petroleum polymer resins and petroleum polymerizate developed at the Research Institute for Physical Chemical Problems of the Belarusian State University, a wasteless manufacturing of bright thermostable resins has been created.

REFERENCES

1. *Mardykin V. P., Gaponik P. N., Popov A. F.* // Russian Chemical Reviews. 1979. Vol. 48, № 5. P. 905.
2. *Gaponik L. V., Mardykin V. P.* // Vestn. Belorussk. Univ. Ser. 2. 1988. № 3. P. 3.
3. *Gaponik L. V., Mardykin V. P., Gavrilenko V. V.* // Organomet. Chem. USSR. 1990. Vol. 3, № 2. P. 111.

4. *Kaputsky F. N., Mardykin V. P., Gaponik L. V.* // Chemical problems of development of new materials and technologies. Minsk. 1998. P. 169.
5. *Kaputsky F. N., Mardykin V. P., Pavlovich A. V.* // Vestsi Natsiyan. Akad. Navuk Belarusi. 1994. № 1. P. 115.
6. *Gaponik L. V., Antipova A. M., Morozova T. K., Mardykin V. P.* // J. Appl. Polym. Sci. 1989. Vol. 38. P. 1979.
7. *Kaputsky F. N., Mardykin V. P., Gaponik L. V., Zimina T. L.* // Vestsi Natsiyan. Akad. Navuk Belarusi. 1996. № 2. P. 110.
8. *Kaputsky F. N., Mardykin V. P.* // Cationic oligomer of 1,3-pentadiene: synthesis, characteristics and application. Minsk. 1997.
9. *Kaputsky F. N., Mardykin V. P., Kostjuk S. V., Gaponik L. V.* Living carbocationic polymerization of styrene and its derivatives. The selected works of the Belarusian State University. Minsk. 2001. Vol. 5. P. 471.
10. *Mardykin V. P., Gaponik L. V.* // Vestsi Natsiyan. Akad. Navuk Belarusi. 1999. № 4. P. 55.
11. *Mardykin V. P., Gaponik L. V., Morozova T. K.* // Vestsi Natsiyan. Akad. Navuk Belarusi. 1987. № 2. P. 67.
12. *Gaponik L. V., Mardykin V. P., Pavlovich A. V.* // Vestsi Natsiyan. Akad. Navuk Belarusi. 1994. № 3. P. 78.
13. *Gaponik L. V., Mardykin V. P., Gaponik P. N.* // USSR P. 706417; Byull. Izobret., 1979. № 48.
14. *Gaponik L. V., Mardykin V. P.* // Izv. Vusov. Khim. I Khim. tehnolog. 1983. Vol. 26, № 1. P. 30.
15. *Gaponik L. V., Mardykin V. P.* // Russian J. Org. Chem. 1977. Vol. 47, № 7. P. 1579.
16. *Gaponik L. V., Mardykin V. P.* // Izv. Vusov. Khim. I Khim. tehnolog. 1979. Vol. 22, № 10. P. 1194.
17. *Gaponik L. V., Mardykin V. P., Gaponik P. N.* // USSR P. 691455; Byull. Izobret., 1979. № 33.
18. *Gaponik L. V., Mardykin V. P.* // Russian J. General Chem. 1985. Vol. 55, № 6. P. 1341.
19. *Gaponik L. V., Lesnyak V. P., Gaponik P. N.* // Horizon of organic and organometallic chemistry. 1999. Moscow. Vol. 2. P. 35.
20. *Mardykin V. P., Pavlovich A. V., Irkhin B. L., Gaponik L. V., Morozova S. G.* // Russian J. General Chem. 1986. Vol. 56, № 10. P. 2311.
21. *Pavlovich A. V., Mardykin V. P., Gaponik L. V.* // Russian J. General Chem. 1992. Vol. 62, № 3. P. 541.
22. *Mardykin V. P., Pavlovich A. V., Gaponik P. N.* // Organomet. Chem. USSR. 1992. Vol. 5, № 4. P. 930.
23. *Mardykin V. P., Pavlovich A. V., Gaponik P. N., Baranov O. M.* // Russian J. General Chem. 1982. Vol. 52, № 11. P. 2620.
24. *Mardykin V. P., Pavlovich A. V., Gaponik P. N., Irkhin B. L.* // Vestn. Belorussk. Univ. Ser. 2. 1986. № 1. P. 69.
25. *Mardykin V. P., Antipova A. M., Gaponik L. V., Listratova G. V.* // Vestn. Belorussk. Univ. Ser. 2. 1978. № 2. P. 14.
26. *Antipova A. M., Gaponik L. V., Sviridov S. V., Mardykin V. P.* // Polym. Sci. Ser. B. 1983. Vol. 25, № 3. P. 170.
27. *Antipin L. M., Shmidel L. E., Larionov O. G.* et al. // Organomet. Chem. USSR. 1990. Vol. 3, № 6. P. 1279.
28. *Mardykin V. P., Antipova A. M., Gaponik L. V.* // Polym. Sci. Ser. B. 1981. Vol. 23, № 1. P. 52.
29. *Antipova A. M., Morozova T. K., Gaponik L. V.* et al. // Vestn. Belorussk. Univ. Ser. 2. 1984. № 2. P. 14.

30. *Antipova A. M., Morozova T. K., Gaponik L. V., Mardykin V. P.* // Polym. Sci. Ser. B. 1986. Vol. 28, № 3. P. 182.
31. *Antipova A. M., Gaponik L. V., Mardykin V. P.* // Complex organometallic catalyst of olefin polymerization. 1980. Chernogolovka. P. 83.
32. *Voronova E. I., Valendo A. J., Gaponik L. V., Mardykin V. P.* // Vestsi Natsiyan. Akad. Navuk Belarusi. 1988. № 5. P. 83.
33. *Ivancheva N. I., Severova N. N., Smolyanova O. V.* et al. // DDR P. 243171.
34. *Mardykin V. P., Morozova T. K.* // Izv. Vusov. Khim. I Khim. tehnolog. 1984. Vol. 27, № 3. P. 357.
35. *Mardykin V. P., Morozova T. K., Pritytskaya T. S.* et. al. // Izv. Vusov. Khim. I Khim. tehnolog. 1981. Vol. 24, № 8. P. 1018.
36. *Antipova A. M., Morozova T. K., Kulevskaya I. V., Mardykin V. P.* // Polym. Sci. Ser. B. 1984. Vol. 26, № 3. P. 170.
37. *Martinovich K. B., Gurash G. V., Mardykin V. P., Gaponik L. V.* // Dokl. Natsion. Akad. Navuk Belarusi. 1978. Vol 22, № 7. P. 631.
38. *Mardykin V. P., Gaponik L. V.* // Vestn. Belorussk. Univ. Ser. 2. 1997. № 3. P. 3.
39. *Mardykin V. P., Pritytskaya T. S., Gurash G. V., Pochernayev N. M.* // Vestn. Belorussk. Univ. Ser. 2. 1981. № 1. P. 27.
40. *Mardykin V. P., Pavlovich A. V.* // Vestn. Belorussk. Univ. Ser. 2. 1991. № 3. P. 24.
41. *Mardykin V. P., Antipova A. M., Gurash G. V., Sviridov S. V.* // Russian J. Appl. Chem. 1979. Vol. 52, № 6. P. 1424.
42. *Mardykin V. P., Irkhin B. L., Pavlovich A. V.* et. al. // Russian J. Appl. Chem. 1984. Vol. 57, № 5. P. 1157.
43. *Pavlovich A. V., Mardykin V. P., Antipin L. M., Kusaev A. I.* // Vestsi Natsiyan. Akad. Navuk Belarusi. 1992. № 3–4. P. 103.
44. *Gaponik L. V., Zimina T. L., Mardykin V. P.* // XVII All-union conference on chemistry of complexes compound. Moscow. 1996. P. 30.
45. *Mardykin V. P., Morozova T. K., Rakhimov R. X.* et. al. // USSR P. 71579032. 1990.
46. *Kaputsky F. N., Vasilenko I. V., Kostjuk S. V., Gaponik L. V.* // Vestn. Belorussk. Univ. Ser. 2. 2002. № 2. P. 15.
47. *Kostjuk S. V., Vasilenko I. V., Gaponik L. V., Kaputsky F. N.* // Modern trends in organometallic and catalytic chemistry. Moscow. 2003. P. 80.
48. *Mardykin V. P., Morozova S. G., Gaponik L. V., Chuprakova L. D.* // Russian J. Appl. Chem. 1998. Vol. 71. P. 1041.
49. *Mardykin V. P., Raysnoy V. D., Pavlovich A. V.* et. al. // Plastmasy. 1986. № 7. P. 57.
50. *Mardykin V. P., Pavlovich A. V., Gaponik L. V., Kaputsky F. N.* // Russian P. 2057764. 1996.
51. *Kaputsky F. N., Mardykin V. P., Gaponik L. V., Zimina T. L.* // Belarusian P. 2331. Byull. Izobret., 1997. № 3.
52. *Kaputsky F. N., Mardykin V. P., Gaponik L. V., Milchanina T. L.* // Vestsi Natsiyan. Akad. Navuk Belarusi. 1998. № 2. P. 91.
53. *Kaputsky F. N., Mardykin V. P., Gaponik L. V., Milchanina T. L.* // Vestn. Belorussk. Univ. Ser. 2. 1998. № 3. P. 11.
54. *Kaputsky F. N., Mardykin V. P., Gaponik L. V., Lesnyak V. P., Kostjuk S. V.* // Vestsi Natsiyan. Akad. Navuk Belarusi. 2000. № 3. P. 48.
55. *Kaputsky F. N., Mardykin V. P., Gaponik L. V., Lesnyak V. P., Kostjuk S. V., Milchanina T. L.* // Russian J. Appl. Chem. 2002. Vol. 75, № 6. P. 1006.
56. *Kaputsky F. N., Mardykin V. P., Gaponik L. V., Lesnyak V. P., Kostjuk S. V.* // Vestn. Belorussk. Univ. Ser. 2. 2000. № 1. P. 3.
57. *Mardykin V. P., Gaponik L. V.* // Vestn. Belorussk. Univ. Ser. 2. 2001. № 1. P. 16.
58. *Kostjuk S. V., Kaputsky F. N., Mardykin V. P., Gaponik L. V.* // Chemistry and physics of polymers in the 21 century. Chernogolovka. 2000. P. 2–64.

59. *Kostjuk S. V., Kaputsky F. N., Mardykin V. P.* et. al // Dokl. Natsion. Akad. Navuk Belarusi. 2002. Vol. 46. P. 74.
60. *Kostjuk S. V., Kaputsky F. N., Mardykin V. P., Gaponik L. V., Antipin L. M.* // Polym. Bull. 2002. Vol. 49. P. 251.
61. *Kostjuk S.V.* // Polym. Bull. 2003. (in press).
62. *Puskas J. E., Lanzendorfer M. G.* // Macromolecules. 1998. Vol. 31. P. 8684.
63. *Kaputsky F. N., Mardykin V. P., Kostjuk S. V., Gaponik L. V.* // Vestsi Natsiyan. Akad. Navuk Belarusi. 1999. № 2. P. 96.
64. *Kostjuk S. V., Mardykin V. P., Gaponik L. V., Kaputsky F. N.* // Vestsi Natsiyan. Akad. Navuk Belarusi. 2000. № 2. P. 47.
65. *Kostjuk S. V., Kaputsky F. N., Mardykin V. P., Gaponik L. V.* Physic and chemistry of polymers: synthesis, properties and application. 2002. Vol. 8. P. 210.
66. *Kostjuk S. V.* Dissertation Ph.D. Institute of Physical Organic Chemistry of the National Academy of Sciences of Belarus. Minsk. 2002. P. 74.
67. *Kostjuk S. V., Mardykin V. P., Gaponik L. V.* et. al. // Polym. Sci. 2003. (in press).
68. *Kaputsky F. N., Mardykin V. P., Gaponik L. V.* // Development of imported- replaced technologies and materials in chemistry industry. Minsk. 1999. P. 142.
69. *Kalishuk D. G., Saevich N. P., Kaputsky F. N.* et. al. // Development of imported- replaced technologies and materials in chemistry industry. Minsk. 1999. P. 144.
70. *Kostjuk S. V., Lesnyak V. P., Gaponik L. V.* et. al. // New technologies of recycling of secondary resources. Minsk. 2001. P. 44.
71. *Lesnyak V. P., Kaputsky F. N., Mardykin V. P.* et. al. // New technologies in chemical industry. Minsk. 2002. P. 67.
72. *Tur V. V., Kaputsky F. N., Ignashova O. E.* // The concrete and ferro-concrete in the third millennium. Rostov-na-Dony. 2002. P. 342.

CHEMICAL PROBLEMS OF THE DEVELOPMENT OF NEW MATERIALS AND TECHNOLOGIES
Minsk 2003

V. V. Egorov,
E. M. Rakhman'ko

ION ASSOCIATION EFFECTS OF LIPOPHILIC QUATERNARY AMMONIUM SALTS IN ION-EXCHANGE AND POTENTIOMETRIC SELECTIVITY

INTRODUCTION

Until the present time the problem of the effects exerted by ion association of lipophilic quaternary ammonium salts (QAS) on the anion-exchange and potentiometric selectivity of the anion-selective electrodes has been practically untackled, both theoretically and experimentally. Moreover, so far lipophilic QAS have been customary assumed as nonselective anion exchangers, the ion exchange constants for which are primarily determined by standard free energies of ion resolvation to conform to Hofmeister's extraction series [1–5]. Indeed, this point of view has been supported by numerous experimental data bearing witness to insignificant dependence of anion exchange constants on the structural features of quaternary ammonium cations (QAC) [1, 4, 6]. However, recently we have found that this situation occurs just in the cases of QAC in which all four hydrocarbon chains are sufficiently long (no less than propyl) and in the cases when single-charged anions are exchanged for the single-charged ones. Otherwise, anion exchange constants and potentiometric selectivity coefficients of QAS-based membranes may be varying by several orders [7–10] pointing to manifestations of the factor of ion association.

It should be noted that the majority of the published reliable information concerning the ion association constants relate to solvents with medium and high dielectric permeability (acetone, methyl ethyl ketone, primary alcohols, dichloroethane, acetonitrile, nitrobenzene, etc.) [11–25], where the values of ion association constants are comparatively low and much leveled. At the same time, in solvents with low dielectric permeability, where the influence of the structural features of cation and anion on the efficiency of electrostatic interaction should be especially essential, the experimental values of the ion association constants are «hard to reach» [26]. Nevertheless, the ion exchange constants revealing the peculiarities of ion association for QAC with exchanging anions are easily accessible experimentally. Unfortunately, the direct assessment of the role played by the ion association factor in exchange selectivity on the basis of ion exchange data is impossible, since the principal part belongs to much more profound solvation effects. However, the relationship between the anion exchange constants and the QAC structure established in Refs. [7, 9, 10] unambiguously demonstrates that

the factor of ion association may have a significant effect on the ion-exchange selectivity too.

In the present work we report some new ideas concerning the role of solvation and ion association processes in the ion-exchange and potentiometric selectivity. In our opinion, a proposed approach based on the linear Gibbs energy relations (LGER) [27–31] and ion association theory by Eigen-Denison-Ramsey-Fuoss [32–35] enables one to compare the role of hydration, solvation and ion association processes in systems involving lipophilic QAS in the ion-exchange (K_i^j) and potentiometric ($K_{i,j}^{Pot}$) selectivity and, consequently, to estimate the limits for purposefull variation of these parameters using the factor of ion association. The obtained results are of great practical importance for the development of extraction systems and ion-selective electrodes with the improved selectivity.

1. LGER-BASED DESCRIPTION OF ION-EXCHANGE EQUILIBRIA

1.1. The first approximation. Comparative estimation of the contributions made by standard free energies of anion hydration and solvation into the anion-exchange selectivity

In solvents with low and medium dielectric permeability QAS exist mainly in the form of ion associates. So the ion-exchange equilibrium in such systems is normally described by the following equation:

$$\overline{R^+ \ldots i^-} \quad j^- \quad \overset{K_i^j}{\rightarrow} \quad \overline{R^+ \ldots j^-} \quad i^- , \tag{1}$$

where $R^+ \ldots i^-$, $R^+ \ldots j^-$ are the ion associates of QAC with anions i^- and j^- respectively, an overscribed bar denotes the phase of organic solvent, K_i^j is the exchange constant.

It should be noted that this relationship is correct provided that ion pairs only occur without the formation of more complex aggregates (approximation of a perfectly associated solution). However, a great body of data obtained during investigations of the anion-exchange properties of trinonyloctadecylammonium (TNODA) relative to a large number of anions in a system water – toluene [6] revealed that there is no relationship between the exchange constants and concentration $R^+ \ldots i^-$ in the organic phase over the concentration range of 10^{-3}–10^{-4} M. This may be indicative of the absence of the aggregation processes or of their course following alike for TNODA salts with different anions (the latter seems to be highly improbable). Because of this, the ion exchange process is further described by the equation (1).

Then the exchange constant may be defined by the following equation:

$$\log K_i^j \quad \frac{G_{h\ j}^0 \quad G_{h\ i}^0 \quad G_{s\ j}^0 \quad G_{s\ i}^0}{2303RT} \quad \log \frac{(k_{ass})_{jR}}{(k_{ass})_{iR}}, \tag{2}$$

where G_h^0 and G_s^0 are the standard free hydration and solvation energies of anions, k_{ass} are ion association constants, and R denotes a quaternary ammonium cation.

Assuming that ion association constants of anions with long-chain QAC are relatively independent of the nature of associating anions (being rather a function of the dielectric permeability of a solvent) the ion exchange constant in the first approximation will be determined solely by the difference in the standard free hydration and solvation energies of exchanging ions*:

$$\log K_i^j \quad \frac{G_{h\ j}^0 \quad G_{h\ i}^0 \quad G_{s\ j}^0 \quad G_{s\ i}^0}{2{,}303RT}. \qquad (3)$$

Since mineral anions are solvated much more effectively by water compared to common organic solvents, the difference in free energies of hydration dominates over the difference in free energies of solvation. Because of this, the position of anions in the exchange series is determined by their hydration energies (Fig. 1).

Table 1

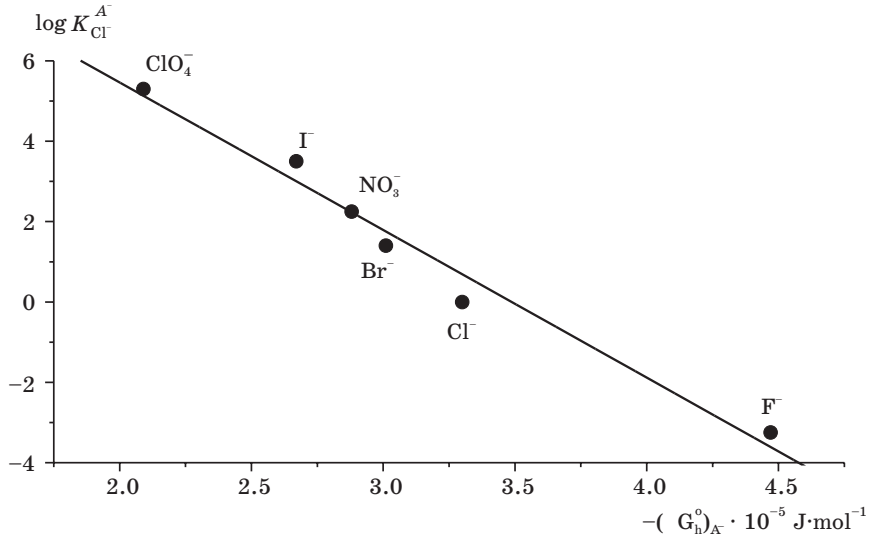

Fig. 1. The logarithms of the anion-exchange constants as a function of their standard free hydration energies. Ion exchanger – TNODA. Data taken from [6, 23].

*Such an assumption is to some extent substantiated as in the absence of some specific interaction between cation and anion, association constant of QAS are actually little dependent on the anion nature as compared to the association constant, e.g. of amine salts exhibiting H-bonding effect, the strength of which is strongly dependent on the anion charge density. This is conclusively demonstrated by the results summarized in Table 1. However, QAS association constants also depend on the anion nature, though to a lesser degree. This aspect will be discussed at greater length in section 1.2.

The logarithmic values of the ion association constants for TNODA and trioctylammonium (TOA) salts in binary systems toluene – nitrobenzene. Data taken from [36].

Anion	log k_{ass}			
	TNODA		TOA	
	30 vol.% of nitrobenzene	50 vol.% of nitrobenzene	30 vol.% of nitrobenzene	50 vol.% of nitrobenzene
Cl^-	5.35	3.6	>12	9.1
Br^-	5.0	3.5	10.5	8.0
J^-	4.88	3.3	7.8	6.2

However, the statement concerning the hydration energies of anions as a governing factor for the value of an exchange constant should not be literally understood. The hydration energies of anions determine their position in the exchange series rather than the exchange constant value. Even in the case of fairly inert organic solvents, e.g. toluene, the transport of anions from aqueous phase to the organic one is accompanied by the compensation of the greater part of free hydration energy by the free energy of solvation. For example, standard free energies of hydration for Cl^- and ClO_4 amount respectively to $-3.3 \cdot 10^5$ and $-2.09 \cdot 10^5$ J · mol^{-1} [23]. Then $K_{Cl}^{ClO_4}{}_{calc}$ calculated from the relationship:

$$K_{Cl}^{ClO_4}{}_{calc} \quad 10^{\frac{(G_h^0)_{ClO_4} \quad (G_h^0)_{Cl}}{2{,}303RT}}, \tag{4}$$

equals to $1 \cdot 10^{22}$, whereas the experimental value of $K_{Cl}^{ClO_4}{}_{exp}$ equals to $2 \cdot 10^5$ [6]. The last value corresponds to the difference in free standard transport energies of these ions approximately $3 \cdot 10^4$ J · mol^{-1}. This suggests that only about of 25 % of the difference in the standard free ions hydration energies are transformed into the ion-exchange selectivity whereas more than 75 % are compensated by the interactions in toluene phase.

The quantitative estimation of free standard energies of ion solvation by different solvents is a rather complex experimental problem. To compare the efficiencies of solvation coupling in different solvents, one can use the empirical polarity scales for solvents [27–31] based on the LGER principle. The essence this principle as applied to the anion solvation consists of the following: should anion A_1 be solvated by solvent S_1 stronger than by solvent S_2, then anion A_2 should be solvated by this solvent S_1 also stronger as opposed to solvent S_2. And the proportionality factor between the standard free solvation energies of one and the same ion by two different solvents is the value (constant in the first approximation) determined by the nature of these solvents and independent of the nature of solvated ions. Clearly, this principle is not and could not be rigorously substantiated theoretically. Moreover, it should be violated provided the interactions of a solvent with one of the ions is specific and distinct from interactions of the same solvent with other ions. For example, in the case of exchanging amphiphilic an-

ions, an individual estimation of the solvation effects is necessary for lipophilic and hydrophilic parts of the anion [37, 38] considering that the proportionality factors for their standard free energies of hydration and solvation differ. Nevertheless, the LGER principle shows itself rather clearly for a great body of experimental data. For example, a linear function $\log K_{Cl}^{A}$ $G_{h\ A}^{0}$ given in Fig. 1 follows directly from this principle.

As applied to the ion-exchange equilibria under study, the LGER principle may be expressed as

$$G_0^S \quad K \quad G_h^0. \tag{5}$$

Then equation (2) can be transformed into the following form

$$\log K_i^j \quad \frac{G_{h\ j}^0 \quad G_{h\ i}^0 \ (1 \quad K)}{2.303RT}, \tag{6}$$

or

$$\log K_i^j \quad K \quad G_{h\ j}^0 \quad G_{h\ i}^0 , \tag{7}$$

where

$$K^* \quad \frac{1 \quad K}{2.303RT}. \tag{8}$$

The K^* factor defines the effect exerted by a solvent nature on the ion-exchange selectivity. Obviously, this factor should increase with the lowering of the solvation ability of a solvent as in this case the difference in the standard free hydration energies of exchanging ions is more completely transformed to selectivity of the exchange process. On the contrary, for active solvents which effectively solvate the anions, when $K \to 1$, $K^* \to 0$, the compensation effect leading to reduced ion-exchange selectivity has to be increased.

Many attempts were undertaken to obtain quantitative correlations between the anion-exchange constants and standard free energies of anion hydration. However, the absence of trustworthy exchange constants determined over a wide range of exchange affinity and of trustworthy G_h^0 values for the majority of anions put obstacles in the way of producing the reliable results [40]. The first problem has been successfully solved, primarily owing to the studies performed at the Analytical Chemistry Department of the Belarusian State University [4, 6, 41–45] as a result of which the values of exchange constants have been found for more than 100 anions in a system water – toluene. As for the standard free energies of hydration, this problem remains to be solved [40] since the values for G_h^0 given in various publications are distinguished by several tens or even hundreds of kJ · mol^{-1} (see also Table 2).

Table 2

The logarithmic values of the anion exchange constants in a system water–toluene (standard ion – Cl^-, ion exchanger – TNODA) and the values of standard free energies of anion hydration. Data taken from the following sources: a – [6], b – [23], c – [46] (experimental values), d – [46] (calculated values).

Anion	$\log K^A_{Cl}$	$G^0_h \cdot 10^{-5}$, J · mol^{-1}		
	a	b	c	d
F^-	–3.25	–4.47	–4.65	–3.45
OH^-	–2.8	–4.64	–4.30	–3.45
H_2PO_4	–2.45	–	–4.65	–2.45
HCO_3	–2.0	–	–3.35	–3.10
CH_3COO^-	–1.6	–	–3.65	–3.00
Cl^-	0	–3.30	–3.40	–2.70
CN^-	0.2	–	–2.95	–2.60
JO_3	0.3	–	–4.00	–2.70
NO_2	0.55	–	–3.30	–2.55
BrO_3	1.0	–	–3.30	–2.60
Br^-	1.4	–3.01	–3.15	–2.50
NO_3	2.25	–2.88	–3.00	–2.75
ClO_3	2.7	–	–2.80	–2.45
J^-	3.5	–2.67	–2.75	–2.20
SCN^-	4.15	–	–2.80	–2.30
BF_4	4.35	–	–1.90	–2.05
ClO_4	5.3	–2.09	–4.30	–1.80
Pic^-	8.15	–	–	–
$TPhB^-$	12.8	–	0.50	0.15

Because of this, the K^* values may vary significantly (nearly twice) depending on the G^0_h set used (Fig. 2), and associated functions $\log K^A_{Cl}$ $G^0_{h\ A}$ $G^0_{h\ Cl}$ 10^{-5} are characterized by low correlation coefficients.

Using a set of G^0_h values for a limited number of anions (F^-, Cl^-, Br^-, NO_3^-, I^-, ClO_4^-), chosen as the most likely values [23], we have derived the values of K, K^* and coefficient $\alpha \equiv 1–K$, that defines the extent to which the difference in the standard free hydration energies of exchanging anions is transformed into the exchange selectivity (for a hypothetical perfectly inert solvent K and α amount to 1 and 0 respectively). The obtained values of K, K^* and α are summarized in Table 3.

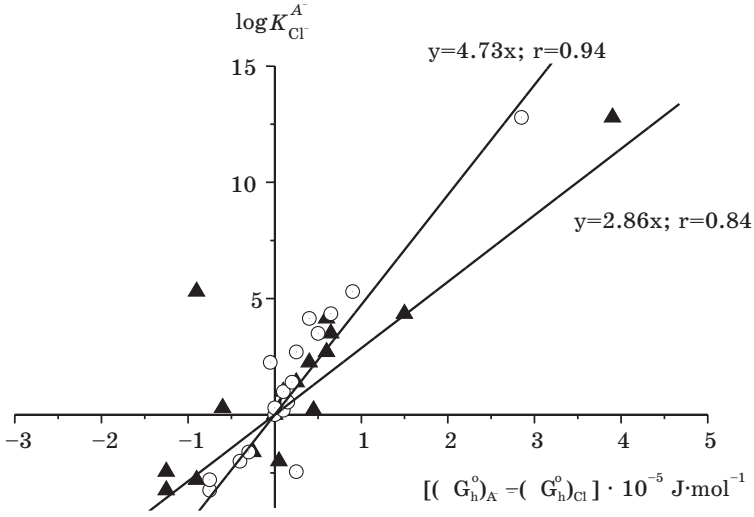

Fig. 2. Logarithms of anion-exchange constants (taken from [6]) as a function of the difference in standard free hydration energies (taken from [46]). | – experimental values of G_h^0;

Table 3

The values of K, K^*, α coefficients characterizing the solvation ability relative to anions and derived from the anion-exchange constants and standard free hydration energies by equations (6), (7). Ion exchanger – TNODA

Solvent	K G_s^0 / G_h^0	$K^* \cdot 10^5$	$\alpha = 1 - K$
n-decanol	0.94	1.1	0.06
chloroform	0.85	2.7	0.15
toluene	0.776	4.0	0.224
n-decane	0.781	3.9	0.219
toluene + nitrobenzene (1:9)	0.75	4.4	0.25

As can be seen, the values of K^* and α increase with the decreasing of the solvents polarity in a sequence decanol < chloroform < toluene in accordance with the above concept. At the same time, when using n-decane instead of toluene the obtained values of K^* and α were surprisingly lower than those of toluene, whereas with the use of a more polar binary mixture toluene – nitrobenzene (1:9) they were somewhat higher. The differences observed in the values of K^* and α for these solvents are not large. However, these differences could not be considered as experimental errors because they are reproducible [6].

A discrepancy between the above-mentioned approach and the experimental results is still larger in the case when double-charged anions are exchanged for the single-charged ones. As applied to the case of chloride exchanged by sulphate, equation (7) takes the following form:

$$\log K_{2Cl}^{SO_4^{2-}} \quad K \quad G_{h\ SO_4^{2-}}^{0} \quad 2 \quad G_{h\ Cl}^{0} \quad . \tag{9}$$

Substituting the value $K^{*}=4\cdot10^{-5}$, obtained for a system water – toluene on the basis of single-charged anions exchange data and $G_{h\ SO_4^{2-}}^{0} = -1.042\cdot10^{6}\ J\cdot mol^{-1}$, $G_{h\ Cl}^{0} = -3.3\cdot10^{5}\ J\cdot mol^{-1}$ [23], into the equation (9) we obtained the $\log K_{2Cl}^{SO_4^{2-}}{}_{calc}$ value of –15.3. The experimental value $\log K_{2Cl}^{SO_4^{2-}}{}_{exp}$ is equal to -2.8. So, the difference between the experimental and the calculated exchange constants is huge (by 12.5 orders). It seems that the most likely explanation for these discrepancies can be the effect of the ion association processes on the ion-exchange equilibrium, which has not been taken into account in the above approach.

1.2. Corrected model. Inclusion of the ion association factor

1.2.1. General approach

On the assumption that the difference in the ion association constants of QAC with exchanging anions has really a pronounced effect on the exchange constant value, equation (2) may be transformed as follows:

$$\log K_i^j \quad K^{**} \quad G_{h\ j}^{0} \quad G_{h\ i}^{0} \quad \log\frac{(k_{ass})_{jR}}{(k_{ass})_{iR}} \tag{10}$$

Apparently, K^{**} factor differs from the K^{*} factor in the equation (7).

In the first approximation the ion association constants are described by Eigen-Denison-Ramsey-Fouss equation [25] as a function of the closest approach parameter of associating ions, charge product, dielectric permeability of the medium and temperature. At T = 293 K this equation assumes the form

$$\log(k_{ass})_{RA} \quad 2.6 \quad 3\log a(Å) \quad 247\frac{|z_R \quad z_A|}{D \quad a(Å)}. \tag{11}$$

where a(Å) is the closest approach parameter in Ångström units, D is the relative dielectric permeability of solvent, z_R, z_A are the cation and anion charges.

It has been found that in solvents with low solvation ability such as toluene so-called contact ion pairs [15, 16] are formed without solvent molecules between the associated cation and anion. In this case the parameter a(Å) is mainly dependent on the geometry of associating ions and primarily on their sizes. Therefore, in media with not very high dielectric permeability, when the last term in equation (11) makes the principal contribution to the association constant, small ions are stronger associated as compared to large ones.

With allowance made for the ion association factor one is enabled to explain an apparent discrepancy between the solvation ability of solvents and K^{*} values calculated from equation (7) for n-decane, toluene and toluene – nitrobenzene mix-

ture (see Table 3). Due to high dielectric permeability of a binary mixture toluene – nitrobenzene containing up to 90 % of nitrobenzene, an extent of ion association of QAS at concentrations of $\leq 1 \cdot 10^{-2}$ M is never in excess of a few per cent. Because of this, the effect of ion association on ion-exchange equilibrium may be neglected. In consequence, K^* factor in this case defines «pure» solvation effects, and its fairly high value compared to other solvents ($4.4 \cdot 10^{-5}$) is conditioned by the fact that nitrobenzene belongs to the solvents poorly solvating the anions, despite its high dielectric permeability, being a weak base rather than Lewis acid.

As for toluene, the solvation effects interfere with the effects of ion association. Since the strength of QAS ion associates increases as the anion size decreases, this causes the leveling of the ion-exchange constants. Because of this a formal description of the exchange equilibrium based on equation (7) that takes no account of the ion association factor gives undervalued K^*, i.e. solvation of the ions by toluene seems higher than is actually the case. In n-decane characterized by a lower dielectric permeability compared to toluene (1.99 and 2.385 respectively) [47] the leveling effect of ion association is enhanced. As seen from the calculations based on equation (11), for ion pairs characterized by the closest approach parameters of 4.0 and 4.5 Å, the ion association constants in toluene should be differing by a factor of 530, whereas in n-decane – by a factor of 2000. As a result, without due regard for ion association the value of K^* will be severely undervalued.

The effect of the ion association factor is still greater in the case of single-charged ions exchanged by the double-charged ones. In this case equation (10) takes the form

$$\log K_{2i}^{j} \quad K^{**} \quad G_{h\ j}^{0} \quad 2 \quad G_{h\ i}^{0} \quad \log \frac{(k_{ass})_{jR} \quad (k_{ass})_{jRR}}{(k_{ass})_{iR}^{2}}, \qquad (12)$$

where $(k_{ass})_{jR}$ is the formation constant for the ion associate $j^{2-}\ldots R^{+}$ formed from a double-charged anion j^{2-} and cation R^{+}; $(k_{ass})_{jRR}$ is the formation constant for the ion associate $R^{+}\ldots j^{2-}\ldots R^{+}$ formed from a negatively charged associate $j^{2-}\ldots R^{+}$ and cation R^{+}; all other designations similar to equation (10).

As seen from the calculations based on equation (11) with the assumption that the closest approach parameters for the associates formed by QAC with single- and double-charged anions are close and equal to e.g. 4.5 and 5 respectively, in toluene (D = 2.385) the contribution of ion association (the last term in equation (12)) to $\log K_{2i}^{j}$ is +16.4. Because of this, the experimental constants characterizing the exchange of double-charged ions for the single-charged ones are much larger than might be expected reasoning from their standard free hydration energies.

1.2.2. Semiquantitative approach to estimation of the contributions made by ion association to anion-exchange selectivity

A theory of Eigen-Dension-Ramsey-Fouss allows for semiquantitative estimation of the ion association constants in media with low dielectric permeability, where these values are experimentally inaccessible. The required values of a(Å) may be iterati-

vely calculated using equation(11) from the association constants values experimentally determined in the media with rather high dielectric permeability. However, it should be taken into consideration that equation (11) has been derived on the basis of a «sphere in a continuous dielectric» model, disregarding a specific interaction of the associating ions with each other and with a solvent dictated by their structural features. Consequently, the values of a(Å) calculated from equation (11) for one and the same pair of ions in different solvents may differ appreciably. At the same time, the values of a(Å) calculated from the data on ion association in solvents similar in nature are, as a rule, in good agreement. All the afore-said is supported by Table 4.

As seen, for ion associates formed by tetraethyl ammonium cation with the same anion in acetone and methyl ethyl ketone the corresponding values of a(Å) are very close and the maximum difference is about 0.2 Å. On the contrary, the difference of the corresponding values in these solvents and in pyridine is approximately 1.5 Å. Therefore, even though the parameter a(Å) is said to be practically constant in binary mixtures of solvents with significantly different dielectric permeabilities [34] and what is more in different solvents [20], to our mind, the reliability of the predicted ion association constants directly depends on similarity of the solvation properties of the solvent for which the values of a(Å) have been calculated and the solvent for which the k_{ass} values are to be predicted. Binary mixtures of toluene and nitrobenzene with as high toluene content as possible for wich reliable k_{ass} values still may be experimentally determined seem to be most suitable for predictions of k_{ass} values in toluene.

Table 4

The logarithmic values of the ion association constants for tetraethylammonium salts in acetone, methyl ethyl ketone and pyridine (data taken from [23]) and the values of the closest approach parameter calculated from equation (11) at T=298 K.

Anion	Acetone (D=19,1)		Methyl ethyl ketone (D=17,8)		Pyridine (D=12,3)	
	$\log k_{ass}$	a(Å)	$\log k_{ass}$	a(Å)	$\log k_{ass}$	a(Å)
Cl^-	2.59	3.62	3.02	3.39	3.51	4.88
Br^-	–	–	2.90	3.55	3.41	5.07
J^-	2.44	3.89	2.63	3.98	3.24	5.44
Pic^-	2.1	4.78	2.36	4.59	2.9	6.42

Table 5

The logarithmic values of the ion association constants for TNODA salts with different anions in binary mixtures of toluene – nitrobenzene (data taken from [36]), the values of the closest approach parameters calculated from equation (11) and the values of radii for the corresponding anions (data taken from [46])

Anion	20 vol.% of nitrobenzene (D=7.1)		10 vol.% of nitrobenzene (D=4.7)		$\overline{a(Å)}$	r_A(Å)
	$\log k_{ass}$	a(Å)	$\log k_{ass}$	a(Å)		
Cl^-	6.95	4.60	11.0	4.52	4.56	1.81
Br^-	6.62	4.86	10.5	4.75	4.80	1.96
J^-	6.48	4.98	9.7	5.17	5.08	2.20
SCN^-	6.6	4.87	9.65	5.20	5.03	2.13
$C_8H_{17}OSO_3$	6.7	4.79	9.8	5.11	4.95	–
Pic^-	5.94	5.51	9.05	5.58	5.55	–
$ТФБ^-$	4.9	7.01	7.5	6.94	6.98	4.21

Table 5 presents the values of ion association constants for TNODA salts with different anions in binary toluene–nitrobenzene mixtures containing from 80 to 90 vol.% of toluene. As is seen, for both compositions of the binary mixture, in wich the values of k_{ass} differ by 3–4 order of magnitude, the calculated values of a(Å) correlate well with each other.

The obtained values of a(Å) enable one to estimate the k_{ass} values in toluene. Based on equation (11), the values of $\log k_{ass}$ calculated for ion associates of $TNODA^+...Cl^-$ and $TNODA^+...TPhB^-$ equal to 22.1 and 14.8 respectively, i.e. they differ by 7.3 orders of magnitude. Compare, in binary toluene – nitrobenzene mixtures containing 50, 20 and 10 % of nitrobenzene this difference amounts to 0.7, 3.0 and 4.5 orders of magnitude [36], whereas in n-decane – to 8.9 orders of magnitude. Thus, even in the case of lipophilic quaternary ammonium salts the factor of ion association may have a profound leveling effect on the values of exchange constants, especially in media with low dielectric permeability.

1.2.2.1. The relationship between the closest approach parameter and the size of associating ions

Proceeding from pure mechanistic ideas about the closest approach parameter as a center-to-center distance between anion and cation, the presence of such a relationship for contact ion pairs is absolutely obvious. However, it should be noted that for QAS the parameter a(Å) is not a sum of the radii of cation and anion since anions penetrate deeply between the hydrocarbon chains of QAC. Besides, the closest approach parameter a(Å) derived from k_{ass} values should not be identified with a distance between the geometrical centers of cation and anion too. This is stipulated by the fact that complex polyatomic ions may be aligned relative each other in such a way that the total efficiency of the interaction of electrostatic charges distributed in individual atoms be a maximum.Quantum-chemical calculations have demonstrated that a positive charge of QAC is predominantly centered at four $-CH_2-$ groups nearest to the nitrogen atom [48]. For example, when QAC interacts with nitrate ion, the resultant mutual orientation may be so that three oxygen atoms of nitrate will be simultaneously interacting with three $-CH_2-$ groups of QAC. Naturally, such an interaction is much more efficient than that of two spherical ions of the same size as above, the charges of which are uniformly distributed over the whole surface of ions. Moreover, mutual polarization of the ions also contributes the interaction efficiency. As a result, in some cases the parameter a(Å) may assume the values below a possible minimum of the distance between the geometrical centers of associating ions that is calculated from the atomic sizes, bond lengths and angles (e.g. the values in Table 4). The parameter a(Å) calculated from the values of k_{ass} could not be also determined as a center-to-center distance between the charges of polarized ions. We are of the opinion that a(Å) is a certain theoretical variable characterizing the integral interaction efficiency of cation and anion, including a change in solvation interaction with a solvent (suggested by the differences in a(Å) values calculated for contact ion pairs in different solvents), and also the effect of entropy due to reduced number of QAC conformations caused by penetration of anion between the alkyl chains, reflected as an increase in a(Å) values with growing length of hydrocarbon chains in QAC (see Table 6).

Table 6

The values of the closest approach parameters for contact ion pairs R_4N^+...Pic^- in 1,2-dichloroethane. Data taken from [12]

QAC	$(CH_3)_4N^+$	$(C_2H_5)_4N^+$	$(C_3H_7)_4N^+$	$(C_4H_9)_4N^+$	$(C_5H_{11})_4N^+$
a(Å)	4.65	5.80	6.00	6.16	6.25

Nevertheless, as seen from Table 5, the values of a(Å) calculated on the basis of the ion association constants correlate well with the radii of the associated anions. A a_{RA}(Å) a_{RCl}(Å) r_A(Å) r_{Cl}(Å) plot yields a straight line for this correlation function starting from the origin and with a slope close to unity (Fig. 3).

Consequently, the values of the closest approach parameters for ion pairs formed by TNODA cations with anions differing in nature may be estimated in the very first approximation by the following equation:

$$a_{RA}(Å) = a_{RCl}(Å) + r_A(Å) - r_{Cl}(Å) \quad (13)$$

The obtained values of a_{RA}(Å) enable one to estimate reliably the ion association constants.

1.2.2.2. Estimations of the limiting values of the exchange constants

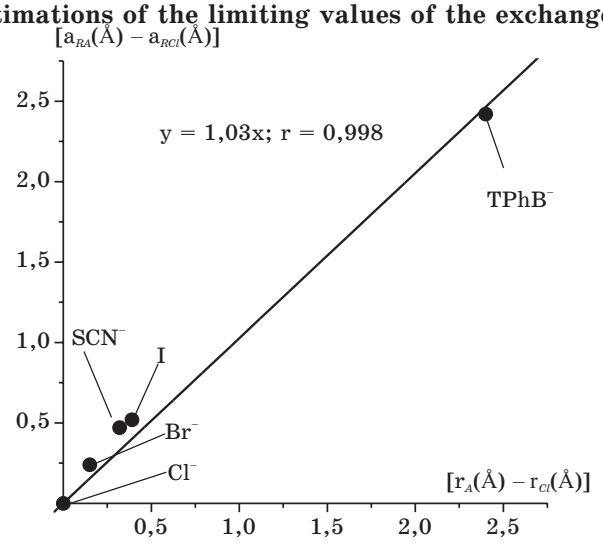

Fig. 3. The differences in the closest approach parameters for various anions and chloride ion in their ion associates with TNODA, calculated from experimental values of the association constants (taken from [36]) as a function of the difference between radii of the corresponding anions and chloride ion (taken from [46])

The experimental values of ion-exchange constants and radii for all anions simultaneously available from the Refs. [6], [46], which to the best of our knowledge are currently most adequately reflecting the actual situation, are listed in Table 7. With the use of equation (13) and the literature data for r_A(Å), the values of a(Å) have been calculated for the corresponding ion associates, and the values of logk_{ass} in toluene have been calculated from equation (11).

Table 7

The logarithmic values of the experimental anion exchange constants in water–toluene system log$(K^A_{Cl})_{exp}$ (standard ion – Cl^-), ion radii r_A (Å), closest approach parameters a(Å), ion association constants in toluene log k_{ass} and limiting exchange constants log$(K^A_{Cl})_{lim}$. Data are taken from the following sources: a – [6], b – [46]; c, d, e – calculated from equations (13), (11) and (14) respectively.

Anion	log $K^A_{Cl\ exp}$	r_A(Å)	a(Å)	log k_{ass}	log $K^A_{Cl\ lim}$
	a	b	c	d	e
F^-	–3.25	1.33	4.08	24.6	-5.75
OH^-	–2.8	1.33	4.08	24.6	-5.3
H_2PO_4	–2.45	2.00	4.75	21.2	-1.55
HCO_3	–2.0	1.69	4.44	22.7	-2.6
CH_3COO^-	–1.6	1.62	4.37	23.0	2.5
Cl^-	0	1.81	4.56	22.1	0
CN^-	0.2	1.91	4.66	21.6	0.7
JO_3	0.3	1.81	4.56	22.1	0.3
NO_2	0.55	1.92	4.67	21.6	1.05
BrO_3	1.0	1.91	4.66	21.6	1.5
Br–	1.4	1.96	4.71	21.4	2.1
NO3–	2.25	1.79	4.54	22.2	2.15
ClO3–	2.7	2.00	4.75	21.2	3.6
J–	3.5	2.20	4.95	20.4	5.2
SCN–	4.15	2.13	4.88	20.7	5.55
BF_4	4.35	2.32	5.07	19.9	6.55
ClO_4	5.3	2.50	5.25	19.3	8.1
Pic^-	8.15	–	5.55*	18.3	11.95
$TPhB^-$	12.8	4.21	6.96	14.8	20.1

* The a(Å) values for Cl^- and Pic^- ion associates with TNODA were taken from table 5.

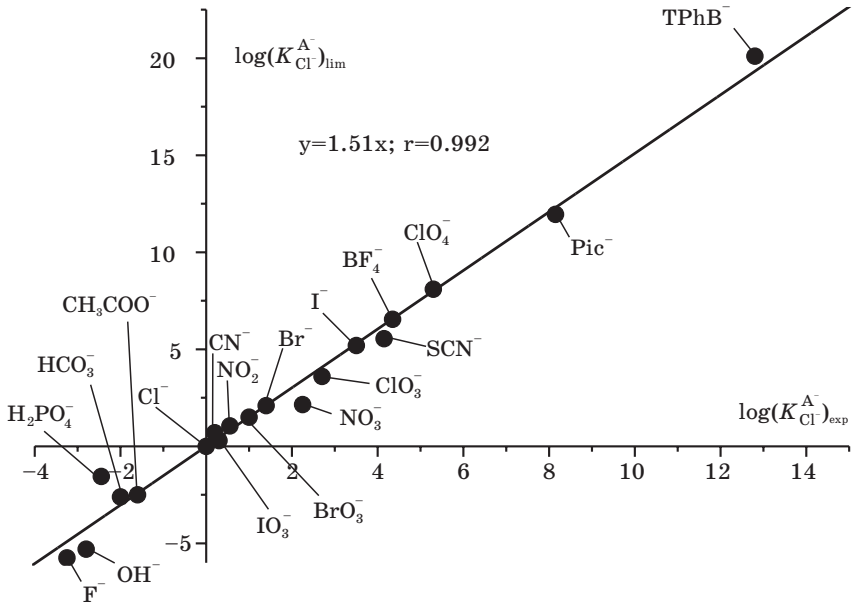

Fig. 4. The logarithms of the limiting values of anion exchange constants calculated from equation (14) in water – toluene system as a function of the logarithms of the experimental exchange constants (taken from [6]). Ion exchanger is TNODA

We have introduced the notion of a «limiting value» for the ion exchange constant $K_i^j{}_{\text{lim}}$ to characterize the net hydration and solvation effects, excluding the effects of ion association, as follows:

$$\log K_i^j{}_{\text{lim}} \equiv \log K_i^j{}_{\text{exp}} \quad \log \frac{(k_{ass})_{jR}}{(k_{ass})_{iR}}. \qquad (14)$$

The values of $K_i^j{}_{\text{lim}}$ obtained in this way represent nothing but the ratio of so-called «individual distribution coefficients» of ions by Eisenman, k_j / k_i [49]. The calculated values of $K_i^j{}_{\text{lim}}$ are present in Table 7.

As seen from Fig. 4, logarithms of the limiting values of exchange constants calculated using equation (14) correlate well with the experimental values.

The observed correlation may be described as follows:

$$\log K_i^j{}_{\text{lim}} \quad 1.51 \quad \log K_i^j{}_{\text{exp}}. \qquad (15)$$

Despite of the fact that the principal contribution into this correlation is made only by two ions (tetraphenylborate and picrate), their exclusion has practically no effect on the form of the correlation function, and the proportionality factor in equation (15) is varying from 1.51 to 1.45. In this case the correlation coefficient remains rather large (r = 0.992 for the whole set of ions and with the exception of picrate and tetraphenylborate r = 0.982). This is a circumstantial confirmation of the proposed approach and realistic character of $K_i^j{}_{\text{lim}}$ values.

As seen, the differences in log $K_{i\ \lim}^{j}$ values are much larger than those for log $K_{i\ \exp}^{j}$. For example, log $K_{Cl\ \lim}^{A}$ and log $K_{Cl\ \exp}^{A}$ values for the most hydrophilic F^- and the most lipophilic $TPhB^-$ ions amount to 26.85 and 16.05 respectively. This suggests that the selectivity of ion exchange may be improved by many orders provided the factor of ion association is excluded or at least reduced.

This may be realized by two ways: (1) using of a solvent with rather high dielectric permeability and as low solvation ability to anions as possible and (2) increasing of the closest approach parameter through the use of anion exchangers with enhanced steric hindrance of the exchange center (e.g. owing to branching hydrocarbon substituents). Unfortunately, these approaches are hardly realizable in practice. As for the solvents with high dielectric permeability, the data on anion exchange in a system water – toluene–nitrobenzene mixture [6] reveal a somewhat better exchange selectivity than in a system water – toluene. At the same time, this improvement is not so great as might be expected reasoning from the values of log k_{ass} given in Table 7. To illustrate, with the use of TNODA solutions in toluene and binary mixture toluene – nitrobenzene (1:9) as ion exchanges the values of log $K_{Cl}^{ClO_4}$ were respectively 5.3 and 6.2 [6],differing by 0,9 of the order of magnitude, whereas the values of k_{ass} were differing by 2.8 orders (see Table 7). This may be explained by a somewhat better solvation ability of nitrobenzene as compared to toluene. As a consequence, the compensation effect due to ion solvation by the solvent increases, leading to a decrease in selectivity. As regards the use of steric hindered anion exchangers, all attempts of the authors aimed at synthesis of such QAS have failed all together: QAS refused to form or were thermodynamically instable decaying in storage.

1.2.2.3. The solvation effect on the ion-exchange selectivity. The refined estimations

From equations (7), (10), (14) it follows that

$$K^{**} \quad K^{*} \ \frac{\log K_{i\ \lim}^{j}}{\log K_{i\ \exp}^{j}}. \qquad (16)$$

Assuming for toluene that log $K_{i\ \lim}^{j}$ amounts to 1.5 log $K_{i\ \exp}^{j}$ (see equation (15)) and $K^{*}=4.0 \cdot 10^{-5}$ (Table 3), we obtain $K^{**}= 6.0 \cdot 10^{-5}$. And assuming identical values of the parameter a(Å) in n-decane and toluene, with proper calculations for n-decane one obtains $K^{**}=1.65$, $K^{*}=6.4 \cdot 10^{-5}$. Such an estimation for chloroform and n-decanol seems fairly risky, since in these solvents effectively solvating anions the values of a(Å) may vary considerably. Besides, in the case of n-decanol it is likely that the formed ion pairs will be separated by the solvent and owing to better solvation ability for small ions the above relationship between a(Å) and r_A(Å) may be changed by the reverse one [18, 21]. Because of this, the consideration is limited to toluene, n-decane and toluene–nitrobenzene mixture. With due regard for the ion association factor the parameters characterizing the efficiency of solvation interaction in these solvents assume the values given in Table 8.

Table 8

K^{**}, K and α values characterizing the solvation properties of solvents relative to anions and calculated for toluene, n-decane and toluene – nitrobenzene (1:9) mixture with due regard for ion association*

Solvent	$K^{**} \cdot 10^{-5}$	K G_s^0 / G_h^0	α 1 K
n-decane	6.4	0.64	0.36
toluene	6.0	0.66	0.34
toluene + nitrobenzene (1:9))	4.4	0.75	0.25

* The value of K was calculated by the equation : K'=1-2.303$RT \cdot K^{**}$.

As seen from the Table 8, after inclusion of the ion association factor everything «goes into place», and the proportionality factor between the standard free energies of hydration and solvation (K) is changing in accordance with varying solvation properties of the solvents to increase in the following sequence: n-decane < toluene < toluene – nitrobenzene mixture.

It is interesting that calculation of the exchange constant for chloride exchanged by sulphate from equation (12) with $K^{**} = 6.0 \cdot 10^{-5}$ and of the ion association constants $\log(k_{ass})_{SO_4R}$=41.3; $\log(k_{ass})_{SO_4RR}$ = 20.4; $\log(k_{ass})_{CIR}$ = 22.1 from equation (11) using a(Å) values of 4.95 and 4.56 derived from the ion-association constants for TNODA with octyl sulphate and chloride ions (Table 5), results in $\log K_{2Cl}^{SO_4^2}$ = –5.4. This value is much closer to the experimental value of –2.8 than that obtained from equation (9) disregarding the factor of ion association (see Section 1.1). Considering that the final result $\log K_{2Cl}^{SO_4^2}{}_{calc}$ is an algebraic sum of two very large values (see equation (12)), it should be accepted as wholly satisfactory.

Thus, the obtained data suggest that the proposed approach on the basis of linear Gibbs energy relations, including the effect of ion association, makes it possible to perform a more adequate estimation of a relative solvation ability of the solvents based on the results for exchange of single-charged ions by single-charged ions and provides a means for better insight into the factors causing extractability of double-charged ions.

1.2.2.4. The steric accessibility effect of QAC exchange center on the ion-exchange selectivity

The presence of such effect follows from the relationship between the closest approach parameter a(Å) and the length of hydrocarbon chains of QAC (see Table 6). In an effort to test the existence at this effect experimentally, we especially have synthesized QAS with different numbers of methyl substituents at the nitrogen atom $(C_{12}H_{25}O)_3C_6H_2CH_2N^+(CH_3)_n(C_8H_{17})_{3-n}$, where n is varying from 1 to 3, and determined the exchange constants between chloride ion and single- or double-charged ions in toluene. Table 9 gives the logarithmic values of the exchange constants for QAS containing three methyl substituents at the nitrogen atom (TMA) and those for TNODA.

Table 9

The logarithmic values of the exchange constants for the case when chloride ions are exchanged by single-charged anions and sulphate ion in a system water – toluene. Ion exchangers – TNODA and TMA: a – experimental values, b –calculated values.

Anion	$\log K_{Cl}^{A}$, $\log K_{2Cl}^{SO_4^2}$		
	TNODA	TMA	
		a	b
SO_4^2	–2.8	0.4	0.1
F^-	–3.25	–1.8	–2.6
CH_3COO^-	–1.6	–1.1	–1.0
Br^-	1.4	0.6	1.0
NO_3	2.25	0.8	2.35
SCN^-	4.15	2.6	3.3
J^-	3.5	2.2	2.6
ClO_4	5.3	3.2	3.8
Pic^-	8.15	6.1	6.25

The comparison of the exchange constants for the appropriate anions obtained using TNODA and TMA as ion exchangers has revealed that the presence of three methyl radicals in QAC is leading to a significant leveling of the exchange constants for single-charged anions. To illustrate, for TNODA the exchange constants K_{Cl}^{F} and K_{Cl}^{Pic} differ by 11.4 orders of magnitude and in case of TMA – by 7.9 orders only. The effect is very strong on exchange of chloride by double-charged sulphate ion when $K_{2Cl}^{SO_4^2}$ increases by a factor of 1600. In general, the observed effects are not unexpected following directly from analysis of equation (11). In media with low dielectric permeability the major contribution to the value of $\log k_{ass}$ is made by the last term in this equation. Because of this, a decrease in the closest approach parameter a(Å) due to better steric accessibility of the exchange center in QAC should result in sharply growing ion-association constants of QAC with small anions. The most profound effect should be exerted by a decreasing a(Å) on the value of the first association constant of double-charged anions with QAC. In an effort of numerical simulation for the effect on the exchange constant value, the following assumptions have been made:

1) a(Å) parameter for the ion pair of a picrate ion with TMA equals 4.65 (the value of a(Å) for tetramethylammonium picrate in dichloroethane, see Table 6);

2) decrease of a(Å) in case of TMA cation substitution for TNODA cation is independent of the anion nature and amounts to 0.9 Å corresponding to a decrease of a(Å) for picrate ion (5.55 – 4.65 = 0.90).

3) the value of a(Å) for ion associates formed by a sulphate ion with TNODA is accepted as 4,95 obtained for the ion pair of TNODA with octyl sulphate (Table 5).

The values of a(Å) parameter for the ion pairs formed by single-charged ions with TNODA are taken from Table 7. In accordance with item 2, the values of a(Å) have been calculated with TMA as ion exchanger, and the values of $\log k_{ass}$ were

calculated from equation (11). The calculated values of exchange constants with TMA as ion exchanger have been obtained from equation (17) as follows:

$$\log K^{A}_{Cl\ \text{ТМА}} \quad \log K^{A}_{Cl\ \text{ТНОДА}} \quad \log \frac{(k_{ass})_{AR}}{(k_{ass})_{CIR}}_{\text{ТМА}} \quad \log \frac{(k_{ass})_{AR}}{(k_{ass})_{CIR}}_{\text{ТНОДА}} . \qquad (17)$$

Changes of the contribution made by ion association into $\log K^{SO_4^{2-}}_{2Cl}$ have been taken into consideration according to equation (12). The calculated values for the logarithms of exchange constants are summarized in Table 9.

The comparison between the calculated and experimental values of the logarithms of exchange constants shows that in the majority of cases the proposed calculation procedure describes adequately a real situation.

However, the exchange constant for nitrate ion falls out of the general pattern: experimental $\log K^{NO_3^-}_{Cl}$ decreases when TMA replaces TNODA as ion exchanger, whereas the calculated value is increased by 0.1. This discrepancy is probably explained by the fact that a compact nitrate ion (r = 1.79 Å), penetrating between alkyl chains of TNODA, is capable to interact simultaneously with hydrogen atoms of three –CH_2– groups, nearest to the nitrogen atom, having an excessive positive charge. In the case of TMA the interaction involves the hydrogen atoms of CH_3–groups, being less efficient due to dispersion of a positive charge over a larger number of hydrogen atoms.

Fig. 5 presents the steric accessibility effect of the QAC exchange center on the value of exchange constant when sulphate is exchanged for single-charged ions.

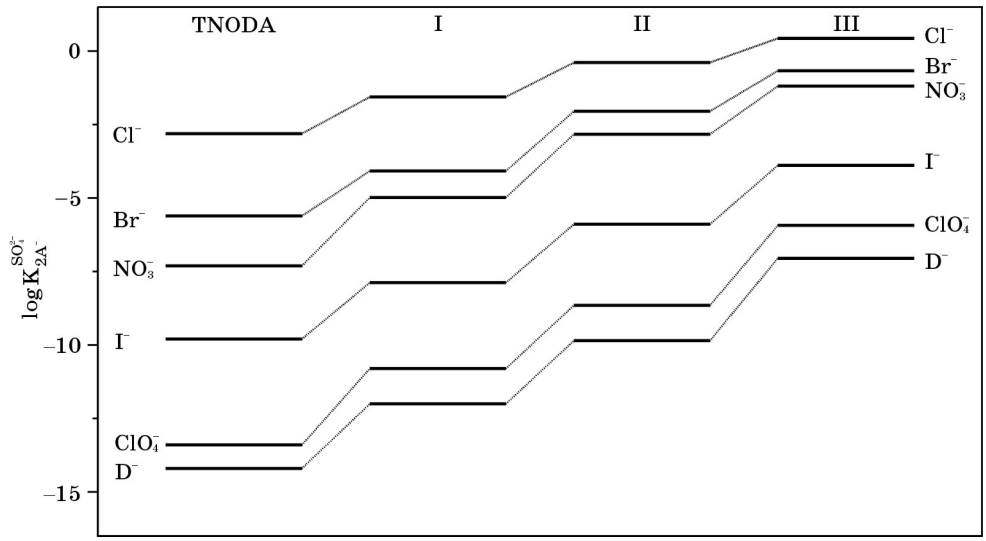

Fig. 5. The logarithms of exchange constants for the case when single-charged anions are exchanged by sulphate in a system water – toluene as a function of the exchange center steric accessibility of anion exchanger: $[(C_{12}H_{25}O)_3C_6H_2CH_2N(CH_3)_n(C_8H_{17})_{3-n}]^+A^-$. Roman numerals in the diagram denote the number of methyl groups in QAC

As seen, affinity of ion exchangers to the sulphate ion regularly grows with increasing of a number of methyl groups at the nitrogen atom. A maximum effect is observed for large ions, namely, perchlorate and 2,4-dinitrophenolate. In the case of chloride exchanged by sulphate the exchange constant increases by 3.2 orders of magnitude, whereas in the case of sulphate exchanged for perchlorate it increases by more than 7 orders. This derives from the fact that the ion association constants of QAC with large-size anions are less dependent on the steric accessibility of QAC exchange center. It should be noted that the observed increase in $\log K^{SO_4^{2-}}_{2ClO_4}$ is in a good agreement with the results of calculations performed in accordance with the above assumptions. The calculations suggest that with TMA used as an ion exchanger the value of $K^{SO_4^{2-}}_{2ClO_4}$ should have an increase by about 6 orders of magnitude.

It has been found that similar behavior is observed for other small-size double-charge anions, for example, tartrate, oxalate too, see Fig. 6.

Thus, the use of QAC with three methyl radicals results in dramatic (by 10^3 –10^7 times) growth of the exchange constants when double-charged anions are exchanged for the single-charged ones. It should be emphasized that all the foregoing is valid only for double-charged anions of small size. This follows directly from equation (11). Since the first term of the equation is a constant and the second (logarithmic term) is little dependent on a(Å), the influence of a(Å) on the value of $\log k_{ass}$ in media with low dielectric permeability is determined mainly by a change in the third term. Disregarding the second term changes, it is easy to show that improvement of the steric accessibility of the exchange center, leading

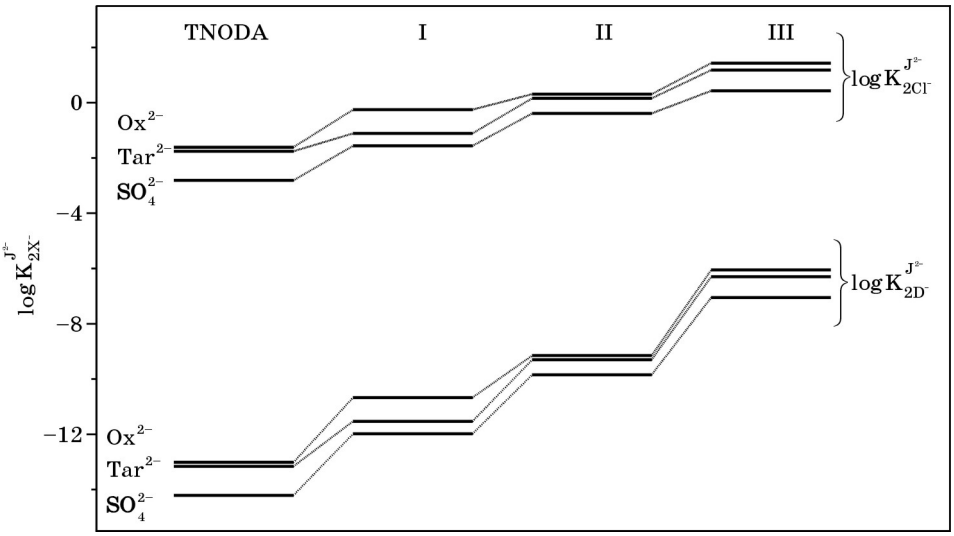

Fig. 6. The logarithms of exchange constants for the case when double-charged anions are exchanged for the single-charged ones in a system water–toluene as a function of the exchange center steric accessibility. Tar^{2-} – tartrate, Ox^{2-} – oxalate, D^- – 2,4-dinitrophenolate. Designations for anion exchangers similar to Fig. 5

to a decrease in a(Å), will be accompanied by an increase of $K_{2i}^{J^2}$ so long as the following relation is fulfilled:

$$a_{Rj}(Å) \quad \frac{3}{2} a_{Ri}(Å), \tag{18}$$

where j is a double-charged ion, i is a single-charged ion.

Otherwise, improvement of the steric accessibility of QAC exchange center should give quite the opposite result. This is confirmed by experimental data (Fig. 7).

As seen, when the largest single-charged anions (ClO_4^-, 2,4-DNF$^-$, Pic$^-$) are exchanged by a large-size double-charged ion, improvement of the steric accessibility of the ion-exchange center is accompanied by increase in the exchange constant (though not so great as in case of sulphate ion, see Fig. 5), whereas in the case of $B_{10}H_{10}^2$ exchanged for smaller single-charged ions the exchange constant passes through a maximum.

Besides, this illustrative example is also of interest since it is modeling the exchange of small-size double-charged anions for single-charged ions in the presence of neutral anion carriers used for the creation of anion-selective electrodes with nontraditional selectivity. Indeed, the picture observed when single-charged anions are exchanged by sulphate in the presence of hexyl 4-trifluoroacetyl benzoate (Fig. 8) is very similar to that observed for the exchange of $B_{10}H_{10}^2$ ion (Fig. 7).

Thus, the obtained results have demonstrated that a change in the steric accessibility of QAC exchange center may have a very strong effect on the value of the exchange constant. In the process, the charge value and sizes of exchanging anions are the key parameters.

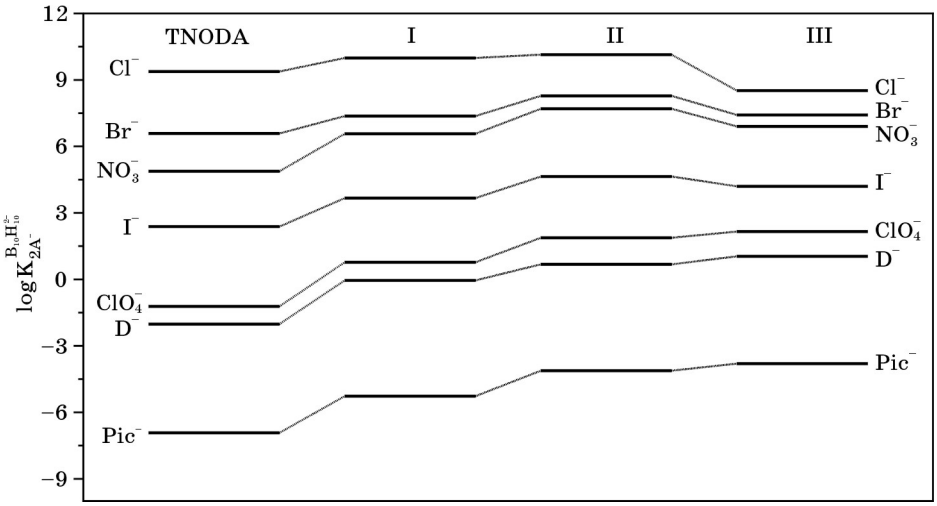

Fig. 7. The logarithms of exchange constants for the case when single-charged anions are exchanged by decaboronhydride anion in a system water – toluene as a function of the exchange center steric accessibility.
Designations for anion exchangers similar to Fig. 5

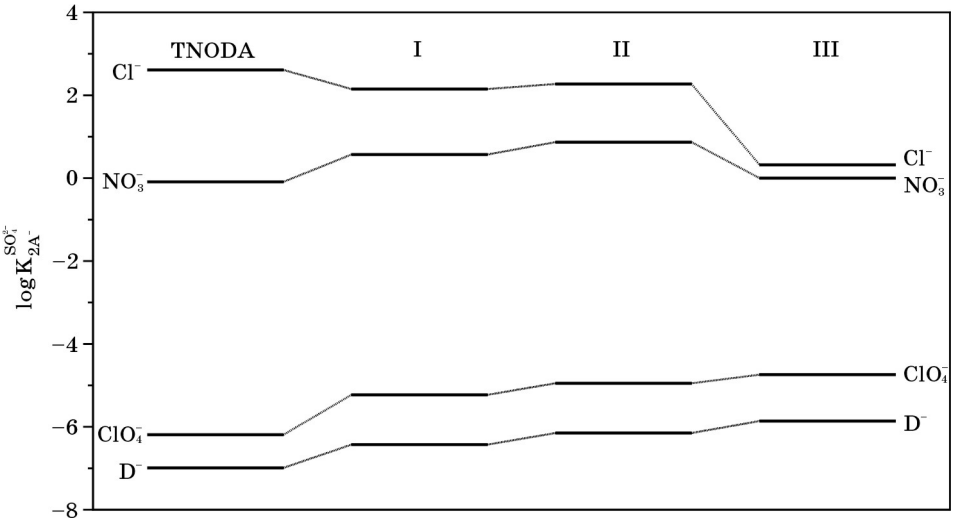

Fig. 8. The logarithms of exchange constants for the case when single-charged anions are exchanged by sulphate in a system water – toluene in the presence of hexyl 4-trifluoroacetylbenzoate (0.06 mol · l^{-1}) as a function of the exchange center steric accessibility. Designations for anion exchangers similar to Fig. 5

2. ION ASSOCIATION EFFECT ON THE POTENTIOMETRIC SELECTIVITY OF QAS-BASED ANION-EXCHANGE MEMBRANES

The data presented in Fig. 9 reveal the effect of the QAC exchange center steric accessibility on the potentiometric selectivity to sulphate ion in the presence of single-charged anions. It is seen that the interfering effect of foreign anions is lowered as the steric accessibility of QAC exchange center is improved. The best selectivity to sulphate ion is observed for the membrane containing trimethyl QAS, and the worst – for the membrane containing monomethyl QAS. The membrane containing dimethyl QAS holds an intermediate position. Data for the TNODA-based membrane are lacking in the figure, because the authors have failed to obtain the sulphate function with a slope close to Nernstian one.

It is interesting that the most significant (approximately by 5 orders of magnitude) improvement of the selectivity to sulphate is achieved in the presence of large single-charged anions (ClO_4^-, SCN^-, I^-), and the smallest improvement (about 1.5 orders of magnitude) is achieved in the presence of chloride. As a whole, the observed picture correlates well with the order of changes in the corresponding ion exchange constants (Fig. 5). Because of considerable differences in the solvation and dielectric properties of PVC membranes plasticized by o-NPOE and toluene solutions of QAS, the agreement is just qualitative.

The findings and results may be interpreted as follows. According to [50], the potentiometric selectivity coefficients determined by the separate solutions

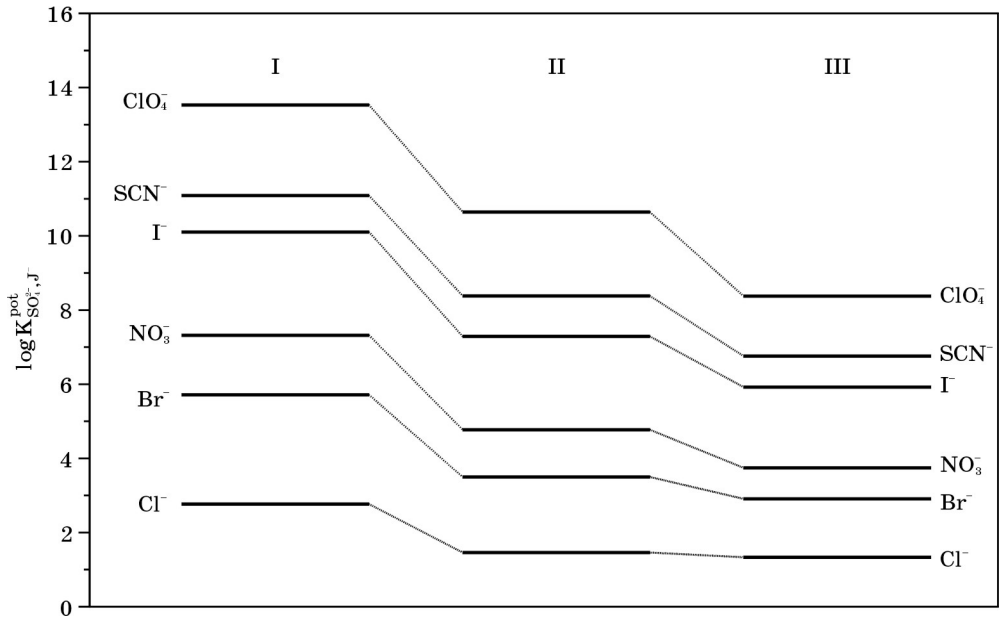

Fig. 9. The logarithms of potentiometric selectivity coefficients of QAS-based sulphate-selective electrodes as a function of the exchange center steric accessibility. Membrane composition: PVC + o-NPOE (1:2) + QAS (0,03 mol · l^{-1}). Designations for anion exchangers similar to Fig. 5.

method for the ions differ in a charge value, are described by the following equation:

$$K_{ij}^{Pot} \quad \frac{\overline{C}_i}{k_i} \quad \frac{k_j}{\overline{C}_j}^{z_i/z_j}, \tag{19}$$

where k_i and k_j are hypothetical individual distribution coefficients of the principal and interfering ions; $\overline{C}_i$ and $\overline{C}_j$ are the concentrations of «free» (forming no ion associates) ions in the membrane phase, provided all the sites in the membrane are occupied only by ions of the same type: respectively *i* or *j*. In the assumption of a perfectly associated solution, when cations and anions occurring in the membrane are predominantly in the form of ion associates and a portion of free ions is relatively small, the concentrations of free ions in the membrane may be easily obtained from analysis of the corresponding equilibria.

For single-charged (foreign) anions we have

$$\overline{C}_j \quad \overline{C}_R \quad \frac{\overline{C}_R^{tot}}{(k_{ass})_{jR}}^{\frac{1}{2}}, \tag{20}$$

where $\overline{C}_R$ is the concentration of free QAC, $\overline{C}_R^{tot}$ is the total concentration of QAS in the membrane.

For double-charged (basic) anions we have

$$\overline{C}_i \quad \frac{\overline{C}_{iR}}{\overline{C}_R \ (k_{ass})_{iR}}, \tag{21}$$

where $\overline{C}_i$ is the concentration of a negatively charged ion associate containing a double-charged anion i and one cation R.

In accordance with electroneutrality condition, the following equation is valid:

$$2\overline{C}_i \quad \overline{C}_{iR} \quad \overline{C}_R. \tag{22}$$

Considering that

$$(k_{ass})_{iR} >> (k_{ass})_{iRR}\ , \tag{23}$$

we have

$$\overline{C}_i << \overline{C}_{iR} \approx \overline{C}_R, \tag{24}$$

from equations (21), (23) we obtain

$$\overline{C}_i \approx \frac{1}{(k_{ass})_{iR}}. \tag{25}$$

Then equation (19) may be written as follows:

$$K_{ij}^{Pot} \quad \frac{k_j^2}{k_i} \frac{(k_{ass})_{jR}}{(k_{ass})_{iR} \ \overline{C}_R^{tot}}. \tag{26}$$

Since individual distribution coefficients for ions i and j are independent of QAC nature and according to equation (11) the first association constant for a double-charged anion i with QAC has stronger dependence on the parameter a(Å) than the association constant of a single-charged anion with the same QAC, it is obvious that improved steric accessibility of the exchange center should result in reduced interference of foreign single-charged anions. Apparently, the greatest improvement of the selectivity to double-charged anions should be observed in the presence of large single-charged anions, the ion association constants of which are less dependent on the steric accessibility of QAC exchange center. A theoretical model under consideration is in a good agreement with the experimental data (Fig. 9).

It should be noted that, similar to the ion-exchange constants for ion associates formed by QAC with single-charged and double-charged anions, there is a critical relationship of the parameters a(Å) when the dependence of K_{ij}^{Pot} on the steric accessibility of QAC exchange center should be changed by just the opposite

one. It should be taken into consideration that the ion association constants involved in the expression for K_{ij}^{Pot} have other relations than in the expression for an exchange constant (equations (12), (26)). Analysis of equations (11), (26) has demonstrated that in the case of membranes with rather low dielectric permeability the improvement in the steric accessibility of QAC exchange center should be accompanied by the enhanced selectivity to a double-charged anion *i* in the presence of a single-charged anion *j* until the following relation is valid:

$$a_{Ri}(\text{Å}) \quad 2a_{Rj}(\text{Å}), \tag{27}$$

Thus, the size restrictions in this case are less stringent than for ion exchange constants (equation (18)).

As seen in Fig. 10, the tendency for improvement of the potentiometric selectivity to sulphate anion in the presence of single-charged anions with improving steric accessibility of QAC exchange center is retained to some extent for the membranes containing a neutral anion carrier, hexyl 4-trifluoroacetylbenzoate. A considerable enhancement of the selectivity to sulphate with increasing number of methyl groups in QAC is observed in the presence of ClO_4, SCN^-, NO_3 ions. Similar selectivity improvement has been revealed by the authors for other double-charged anions (hydrophosphate, tartrate, oxalate) as well.

It is of interest that using of the secondary amine salt $(C_{12}H_{25}O)_3C_6H_2CH_2NH(CH_3)\cdot HCl$ as anion exchanger (membrane IV) results in further significant (about an order) enhancement of the selectivity to sulphate an-

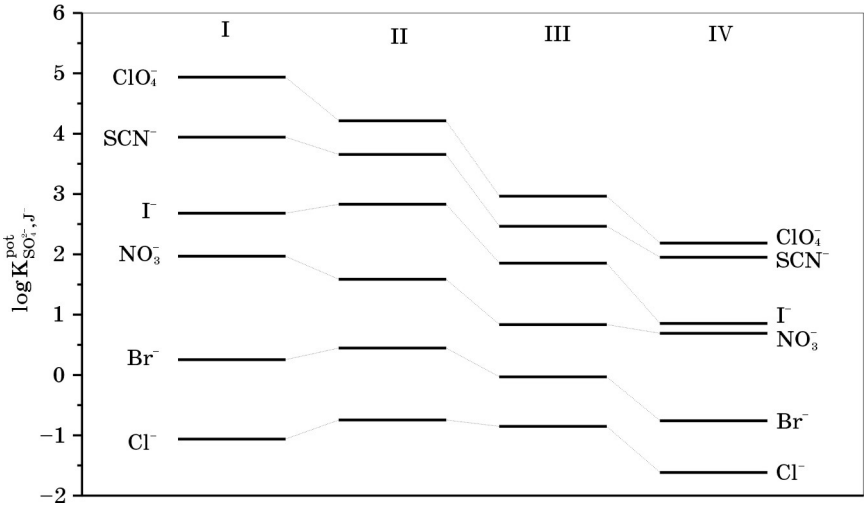

Fig. 10. The logarithms of potentiometric selectivity coefficients of neutral carrier-based sulphate-selective electrodes as a function of the nature of liquid anion exchanger. Membrane composition: PVC + 1-chloronaphtalene (1:2) + hexyl 4-trifluoroacetylbenzoate (8 % of the weigh of other membrane components) + anion exchanger (0.03 mol · l^{-1}). Designations I, II, III in the diagram are similar to Fig. 5, and IV denotes hydrochloride of the secondary amine $(C_{12}H_{25}O)_3C_6H_2CH_2NH(CH_3)\cdot HCl$

ion in the presence of single-charged anions. It is likely that along with enhanced steric accessibility of the exchange center this is due to hydrogen bonding between hydrogen atoms of the secondary ammonium cation and sulphate ion. Specifically, the complex of the following structure may be formed:

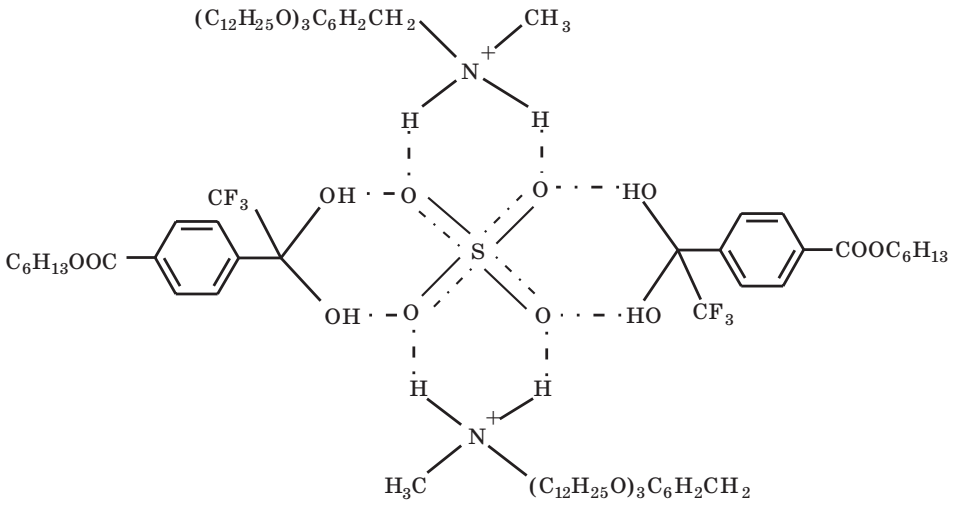

The obtained results bear witness to the fact that the selectivity of the neutral carriers-based membranes to double-charged anions is not indifferent to the structure of liquid ion exchanger, in particular to the steric accessibility of its exchange center. This is of great importance in practice, since major progress that has been made recently in the development of anion-selective electrodes with non-traditional selectivity is due primarily to synthesis of neutral anion carriers [51–55]. A critical requirement for normal functioning of such electrodes is the presence of a liquid anion exchanger in the membrane [50]. Until the present time, the selectivity of these ISE has been attributed solely to a neutral carrier, whereas the role of a liquid ion exchanger has been reduced to the provision of anion permselectivity of the membranes and, hence, the Nernstian slope of the electrode function. Based on the results of the present study, it might be expected that proper selection of anion exchanger may be an additional means of controlling the selectivity of this type electrodes reversible to double-charged anions.

3. CONCLUSION

This paper is actually the first attempt at individual estimation of the contributions made by solvation and ion association effects to the exchange and potentiometric selectivity for the systems based on lipophilic QAS. The authors perceive clearly that the approaches used here are far from being perfect and necessitate further refinement. Specifically, valuable information may be acquired by a direct experimental study of the effect exerted by the steric accessibility of QAC exchange center on the ion association constants with different anions, as

well as quantum-chemical calculations of the closest approach parameters including complete structural and energy optimization for the ionic associates formed.

The most important outcome of this paper is substantiation of the effect of ion association factor on the ion exchange selectivity in QAS-based systems, the contribution of which to the ion exchange constant in solvents with low dielectric permeability may come to 10 orders and more, being comparable to the contribution of solvation interactions. A better understanding has been gained of the possibility to control the anion-exchange selectivity in such systems both by leveling and differentiation of the association constants. The revealed strong steric-accessibility effect of the exchange center of QAS (previously considered as «non-selective» anion exchangers) on the anion-exchange selectivity is of particular interest, especially when double-charged anions are exchanged for the single-charged ones producing a huge (up to 10^7-fold) increase in the selectivity. This makes it possible to consider QAS with enhanced steric accessibility of the exchange center as anion exchangers selective to double-charged anions.

Among the findings of the authors, the fact that the effect of a sharp increase in the anion-exchange selectivity to double-charged anions, attained when using QAS with enhanced steric accessibility of the exchange center is of great practical significance, as this effect has been also revealed in the potentiometric selectivity of the QAS-based anion-exchange membranes and more important in the selectivity of the neutral-carriers-based membranes doped with QAS to provide the anion permselectivity.

This looks promising for a considerable improvement of ISE selectivity to SO_4^{2}, HPO_4^{2}, $C_2O_4^{2}$ and some other double-charged anions, and achievement of the selectivity characteristics enabling wide use of these ISE in analytical practice.

4. ACKNOWLEDGEMENT

The authors would like to thank Dr. Sc. A.L. Gulevich for experimental data on ion association of TNODA salts in toluene – nitrobenzene mixtures. Special thanks are due to Dr. Ph. E.B. Okaev who has synthesized the samples of QAS with different steric accessibilities of the exchange center, to the post-graduates and students of the Analytical Chemistry Department E. V. Pomelenok, E. I. Yankowski, V. A. Nazarov, V. V. Sviridov. The authors would like to acknowledge the many contributions by Dr.Ph. A. A. Rat'ko and E. L. Rogach to this paper.

The present work has been performed with the support of the Belarus Republican Foundation for Fundamental Research (Grant №X02P-018).

REFERENCES

1. *Ivanov M. I., Gindin L. M., Mironova L. Ya., Nalkina Z. A.* // Izv. SO AN SSSR. Ser. Khim. 1966. Is.3, №11. P. 34–39.
2. *Ivanov M. I., Gindin L. M., Chichagova G. N.* // Izv. SO AN SSSR. Ser. Khim. 1967. Is. 3, № 7. P. 100–104.
3. *Wegmann D., Weiss H., Ammann D., Morf W. E., Pretsch E., Sugahara K., Simon W.* // Microchim. Acta. 1984. Vol. 3, №1. P. 1–16.

4. *Rakhman'ko E. M., Starobinets G. L., Egorov V. V., Gulevich A. L., Lestchev S. M., Borovski E. S., Tsyganov A. R.* //Fresenius Z. Anal. Chem. 1989. Vol. 335, № 1. P. 104–110.
5. *Pretsch E., Buhlmann P., Bakker E.* // Trends in Anal. Chem. 2002. Vol. 21, № 12. P. 16–18
6. *Rakhman'ko E. M.* Physico-Chemical bases on the application of extraction by quaternary ammonium salts in analysis: Dr. Sc. Theses. Minsk, 1994. 141 p.
7. *Rakhman'ko E. M., Sloboda N. A.* // Zh. Neorgan. Khim. 1993. Vol. 37, № 8. P. 1254–1256.
8. *Smirnova A. L., Tarasevich V. N. Rakhman'ko E. M.,// Sens. and Actuators. B.* 1994. Vol. 18–19. P. 392–395.
9. *Egorov V. V., Borisenko N. D., Rakhman'ko E. M.* // Zh. Anal. Khim. 1997. Vol. 52, № 11. P. 1192–1198.
10. *Egorov V. V., Borisenko N. D., Rakhman'ko E. M., Lushchik Ya. F., Kacharsky S. S.* // Talanta. 1997. Vol. 44, № 11. P. 1735–1747.
11. *Gleysten L. F., Kraus C. A.* // J. Amer. Chem. Soc. 1947. Vol. 69, № 2. P. 451–454.
12. *Tucker L. M., Kraus C. A.* // J. Amer. Chem. Soc. 1947. Vol. 69, № 2. P. 454–456.
13. *Witschonke C. R., Kraus C. A.* // J. Amer. Chem. Soc. 1947. Vol. 69, № 10. P. 2472–2481.
14. *Luder W. F., Kraus C. A.* // J. Amer. Chem. Soc. 1947. Vol. 69, № 10. P. 2481–2483.
15. *Abraham M.* // J. Chem. Soc. Perkin Trans. Part II. 1972. Vol. 10. P. 1343–1350.
16. Kraus C. A. // J. Phys. Chem. 1956. Vol.60, № 2. P. 129–141.
17. Fuoss R. M., Kraus C. A. // J. Amer. Chem. Soc. 1957. Vol. 79, № 13. P. 3304–3310.
18. Kay R. L. // J. Amer. Chem. Soc. 1960. Vol. 82, № 9. P. 2099–2105.
19. Berns R. S., Fuoss R. M. // J. Amer. Chem. Soc. 1960. Vol. 82, № 21. P.5585–5588.
20. Bodenseh H. K., Ramsey J. B. // J. Phys. Chem. 1965. Vol. 69, № 2. P. 543–546.
21. *Evans D. F., Nadas J. A.* // J. Phys. Chem. 1971. Vol. 75, № 11. P. 1708–1713.
22. *Evans D. F., Zawoyski C., Kay R. L.* // J. Phys. Chem. 1965. Vol. 69, № 11. P. 3878–3885.
23. *Izmajlov N. A.* Electrochimiya rastvorov. M.: Mir, 1986. 488 p.
24. *Robinzon R., Stokes R.* Electrolyte solutions. M.: Inostr. literatura, 1963.–646 p.
25. *Gordon J.* Organic Chemistry of Electrolytes Solutions. M.: Mir, 1979. 712 p.
26. *Fuoss R. M., Kraus C. A.* // J. Amer. Chem. Soc. 1933. Vol. 55, №20. P. 3614–3620.
27. *Swain G. G., Swain M. S., Powells A. L., Alunn S.* // J. Amer. Chem. Soc. 1983. Vol. 105, № 3. P. 502–513.
28. *Kamlet M. J., Abboud J. L. M, Taft R. W.* // Progress in Physical Organic Chemistry / Ed. R. W. Taft. N.-Y.: Wiley and Sons. 1981. Vol. 13. P.485–630.
29. *Krygowski T. M., Milczarek E., Wrona P.* // J. Chem. Soc. Perkin Trans. Part II. 1980. № 11. P. 1563–1568.
30. *Shmidt V. S.,* // Uspekhi Khimii. 1978. Vol. 47, №10. P. 1730–1755.
31. *Shmidt V. S., Rybakov K. A., Rubisov V. I.* // Zh. Neorgan. Khim. 1980. Vol. 25, № 7. P.1915–1919.
32. *Eigen M.* // J. Phys. Chem. (Frankfurt). 1954. Vol. 1, № 1. P. 176–200.
33. *Denison J. T., Ramsey J. B.* // J. Amer. Chem. Soc. 1955. Vol. 77, №9. P. 2615–2621.
34. Fuoss R. M. // J. Amer. Chem. Soc.–1958.–Vol. 80, №19. P. 5059–5061.
35. *Fuoss R. M.* // J. Amer. Chem. Soc. 1957. Vol. 79, № 13. P. 3301–3303.
36. *Gulevich A. L.* Extraction of alkylsulphates and lipophilic carbonic acids by quaternary ammonium salts and its analytical application. Ph. D. Theses. Minsk, 1982. 204 p.
37. *Rakhman'ko E. M., Kosenkova N. M., Starobinets G. L.* et. al. // Izv. vuzov SSSR. Khimiya i khimicheskaya tekhnologiya. 1985. Vol. 28, №10. P. 57–60.
38. *Rakhman'ko E. M., Starobinets G. L.* //Vestnik BGU, Ser. Khim. 1986. № 2. P. 12–16.
39. *Rakhman'ko E. M., Starobinets G. L., Gulevich A. L., Snigireva N. M., Prilutskaya J. S., Borshchenskaya T. I.* // Papers of ISEC 88, Moscow. Vol. 3. P. 330–333.
40. *Abramov A. A., Dzhigirkhanov M. S.-A., Jofa B. Z., Volkova S. V.* // Radiokhimia. 2002. Vol. 44, № 3. P. 248–251.

41. *Starobinets G. L., Rakhman'ko E. M., Soroka J. S.* // Zh. Neorgan. Khim. 1978. Vol. 23, №6. P.1628–1631.
42. *Rakhman'ko E. M., Gulevich A. L., Starobinets G. L.* // Dokl. AN BSSR. 1980. Vol. 24, №11. P. 1015–1017.
43. *Gulevich A. L., Rakhman'ko E. M., Starobinets G. L.* // Izv. AN BSSR. Ser. Khim. Nauk. 1980. №5. P. 40–44.
44. *Rakhman'ko E. M., Tsyganov A. R., Starobinets G. L.* // Zh. Neorgan. Khim. 1981. Vol. 26, №9. P.2510–2514.
45. *Starobinets G. L., Rakhman'ko E. M., Gulevich A. L.* // Zh. Phys. Khim. 1981. Vol. 55, № 2. P. 490–494.
46. *Marcus Y.* // J. Chem. Soc. Faraday Trans. 1991. Vol. 87, № 13. P. 2995–2999.
47. *Dobos D.* Electrochemical Data.–M.: Mir, 1980. 368 p.
48. *Egorov V. V.* Extraction and Ion Association Effects in Functioning of Liquid Ion-Selective Electrodes. Dr. Sc. Theses.–Minsk, 1999. 412 p.
49. *Sandblom J., Eisenman G., Walker J. L.* // J. Phys. Chem. 1967. Vol. 71, № 12. P. 3862–3870.
50. *Schaller U., Bakker E., Spichiger U. E., Pretsch E.* // Anal. Chem. 1994. Vol. 66, №3. P. 391–398.
51. *Buhlmann P., Pretsch E., Bakker E.* // Chem. Rev. 1998. Vol. 98, № 4. P. 1593–1687.
52. *Antonisse M. M. G., Reinhoudt D. N.* // Electroanalysis. 1999. Vol. 11, № 14. P. 1035–1048.
53. *Nishizawa S., Buhlmann P., Xiao K. P., Umezawa Y.* // Anal. Chim. Acta. 1998. Vol. 358. P. 35–44.
54. *Fibbioli M., Berger M., Schmidthen E. P., Pretsch E.* // Anal. Chem. 2000. Vol. 72, № 1. P. 156–160.
55. *Tsagkatakis J., Chaniotakis N., Jurkschat K., Willem R., Quin Y., Bakker E.* // Helv. Chim. Acta. 2001. Vol. 84, № 14. P. 1952–1961.

ABSTRACTS

Ivashkevich O. A., Nechepurenko Yu. V. and Rakhmanov S. K. **Research Institute for Physical Chemical Problems of the Belarusian State University celebrates the 25th anniversary** // Chemical problems of the development of new materials and technologies: Сб. ст. Вып. 1. Minsk, 2003. P. 5–8.

The main stages of the Institute development, the basic directions of investigations carried out at the Institute and the fundamental results of investigations carried performed at the Institute over 25 years of its activity are considered.

Sviridov V. V., Gaevskaya T. V., Stepanova L. I., Vorobyova T. N. **Electroless and Electroplating of Metals** // Chemical problems of the development of new materials and technologies: Сб. ст. Вып. 1. Minsk, 2003. P. 9–59.

The present paper summarizes the main results of the research on the electroless and electrochemical metal deposition from aqueous solutions, which has been carried out in the Research Institute of Physical-Chemical problems of the Belarussian State University and at the Department of Inorganic Chemistry of the BSU for the last three decades. The paper covers the following problems: the main peculiarities of electroless and electrochemical deposition of copper, nickel, Ni-B, Ni-P, gold films 0.1–30 μm and more in thickness, their phase composition, morphology and properties; the characteristic features of of hydrometallurgic allowing (e.g. electroless and electrochemical deposition of a number of binary alloy coatings such as Cu-Ni, Cu-Cd, Cu-Sn, Cu-Zn, Ni-Sn, Ni-W, Ni-Mo), methods of their chemical and phase composition and microstructure regulation, together with correlation between these parameters and alloy properties; the methods for composite metal and alloy film plating from solutions with production of materials including metal oxides and thus possessing unusual and useful properties; the peculiarities of metal film plating onto dielectrics with production of continuous films and metal conductive patterns without the use of photoresists.

Kulak A. I., Streltsov E. A., Sviridov D. V. **Electronic structure and catalytic properties of oxide semiconductors modified with fine metal particles** // Chemical problems of the development of new materials and technologies: Сб. ст. Вып. 1. Minsk, 2003. P. 60–87.

The morphology of metal nanophase formed on the surface of wide-bandgap semiconductor oxides via the contact, photocatalytic, or photoelectrochemical de-

position is substantially dependent on concentration, bulk distribution, and energy characteristics of donor defects in the semiconductor substrate. The generation of electronic surface states in a forbidden zone of the semiconductor by the deposition of metal nanoparticles is the major factor determining the efficiency of electron exchange between metal particles and semiconductor bulk and the efficiency of electrocatalytic process as a whole. According to the electrolyte electroreflectance spectroscopic measurements, Ag, Pd, and Pt nanoparticles induce the «shallow» (with respect to the c-band edge) surface states in the forbidden zone of TiO_2, which provide near-unimpeded electron exchange between metal particles and semiconductor c-band. As the size of metal particles increases, the surface state levels in TiO_2 become more «deep» in relation to the edge of c-band. Thus the modification of the energy structure of surface states, e.g. by depositing metal nanophase of definite morphology or using the successive deposition of different metals opens the fresh opportunities in exerting an effective control over the electrocatalytic, photocatalytic, and photoelectrochemical properties of metal-loaded semiconductors.

Sviridov D. V. **Ion implantation in polymers: chemical aspects** // Chemical problems of the development of new materials and technologies: Сб. ст. Вып. 1. Minsk, 2003. P. 88–106.

The review summarizes results of the investigations on the nature of chemical processes occurring in the polymer matrix under ion bombardment and the role of these processes in modification of electrical and optical properties of ion-implanted polymers. The fate of the implanted species, structure of ion-implanted layer and possible microelectronic applications of ion-implanted polymers are also discussed.

Artemyev M. V. **Semiconductor nanocrystals inside spherical microcavities: A case of quantum dots in photonic dots** // Chemical problems of the development of new materials and technologies: Сб. ст. Вып. 1. Minsk, 2003. P. 107–118.

Quantum dots in photonic dots, a new type of microstructures involving highly luminescent II–VI semiconductor nanocrystals has been proposed and realized by incorporating nanocrystals (quantum dots) into glass and polymeric microspheres. The high quality micron-size microspheres represent simplest fully three-dimensional microcavities (photonic dots). Coupling of discrete electron states of quantum dots and photon states inside photonic dots strongly affects onto both stationary and dynamic photoluminescence properties of nanocrystals. Quantum dots in photonic dots possess a number of interesting optical effects which are demonstrated in this paper. These effects include an increase in radiative recombination rate in the vicinity of ultranarrow photon modes (Purcell effect), room temperature nearly thresholdless lasing; blinking of photon modes; single photon mode switching by single quantum dot emission.

Gurin V. S., Alexeenko A. A. **Silica sol-gel materials with metal and semiconductor nanoparticles: synthesis, structure and optical features** // Chemical problems of the development of new materials and technologies: Сб. ст. Вып. 1. Minsk, 2003. P. 119–137.

Recent achievements on fabrication, structure and optical features of the metal- and semiconductor-doped silica sol-gel materials are reviewed. The nanoparticles of copper and copper compounds (oxides, sulfides and selenides) have been produced by means of the modified silica-based sol-gel technique within the two types of materials: amorphous silica films and monolithic glasses. The features of optical absorption are discussed in dependence on chemical composition. They are variable by stoichiometry of the compounds, size of particles, their concentration and localization in the matrix. These factors determine optical properties of materials and open pathways of their application, in particular, as switching and beam-controlling elements in near-IR lasers. The quantum confinement and a partial surface chemical modification of the nanoparticles are considered as possible reasons for occurrence of the optical features specific for the copper multivalent compounds.

Ragoisha G. A., Bondarenko A. S. **Potentiodynamic electrochemical impedance spectroscopy** // Chemical problems of the development of new materials and technologies: Сб. ст. Вып. 1. Minsk, 2003. P. 138–150.

Potentiodynamic electrochemical impedance spectroscopy (PDEIS) is a technique for simultaneous ac and dc electrochemical response investigation on the potential scale. Analogous to the potentiodynamic voltammetry, PDEIS gives the variation of the dc current and, additionally, the variation of impedance spectra in the same potential scan. Thus, a comprehensive dc and ac response is acquired in a simple experiment similar to the acquisition of a common cyclic voltammogram. This is provided by the virtual instruments that also analyse the response in terms of equivalent electric circuits, giving at the output the dependence on the potential of several key parameters of electrochemical interface. The new technique simplifies considerably the investigation of stationary electrochemical systems and provides the unique possibility for the comprehensive electrochemical characterisation of unstable systems and transient states. A lot of examples is presented in the review to illustrate these new possibilities.

Ivanovskaya M., Kotsikau D., Orlik D. **Gas-sensitive properties of oxide systems based on In_2O_3 and SnO_2 obtained by sol-gel technology** // Chemical problems of the development of new materials and technologies: Сб. ст. Вып. 1. Minsk, 2003. P. 151–175.

The influence of structural features of In_2O_3, SnO_2, MoO_3 and Fe_2O_3 simple oxides and their composites on the properties of the corresponding semiconductor gas sensors with regards to different gases (CO, CH_4, NH_3, C_2H_5OH, CH_3OH, NO, NO_2, O_3) have been studied. Structural peculiarities of oxide systems obtained by

sol-gel technology have been considered. It was shown the possibility to control the sensor sensitivity to the mentioned above gases by varying chemical composition of sensitive materials and adjusting their structure, as well as by regulating of detecting temperature.

Kabo G. J., Blokhin A. V., Kabo A. G. **Investigation of thermodynamic properties of organic compounds** // Chemical problems of the development of new materials and technologies: Сб. ст. Вып. 1. Minsk, 2003. P. 176–192.

Scientific and ptactical significance of the investigations in the field of thermodynamics of organic compounds is discussed. The apparatuses and methods used in LTOC (the Laboratory of Thermodynamics of Organic Compounds, Research Institute for Physical Chemical Problems, Belarusian State University) for experimental determination of thermodynamic properties of substances are described. They are adiabatic calorimetry and DSC of the heat bridge type for the measurements of heat capacities and enthalpies of phase transitions in the condensed state, heat flow differential microcalorimeter of the Calvet type to obtain enthalpies of evaporation, calorimeters for combustion of organic substances for determination of the enthalpies of combustion and formation, the apparatus for measurements of saturated vapor pressure by the integral effusion Knudsen method. The main results of studies of chemical and phase equilibria, thermodynamics of isomerization, improvements of additive methods for calculation of thermodynamic properties, investigations of plastic crystals of organic compounds and ionic liquids, calculations by the methods of statistical thermodynamics are reported. The information concerning development of the methods of calculation of chemical exergies in LTOC and thermodynamic substantiation of energy and resource saving technologies of organic production of Republic of Belarus is given.

Gaponik P. N., Ivashkevich O. A. **Tetrazoles: Synthesis, Structures, Physico-Chemical Properties and Application** // Chemical problems of the development of new materials and technologies: Сб. ст. Вып. 1. Minsk, 2003. P. 192–233.

The paper represents a brief review of works published by the authors over a period of 1980-2003 years in the field of synthesis and investigations of properties of tetrazole derivatives. The main attention is given to problems of regioselective functionalization of the tetrazole ring and the development of simple and convenient methods for the synthesis of N- and C-substituted tetrazoles, to peculiarities of structure of crystalline tetrazoles including quaternary salts and complexes with transition metal salts as well as to the data on electronic, spatial structure and energetic characteristics of tetrazoles obtained using both quantum-chemical methods and IR-, ^{1}H , ^{13}C and ^{15}N NMR spectroscopy. The features of thermal decomposition and combustion of various tetrazoles and polyvinyltetrazoles determining the prospects of their use as effective components of different kind combustible and thermally decomposing systems, including those capable of liquid-flame combustion, which has been revealed for the first time, are considered.

Lesnikovich A. I., Vorobyova S. A. **Preparation and investigation of the heterogeneous systems, containing highly dispersed components** // Chemical problems of the development of new materials and technologies: Сб. ст. Вып. 1. Minsk, 2003. P. 234–247.

The results of the investigation of the different materials containing highly dispersed substances are reported. The following materials, including colloidal, supported and fibrous regulators of intraballistic characteristics of composite solid propellants; X-ray contrast neutron-capturing magnetic liquid for radiation examinations, neutron-capture therapy of malignant neoplasms and X-ray diagnostics; magnetoabrasive tools combining high magnetic, cutting and abrasive characteristics; magnetic sorbents for the purification of the waste water of the industrial enterprises; antifriction and antiwear additives to mineral oils; developers for latent fingerprint visualization on wet, greasy and adhesive surfaces; different gas-generating systems for sickness diagnostics; silver and silver/palladium powders for conducting pasters are considered. The preparative peculiarities of the interphase synthesis and the properties of the nanosized metals and their compounds obtained by this method are discussed. The state (sediment, film, colloidal solution) and the phase of the reaction product's localization (organic, water or interface) is shown to depend on such factors as the nature, concentration and ratio of the reagents, reaction temperature, volume of the phases and interface area. The properties of the formed metals and their compounds are differ from one's of the corresponding substances precipitated from the homogeneous (aqueous) solutions.

Naumovich E. N, Yaremchenko A. A, Viskup A. P., Kharton V. V. **Perovskite-related oxide materials for oxygen-permeable electrochemical membrans** // Chemical problems of the development of new materials and technologies: Сб. ст. Вып. 1. Minsk, 2003. P. 248–263.

This brief review is focused on the studies of mixed ionic-electronic conductors on the basis of lanthanum gallate doped with transition metal cations in the B sublattice. The substitution of gallium with iron, cobalt or nickel results in greater electronic conductivity, simultaneously keeping high level of the oxygen ionic transport. In particular, $La_{0.90}Sr_{0.10}Ga_{0.65}Ni_{0.20}Mg_{0.15}O_{3-d}$ perovskite exhibits attractive oxygen permeability, which is quite similar to that of La_2NiO_4- and (La,Sr)CoO_3-based phases The combination of appropriate transport and thermomechanical properties with sufficiently high thermodynamic stability enables to use Ni- or Fe-substituted $LaGaO_3$-based mixed conductors for the membrane electrocatalytic reactors for partial oxidation of light hydrocarbons.

Kaputskii F. N., Gert E. V., Torgashov V. I., Shishonok M. V. and Zubets O. V. **Multifunctionality of nitrogen oxide compounds as a basis for preparation of practically important cellulose materials** // Chemical problems of the development of new materials and technologies: Сб. ст. Вып. 1. Minsk, 2003. P. 264–294.

The experience of using the multifunctional character of nitrogen oxide compounds (N_2O_4, NO_2, N_2O_3, HNO_3) in cellulose chemistry and technology is summarized. The approach discussed is based on the ability of the nitrogen oxide compo-

unds to act as multi-purpose reagents with respect to cellulose, enabling oxidation, nitrosation, nitration, hydrolytic cleavage or adduct formation to be performed on cellulose, depending on reaction conditions. It is often possible to perform simultaneously several chemical or/and structural cellulose modifications using a sole reagent in a «one-pot» process.

High solubility of nitrates formed from mineral components of vegetal tissues, along with high reactivity of HNO_3 toward lignin that occurs together with cellulose, provide the possibility of selective extraction of radionuclides in the course of nitric acid delignification of contaminated vegetal material. In this review, examples are given of effective use of multiple functionality of nitrogen oxide compounds in the preparation of such practically important materials as totally or partially substituted cellulose acetates soluble in organic solvents, water-soluble polysaccharide sulphates with low degree of substitution, powder forms of cellulose hydrate and of carboxylated cellulose in both structurally disordered and microcrystalline forms, as well as in isolation of radionuclide-free cellulose and nitrolignin from contaminated agricultural residues.

Grinshpan D. D., Savitskaya T. A., Tsygankova N. G. **Non-traditional solutions of cellulose and it's derivatives and their processing products** // Chemical problems of the development of new materials and technologies: Сб. ст. Вып. 1. Minsk, 2003. P. 295–326.

The main achievements of the Laboratory of cellulose solutions and their processing products in the field of the elaboration of new cellulose dissolving processes, the homogeneous synthesis of cellulose derivatives, the elaboration of the incompatible polymer solutions stabilization, the creation of new film – fabric materials and filtering equipments on their base, the preparation of hard quickly disintegrated drug forms (tablets, granules) using new water soluble cellulose derivative have been summarized.

Kostjuk S.V., Lesnyak V. P., Gaponik L. V., Mardykin V. P., Kaputsky F. N. **The complexes of Lewis acids: synthesis and application in polymerization** // Chemical problems of the development of new materials and technologies: Сб. ст. Вып. 1. Minsk, 2003. P. 327–339.

The published works by the present authors on the synthesis of organoaluminium compounds and complexes thereof are summarized. The study of the reactivity of these latter in stereospecific and alternating polymerization made it possible to produce effective catalysts for synthesizing superhigh molecular weight polyolefins, alternating copolymers. The detailed investigation of the properties of the organoaluminium complexes with ethers allowed working out new catalytic systems capable of initiating styrene living cationic polymerization. The revealed regularities of living polymerization of styrene allows to realize for the first time the controlled polymerization of industrial C_9-fraction, with the obtained results being used for developing technology for production of aromatic hydrocarbon resins from C_9-fraction. An industrial process was developed and employed to pro-

duce oligopiperylene and aromatic hydrocarbon resins, which are used as film-forming components in paint and varnish composition.

Egorov V. V., Rakhman'ko E. M. **Ion Association Effects of Lipophilic Quaternary Ammonium Salts in Ion-Exchange and Potentiometric Selectivity** // Chemical problems of the development of new materials and technologies: Сб. ст. Вып. 1. Minsk, 2003. P. 340–367.

Strong effects of ion association on the anion-exchange selectivity in systems water – solutions of high quaternary ammonium salts (QAS) in organic solvents as well as on the potentiometric selectivity of plasticized polyvinylchloride (PVC) membranes containing QAS as ion exchangers have been established experimentally and substantiated theoretically. Based on the linear Gibbs energy relations (LGER) and ion association theory by Eigen-Denison-Ramsey-Fuoss, an approach to separate estimation of the parts played by the solvation and ion association factors in ion-exchange and potentiometric selectivity has been proposed. The results obtained serve as the basis for revision of the formed notions about QAS as of «nonselective» ion exchangers and enable the development of methods for the control of ion-exchange and potentiometric selectivity using the factor of ion association. Specifically, it has been demonstrated that variation of steric accessibility of the QAS exchange center is a powerful means to control the selectivity.

It has been found experimentally that due to varying steric accessibility of the QAS exchange center the selectivity values have changed by 3 orders of magnitude in case of single- charged anions exchanged for single-charged ones and by more than 7 orders – in case of double-charged anions exchanged for the single-charged ones. The above-mentioned effects revealed also in the potentiometric selectivity of QAS-based PVC membranes and to some extent - in the potentiometric selectivity of the membranes based on neutral anion carriers, doped with QAS for provision of anion permselectivity, are of great practical importance for the development of ISE with improved selectivity.

CONTENTS

Научное издание

ХИМИЧЕСКИЕ ПРОБЛЕМЫ СОЗДАНИЯ НОВЫХ МАТЕРИАЛОВ И ТЕХНОЛОГИЙ

СБОРНИК СТАТЕЙ

Выпуск 1

На английском языке

В авторской редакции

Художник обложки *Л. А. Стрижак*
Технический редактор *Т. К. Раманович*
Компьютерная верстка *А. А. Микулевича*

Подписано в печать с оригинала-макета заказчика 03.10.2003. Формат 70×100/16.
Бумага офсетная. Гарнитура SchoolBook. Печать офсетная.
Усл. печ. л. 30,31. Уч.-изд. л. 32,59. Тираж 500 экз. Зак. 2237.

Белорусский государственный университет.
Лицензия ЛВ № 315 от 14.07.2003.
220050, Минск, проспект Франциска Скорины, 4.

Республиканское унитарное предприятие
«Издательство «Белорусский Дом печати».
220013, Минск, проспект Франциска Скорины, 79.